

Chaos, Solitons and Fractals: the interdisciplinary journal of Nonlinear Science, and Nonequilibrium and Complex Phenomena

From experimental phenomena to computational models: Exploring the synchronization mechanisms of phase-locked stimulation in the hippocampal-thalamic-cortical circuit for memory consolidation
--Manuscript Draft--

| | |
|------------------------|---|
| Manuscript Number: | CHAOS-D-24-06617R1 |
| Article Type: | Full length article |
| Section/Category: | Interdisciplinary applications in systems biology, social sciences and econophysics |
| Keywords: | Memory consolidation · hippocampal-thalamocortical (HTC) circuit · closed-loop electrical stimulation · magnetic ultrasonic stimulation · mass discharge rate |
| Corresponding Author: | Qingyun Wang Beihang University Beijing, CHINA |
| First Author: | Denggui Fan |
| Order of Authors: | Denggui Fan Jin Chen Songan Hou Zhengyong Song Gerold Baier Qingyun Wang |
| Abstract: | <p>Closed-loop phase-locking stimulation has been experimentally demonstrated to facilitate memory consolidation, which is believed to rely on the coordinated interactions among slow waves in multi-regional cortex, thalamocortical sleep spindles, and hippocampal ripples. However, the mechanisms through which this stimulation influences memory consolidation have not been thoroughly investigated. Therefore, starting from experimental phenomena, we computationally explored the synchronization mechanisms of memory consolidation in the hippocampal-thalamocortical (HTC) loop based on a firing rate model, and further reproduced the established effects of stimulation therapy on memory consolidation. The results indicate that excitatory connections between the cortex and hippocampus play a crucial role in the memory consolidation process. Additionally, our improved inhibitory closed-loop phase-locking stimulation protocol exhibits a more enhanced effect on memory consolidation compared to previous experimental stimulation schemes. Moreover, noninvasive stimulation shows lower side effects, costs, and implementation difficulties compared to invasive stimulation. Consequently, we further designed and explored the modulatory effects of a non-invasive magnetic-acoustic stimulation protocol. The results suggest that this non-invasive magnetic-acoustic stimulation yields effects comparable to those of existing invasive experimental deep brain stimulation. Our findings may provide new evidence and perspectives for understanding the neural mechanisms of memory processes and offer potential theoretical foundations for innovative non-invasive therapeutic strategies.</p> |
| Suggested Reviewers: | Jianzhong Su su@uta.edu Mingming Chen mmchen@zzu.edu.cn |
| Response to Reviewers: | |

Dear editor,

We are resubmitting the revision version of our manuscript entitled “From experimental phenomena to computational models: Exploring the synchronization mechanisms of phase-locked stimulation in the hippocampal-thalamic-cortical circuit for memory consolidation” for reconsideration by Chaos, Solitons and Fractals.

Thank you to the reviewers for their pertinent comments, which have greatly assisted us in improving the paper. We have carefully reviewed all the comments and made the necessary modifications in the corresponding sections of the paper. Furthermore, these comments have provided valuable insights for our scientific research and writing, enriching our research and writing experience and offering some guidance for our future studies. The changes made are highlighted in a light color in the main manuscript.

We also extend our special thanks to Editor for all the efforts made to improve this paper.

Please address all correspondence concerning this manuscript to me at nmqingyun@163.com; worldfandenggui@163.com

Thank you for your reconsideration of this manuscript.

Prof. Qingyun Wang and Denggui Fan

QW: Dynamics and Control, Beihang University

DF: School of Mathematics and Physics, University of Science and Technology Beijing

Graphical Abstract

From experimental phenomena to computational models: Exploring the synchronization mechanisms of phase-locked stimulation in the hippocampal-thalamic-cortical circuit for memory consolidation

Denggui Fan, Jin Chen, Songan Hou, Zhengyong Song, Gerold Baier, Qingyun Wang

Figure 1: The structure of synaptic connections between neurons of the HTC network. This network model consists of three subnetworks: hippocampus, cortex, and thalamus.

Figure 2: Generation of SOs, spindles, and ripple in the full hippocampo-cortico-thalamic model and their firing characteristics.

Figure 3: Three type of invasive stimulus therapies and one type of non-invasive stimulation pattern (magnetic ultrasonic stimulation), and their performing process and physical mechanism, stimulation waveforms as well as mathematical expressions.

Figure 4: The impact of the strength of cortico-hippocampal excitatory connections on their firing rate and their facilitation effects to memory consolidation. It is shown that this excitatory connection has significant implications for the promotion of memory consolidation.

Figure 5: The impact of varying connection strengths on the firing rate of thalamic neurons. Under varying connection strengths among different neurons, there is almost no effect on the firing rate of thalamic neurons.

Figure 6: Under a fixed connection strength, changing the stimulus intensity has little effect on the discharge rate of the nucleus, further explaining the important role of excitatory connections in the cortical-hippocampal nucleus neurons in promoting memory consolidation.

Figure 7: Numerical simulations reproduce the experimental results, namely that under real-time closed-loop stimulation, synchronization increases and the number of ripple events decreases, while the number of other events increases; without precise temporal stimulation, the results are qualitatively consistent with the experimental findings. The significant reduction in the number of slow oscillation events may counteract the decreased synchronization between hippocampal ripples and cortical slow oscillations, leading to no significant changes after stimulation or potentially being detrimental to memory consolidation.

Figure 8: Heatmap of exponential changes under dual-parameter experimental stimulation. This further affirms the rationality of the experimental stimulation frequency (100Hz) chosen in the numerical simulations.

Figure 9: Results of the inhibitory stimulation protocol. The low-current inhibitory stimulation scheme is more effective than the existing experiments (with significant increases in synchronization values as well as the number and characteristics of events), further demonstrating the rationality and superiority of real-time closed-loop stimulation.

Figure 10: Dual-parameter inhibitory stimulation. Similarly, it also further confirms the rationality and superiority of our chosen stimulation frequency (500Hz).

Figure 11: Results of magneto-ultrasound stimulation, compared with the effects of experimental closed-loop intracranial stimulation. It indicates that the effects of magneto-ultrasound stimulation are comparable to those of experimental closed-loop intracranial stimulation. That is, the synchronization gain of thalamo-cortical spindle waves with hippocampal ripples and the increase in the number of cortical slow oscillation events show no significant difference, and the reduction in the number of ripple events is roughly consistent. The increase in spindle events under magneto-ultrasound stimulation is slightly inferior, but in comparison, the enhancement of cortical slow oscillation and hippocampal ripple synchronization under magneto-ultrasound stimulation is significantly higher than that under closed-loop intracranial electrical stimulation. This improvement may offset the insufficiency in the number of spindle events.

Figure S1: The time-frequency plots of the three types of waves and the percentage of their co-occurrence (So and spindle have approximately 85% co-occurrence, spindle and ripple have approximately 75% co-occurrence, So and ripple have approximately 50% co-occurrence).

Figure S2: Discharge rates of hippocampal and cortical nucleus neurons under different connection strengths. (Apart from the change in cortical excitatory connections to the hippocampus affecting the discharge rate of neurons, there are almost no changes in the others).

Figure S3: Changes in memory consolidation-related indicators with altered connection strengths other than the excitatory connections from the cortex to the hippocampal neurons. It does not promote memory consolidation.

Figure S4: Changes in memory consolidation indicators under different inhibitory stimulation intensities. None of the above stimulation intensities can simultaneously increase all indicators of memory consolidation, and may

even significantly impair memory consolidation.

Highlights

From experimental phenomena to computational models: Exploring the synchronization mechanisms of phase-locked stimulation in the hippocampal-thalamic-cortical circuit for memory consolidation

Denggui Fan, Jin Chen, Songan Hou, Zhengyong Song, Gerold Baier, Qingyun Wang

- **Based on the hippocampal-thalamic-cortical circuit dynamics network model, we provided the theoretical evidence for the experimental results, i.e., the promoting effect of real-time closed-loop electrical stimulation on memory consolidation**

In this study, we used a computational model to simulate the experimental stimulation process and quantify the memory consolidation indicators. We successfully reproduced the promoting effect of real-time closed-loop electrical stimulation on memory consolidation as designed in the experiment.

- **We proposed two type of improving stimulation therapies, i.e., the low current inhibitory stimulation and non-invasive magneto-ultrasonic stimulation.**

The results show that this inhibitory stimulation protocol can promote memory consolidation more efficiently. In addition, the predictive effects of non-invasive stimulation protocol is comparable to the commonly invasive intracranial stimulation, but has significant advantages in terms of side effects, cost, and difficulty of implementation. These findings provide new solutions for the treatment of memory disorders and may advance the development of clinical stimulation devices.

- **We verified the complex nonlinear properties of memory consolidation using the Mean Firing Rate (MFR) and the key role of excitatory connections between the cortex and the hippocampus in modulating dominantly memory consolidation, which providing new ideas for understanding the neural mechanism of memory process.**

From experimental phenomena to computational models: Exploring the synchronization mechanisms of phase-locked stimulation in the hippocampal-thalamic-cortical circuit for memory consolidation

Denggui Fan^a, Jin Chen^a, Songan Hou^b, Zhengyong Song^a, Gerold Baier^c,
Qingyun Wang^b

*^aSchool of Mathematics and Physics, University of Science and Technology
Beijing, Beijing, 100083, China*

^bDynamics and Control, Beihang University, Beijing, 100191, China

*^cCell and Developmental Biology, University College London, London, London WC1E
6BT, United Kingdom*

Abstract

Closed-loop phase-locking stimulation has been experimentally demonstrated to facilitate memory consolidation, which is believed to rely on the coordinated interactions among slow waves in multi-regional cortex, thalamocortical sleep spindles, and hippocampal ripples. However, the mechanisms through which this stimulation influences memory consolidation have not been thoroughly investigated. Therefore, starting from experimental phenomena, we computationally explored the synchronization mechanisms of memory consolidation in the hippocampal-thalamocortical (HTC) loop based on a firing rate model, and further reproduced the established effects of stimulation therapy on memory consolidation. The results indicate that excitatory connections between the cortex and hippocampus play a crucial role in the memory consolidation process. Additionally, our improved inhibitory closed-loop phase-locking stimulation protocol exhibits a more enhanced effect on memory consolidation compared to previous experimental stimulation schemes. Moreover, non-invasive stimulation shows lower side effects, costs, and implementation difficulties compared to invasive stimulation. Consequently, we further designed and explored the modulatory effects of a non-invasive magnetic-acoustic stimulation protocol. The results suggest that

this non-invasive magnetic-acoustic stimulation yields effects comparable to those of existing invasive experimental deep brain stimulation. Our findings may provide new evidence and perspectives for understanding the neural mechanisms of memory processes and offer potential theoretical foundations for innovative non-invasive therapeutic strategies.

Keywords: Memory consolidation;hippocampal-thalamocortical (HTC);circuit closed-loop electrical stimulation;magnetic ultrasonic stimulation;mass discharge rate

1. Introduction

Precise timing relationships among the three primary non-rapid eye movement (NREM) rhythms cortical slow oscillations (SOs), thalamic spindle waves, and hippocampal ripples—are deemed crucial for memory consolidation during sleep [1, 2, 3, 4, 5]. The interlocking of these distinct NREM rhythms serves as the coupled mechanism for memory consolidation [6, 7, 8, 9, 10, 11, 12].

Electrical stimulation has been extensively applied in the treatment of various neurological disorders, such as epilepsy and Parkinson’s disease, serving as a complementary approach to pharmacotherapy and playing a significant role in the management of these conditions [13, 14, 15, 16]. In relation to neurodegenerative diseases associated with cognitive impairment, electrical stimulation has also demonstrated the potential to improve cognitive functions. Meanwhile, external intervention can facilitate memory consolidation, with the majority of evidence supporting these theories derived from studies involving either non-invasive experiments on humans or neuronal recordings in rodents. For instance, closed-loop acoustic stimulation is employed to demonstrate that bolstering slow-wave oscillations and sleep spindles in the neocortex enhances memory [17, 18]; By enhancing the synchronization of hippocampal prefrontal neurons during sleep through closed-loop electrical stimulation, human memory consolidation is strengthened [19]; Transcranial electrical stimulation influences sleep-related memory consolidation by altering the excitability of nerve cells, thereby modifying the resting potential to achieve depolarization or hyperpolarization, which in turn fosters more slow-wave oscillatory activity and enhances memory consolidation [20, 21]. However, the effects of stimulus regulation in the aforementioned protocols have thus far been validated solely through physiological means, with a no-

table absence of direct computational theoretical evidence, the dynamics of memory consolidation remain unclear, and the outcomes of current experimental protocols fall short of enhancing various criteria pertinent to memory consolidation.

Modeling the nervous system provides a more diverse arsenal for the study of various neural functions, offering theoretical and simulation support for clinical trials[22, 23, 24, 25]. Currently, numerous neurodynamic models focused on the cortex, hippocampus, and thalamus have significantly contributed to the understanding of related neurological disorders and the mechanisms underlying brain function [26, 27, 28, 29, 30]. Prior model studies were confined to either the hippocampal-cortical or cortical-thalamic networks alone [31]. Taking into account the mediating role of thalamic spindle waves, this study employs the simplified hippocampal-thalamic-cortical neural mass model (HTC) introduced by Azimi et al. to investigate the network dynamics underlying memory consolidation [9]. This model is capable of spontaneously generating slow oscillations, slow/fast spindles, and hippocampal ripples. Without providing any code, we utilized this model to simulate the neuronal membrane potentials in the hippocampus, thalamus, and cortex. Through filtering, we identified the slow oscillations, slow/fast spindles, and hippocampal ripple events that occur during the memory consolidation process. Using the events detected post-filtering, we will explore the intrinsic mechanism of memory consolidation and study the effect of different electrical stimulation schemes on enhancing brain memory consolidation[32, 33, 34, 35].

Inspired by the above, this paper will explore the promoting effect of stimulus regulation on memory consolidation from the perspective of calculation. Referring to the experimental scheme of intracranial real-time closed-loop electrical stimulation promoting memory consolidation recently proposed in nature neuroscience [19], we will conduct numerical simulation of the experimental process through the model to make up for the shortage of computational evidence. Although the participants in the experiment were patients with medically intractable temporal lobe epilepsy, it was clearly explained that there was no correlation between the accuracy of recognition memory and the impact of stimuli on interactive epileptiform discharges (IED). It shows that epilepsy patients as the re-search object in this experiment do not affect the regulation of stimulus on memory consolidation. Therefore, we combined the HTC model to simulate the numerical calculation of the human stimulation experiment and verified the results of experiment [19]. In addition, we also designed a specific real-time closed-loop inhibitory stimulus,

and verified for the first time that adding a specific low current inhibitory stimulus can also improve the indicators related to memory consolidation, thus promoting memory consolidation. In contrast, the same stimulus without such precise time locking has no good effect on memory consolidation, which reflects the scientificity and rationality of real-time closed-loop to a certain extent. In particular, our proposed electrical stimulation scheme may better promote memory consolidation. More importantly, we have also developed a promising noninvasive stimulation scheme, namely, magnetic ultrasound stimulation, which has the same effect as experimental intracranial stimulation. All these may contribute to the development of clinical stimulation equipment for memory impairment and dementia in the future, and provide a new means to solve memory impairment. In addition, the model also predicted that altering the excitatory connection between the cortex and hippocampus has a greater impact on the discharge rate of the nucleus. Under the same stimulation, a larger change in discharge rate, compared to a smaller one, would positively enhance memory consolidation. It provides new ideas for promoting memory consolidation.

2. Materials and Methods

2.1. *Experimental Data*

This paper is referring to the experimental data from eighteen participants with pharmacologically intractable temporal lobe epilepsy. It was shown that epilepsy patients as the research object in this experiment do not affect the regulation of stimulus on recognition memory consolidation [15]. Participants were tested in two experimental nights: intervention night and undisturbed night. At the intervention night, real-time closed-loop (RTCL) stimulation was used in NREM early sleep. One intracranial electroencephalogram (iEEG) electrode in the medial temporary lobe is used as a synchronous probe to determine the time of closed-loop control, while the second neocortical iEEG electrode is used as a stimulation site (usually in the white matter of the orbital frontal cortex, 15 of the 19 stimulation nights). The slow wave activity of the probe was monitored and analyzed in real time to trigger a short (50ms) high frequency (100Hz) electrical stimulation event at the neocortical stimulation site about every 4 seconds. There are two operation modes of intervention, namely (I) "synchronous stimulation" (II) "mixed stage stimulation", which are respectively applied to two groups of different participants.

2.2. Structure of HTC

As shown in Figure 1, this HTC circuit structure consists of two hippocampal networks, representing the CA1-CA3 network, one thalamic network, and two cortical networks, respectively. The strength of short-range synaptic connections between neurons in a separate CA3-CA1 network and a separate cortical thalamic network is much greater than that of the CA3-CA1 network and cortical network neurons in remote synaptic connections, similar to the three small world networks[9].

2.3. Network Dynamics of HTC

The HTC network is modelled with the rate model[9]:

$$\begin{aligned} \frac{dV_q^k}{dt} = & -\frac{V_q^k}{\tau_q} - \sum_{n=1}^3 x_n N_{j_n}^{k_{n1}} P_{j_n i}^{k_n} J_{j_n i}^{k_n} (c^k) r(V_{j_n}^{k_{n1}}) \\ & + \sum_{m=1}^5 x_m N_{j_m}^{k_{m1}} P_{j_m q}^{k_m} J_{j_m q}^{k_m} r(V_{j_m}^{k_{m1}}) + k_l \frac{f(u_l)}{A_l} \end{aligned} \quad (1)$$

$$\frac{dc^k}{dt} = -\frac{c^k}{\tau_c} + \sum_{n=1}^3 y_n N_e^{k_n} P_{ee}^{k_{n1}} \Delta c^k r(V_e^{k_n}) \quad (2)$$

where, V_q^k is the membrane potentials, A_l is the specific membrane capacitance, c^k and Δc^k are respectively the adaptation variable of neuron k and its increment, $N_{j_n}^{k_{n1}}$ and $N_{j_m}^{k_{m1}}$ are the number of neurons, where $x_n, x_m, y_n, k_l \in \{-1, 0, 1\}$; $n = 1, 2, 3$; $m = 1, 2, 3, 4, 5$; $l \in \{t, r\}$; $q, j_n \in \{i, e, t, r\}$; $k, k_{n1} \in \{CA1, CA3, CX1, CX2, TH\}$; $k_n, k_m \in \{CA1, CA3, CX1, CX2, TH, CA3 - CA1, CX1 - CA1, CA1 - CX, CX2 - CA3, CX2 - CX1, CX1 - TH, TH - CX1, CX2 - TH\}$.

The probability and strength of the network from neurons m to neurons n are determined by P_{mn}^{k-h} and J_{mn}^{k-h} , where k and h can be CA1, CA3, CX (representing the cortex) or TH (representing the thalamus), n can take t (representing TC neurons), r (representing thalamic RE neurons), e (representing cortical or hippocampal excitatory neurons), and i (representing cortical or hippocampal inhibitory neurons), while m can only take one of the excitatory neurons t or e .

The firing rate (r) of Hippocampal and cortical neurons is a sigmoid function of the membrane potential (V_m^k) as follows:

$$r(V_m^k) = r_0 + \frac{r_1}{1 + \exp[-(V_m^k - V_m^{*k})/g_m^k]} \quad (3)$$

$$\{m\} \in \{e, i\}, \{k\} \in \{CA1, CA3, CX\}$$

where $r_1(r_0)$ is the maximum (minimum) discharge rate of neurons m in a completely depolarized state, V_m^{*k} is the threshold discharge potential of neurons m , g_m^k is the dependence of discharge rate on membrane potential.

J_{mn}^k indicates the strength of the connection from neuron m to neuron n . Dendritic spike frequency adaptation (DSFA) is considered applicable to all excitatory to excitatory connections, J_{ee}^k is a decreasing sigmoid function of an adaptation variable, c , representing the mean adaptation level of an excitatory neuron:

$$J_{ee}^k(c^n) = \frac{J0_{ee}^k}{1 + \exp[(c^n - c^*)/g_c]} \quad (4)$$

$$\{n\} \in \{CA3, CA1\}, \{k\} \in \{CA3, CA3 - CA1\}$$

where, $J0_{ee}^k$ is the maximal synaptic strength corresponding to adaptation level at equilibrium value (set to be zero). $c^* = 10$ is the threshold adaptation level and $g_c = 3$ shows the sharpness of the excitatory to excitatory connection dependence on the adaptation variable. The adaptation level increases by Δc_n .

The function $f(u_l)$ in Eq.(1) is a sigmoid function that can be expressed as:

$$f(u_l) = \frac{-f_l^{\max}}{1 + \exp\left[\frac{(u_l + f_{th}^l)}{q_l}\right]}, \{l\} \in \{t, r\} \quad (5)$$

where u_l is a bursting variable particularly defined for thalamic neurons to model T-type calcium currents:

$$\frac{du_l}{dt} = \frac{b_l - u_l}{\tau_l^u} \quad (6)$$

where τ_l^u is the time constant, $b_l = 0$ is $V_r^{TH} > 0mV$ or $V_t^{TH} > -0.1mV$, otherwise $b_l = -200mA$. Then the discharge rate of thalamic neurons is

defined as:

$$r(V_m^{TH}) = \frac{R_m^T}{1 + \exp\left[\frac{V_m^{TH} - V_m^T}{g_m^T}\right]} (\exp[L_m u_m]) + \frac{R_m^B}{1 + \exp\left[\frac{V_m^{TH} - V_m^B}{g_m^B}\right]} (1 - \exp[L_m u_m]) \quad (7)$$

where, R_m^T (R_m^B), V_m^T (V_m^B) and g_m^T (g_m^B) is maximum firing rate, threshold firing potential, and the sharpness of the firing rate.

The corresponding parameter values of HTC model network can be found in Supplementary Materials. The numerical calculation is conducted by the MATLAB software and using the fourth-order Runge Kutta method with a time step of $1ms$.

2.4. Transcranial magneto-acoustical stimulation

Utilized standard Cartesian coordinates, assuming longitudinal pressure waves along the z axis and a magnetostatic field along the x axis, with current density aligned with the y axis. The longitudinal wave follows the classical wave equation[32].

$$\frac{\partial^2 u}{\partial z^2} = \frac{1}{c_0^2} \frac{\partial^2 u}{\partial t^2} \quad (8)$$

The displacement u represents the distance of an ion from its equilibrium position, with c_0 denoting the ultrasonic velocity. For a progressive sine wave, the instantaneous velocity v of an ion can be described as:

$$v_z = W \sin(\omega t - \varphi) \quad (9)$$

where W is the ion velocity, $\omega = 2\pi f$ is the angular frequency, and f is the ultrasonic frequency. The relationship between fluid velocity and instantaneous pressure P can be expressed as

$$P = \rho c_0 \omega \quad (10)$$

where ρ is the tissue density. According to Montalibet's theory, the current density J_y can be expressed as

$$J_y = \sigma \frac{w B_x}{1 + \tan^2 \psi} \sin(\omega t - \psi) \quad (11)$$

where σ is the tissue conductivity, with a typical value of 0.5 siemens /m. B_x is the static magnetic field strength, and ψ is the phase angle.

$$\tan \psi = \omega \tau \quad (12)$$

where τ is the time constant, typically femtoseconds for an electrolyte, and can be neglected for medical ultrasonic frequencies (200 – 700kHz) . From this, we derive a simplified formula for neuronal discharge induced by ultrasound:

$$J_y \approx \sigma w B_x \sin \omega t \quad (13)$$

The relationship between ultrasonic power intensity and ultrasonic pressure satisfies the following equation

$$\Gamma = \frac{1}{2} \frac{P^2}{\rho c_0} \quad (14)$$

Combine the above equations to get the final formula

$$J_y \approx \sigma B_x \sqrt{\frac{2\Gamma}{\rho c_0}} \sin(2\pi f t) \quad (15)$$

Thus, in transcranial Magnetoacoustic stimulation, we can intermittently switch the magnetic field stimulation, so that the pulse ultrasound can better simulate the pulse current in DBS.

2.5. Firing Characteristics of HTC on the Memory Consolidation

2.5.1. Events Detection Methods

In the second stage of non rapid eye movement sleep, the appearance of spindle waves marks a specific pattern of brain activity, closely related to cognitive functions such as sensory signal transmission, synaptic plasticity, memory consolidation, and intellectual development. Ripple waves mainly appear in the hippocampus and are related to the process of memory consolidation, although they have also been observed in areas outside the hippocampus. Slow waves and oscillations are associated with deep sleep and are important manifestations of synchronized brain activity. The specific detection method is as follows:

Spindle Similar to existing methods [36], The 4th order zero phase delay Butterworth bandpass filter is applied to the local field potential (LFP)

of cortical network 2, and the frequency is adjusted to 9Hz-16Hz. In the experiment, it is adjusted to 12Hz-16Hz. Then we use Hilbert transform to extract the phase and calculate the instantaneous amplitude, which is smoothed through a 300 millisecond Gauss window (standard deviation=0.65). Spindle events are identified by amplitude exceeding the threshold by one standard deviation and duration between 0.5 and 3.5 seconds. Adjacent events with an interval of less than 0.5 seconds are merged.

Ripple Similar to previous research [37], firstly, the fourth-order zero phase delay Butterworth bandpass filter was applied to the membrane potential of CA1 pyramidal neurons. The target frequency range was 80hz-150hz, and the experimental focus was 80hz-100hz. The instantaneous amplitude is calculated by deriving the phase through Hilbert transform. Subsequently, a 50 millisecond Gaussian smoothing window is used to enhance the signal definition. Our criteria for identifying ripple events include amplitude exceeding the median plus two standard deviations and a minimum duration of 30 milliseconds.

Slow Oscillation Similar to [9], we first perform the bandpass filtering (12Hz-16 Hz, 3th order zero phase delay Butterworth) to the membrane potential of excitatory neuron of cortical network 2. Afterwards, the positive and negative peaks of the signal are calculated. When the distance between two consecutive positive and negative zeros in different directions is between 0.5s and 2s (corresponding to 0.5Hz to 2 Hz), the difference between the positive and negative peaks of the signal is greater than the threshold (1.4SD of the average negative peak), and the negative peak is greater than the threshold (1.4SD of the average negative peak), an slow oscillation (So) event can be identified.

Slow Wave Refer to [38], firstly, the membrane potential signal of excitatory neuron of the hippocampal network is band-pass filtered (0.125Hz-1.6Hz, two pass fir band pass filter, order = three cycles of the low frequency cut-off); Secondly, the positive and negative peaks of the signal are calculated. When the distance between the positive and negative zeros in two consecutive directions is between 0.8s and 2s, and the amplitude standard is met at the same time, the difference between the positive and negative peaks of the signal is greater than the threshold (1.4SD of the average negative peak), and the negative peak is greater than the threshold (1.4SD of the average negative peak), the slow wave event can be identified.

2.5.2. Temporal nesting of cortical slow oscillations, thalamic spindles, and hippocampal ripples

The neuronal membrane potentials of the hippocampus and thalamic cortex were processed using the aforementioned filtering methods to obtain ripple (100-250Hz), So (0.5-2Hz), and spindle waves (12-16Hz) (Figure 2a). Their time-frequency charts (see Figure S1, using a Molet wavelet transform with a cycle of 3 and scaling factor of 0.8) and ripple frequency spectra (Walch's method) (Figure 2b) can be derived from the eeglab toolbox. Existing experiments demonstrate that during the slow-wave sleep (SWS) process, most ripples and slow oscillations coincide with spindle waves [9, 39]. To investigate the coupling mechanisms among spindle waves, ripples and slow oscillations, we contrasted the characteristics of spindle waves both isolated (8Hz-12Hz, 12Hz-16Hz) and in conjunction with ripples (100Hz-250Hz), measuring the amplitude and duration of those occurring concurrently with the ripples (within ± 0.1 s of the ripple's peak) and those not. Our simulation findings align with experimental results presented in Figure 10 (f) of [10]. Slow and fast spindle waves, in conjunction with ripples, exhibit greater duration and amplitude than those occurring in isolation. Specifically, fast (or slow) spindle waves synchronized with ripples demonstrate a higher amplitude and longer duration than isolated ones. Differently, 72.59% of fast spindle waves are coupled with ripples, while 83.47% of slow spindle waves are coupled with ripples (Figure 2d,e).

Additionally, during the SWS process, slow oscillations, spindle waves, and ripples tend to co-occur, fostering memory consolidation. To further investigate the interactions among these factors in enhancing memory consolidation, we will calculate the percentage of pairwise co-occurrences, using the same detection method as before. Our numerical findings align with existing experimental results [9] (Figure 2c, Figure S1).

2.6. Indexes measuring memory consolidation

2.6.1. Phase Locked Value (PLV)

The signal should first be filtered and the phase is obtained by Hilbert transform. The closer the PLV is to 1, the closer the two signals are to synchronization, which is calculated by:

$$PLV = \frac{1}{N} \left| \sum_{n=1}^N \exp(j\theta(t, n)) \right| \quad (16)$$

where N represents the number of trials, i.e. trials $n[1 \dots N]$, $\theta(t, n)$ represents the instantaneous phase difference of the same trial for different leads, $\exp(j\theta(t, n))$ represents the using of Euler's formula to obtain complex phase, $\sum_{n=1}^N$ overlays the complex signals of all trials, $\frac{1}{N} |\cdot|$ obtain the amplitude of the superimposed complex signal and calculate the average.

2.6.2. Duration of slow wave sleep ripple

Ripples, typically occurring within the valleys of spindle waves, signify the active phase of these oscillations. Prior research indicates that optogenetic stimulation can extend the duration of spontaneous hippocampal ripples, thereby enhancing memory consolidation. Consequently, the total duration of ripples is a key metric for assessing the impact of stimulation protocols on memory consolidation during spatial learning tasks.

2.6.3. Amplitude, duration and number of spindles in slow wave sleep

Sleep spindles, characteristic of stage 2 NREM sleep, are linked to enhanced memory consolidation through their amplitude and duration[40, 41, 42, 43], which reflect multiregional brain interactions. Evidence supports the positive correlation between spindle characteristics and memory improvement. Here, we focus on the total count, cumulative duration, and average amplitude of spindles to explore their role in memory consolidation.

2.6.4. Number of slow wave sleep So

Transcranial electrical stimulation (tDCS) experiments[44] have shown that enhancing slow oscillation activity during sleep bolsters memory consolidation. Accordingly, we will assess the total slow oscillation (So) activity generated during sleep for its impact on memory.

2.6.5. Percentage of co-occurring oscillations

Memory consolidation at night is closely tied to the synchronized presence of spindle waves, slow oscillations (So)[45], and hippocampal ripples. Direct evidence indicates that their combined occurrence extends both their duration and amplitude, which is more effective than when they occur alone. Increasing the co-occurrence of these oscillations is key to improving memory consolidation.

2.7. Stimulation settings

Stimulation protocols will be introduced into the cortical subnetwork of HTC circuit to regulate cortical activity during sleep, and to assess its impact

on sleep electrophysiology and the consolidation of memory throughout the night.

2.7.1. *Experiment Protocol*

The experiment [19] used a real-time closed-loop method to monitor and analyze slow-wave activity in the hippocampus, with a five-minute pause block, and a short (50 ms) high-frequency (100 Hz) electrical stimulation event was triggered at neocortical stimulation sites approximately once every 4s with a 5-min stimulation block of 1 ms per pulse width (Figure 3). For stimulation open-loop control, the method was added directly to the cerebral cortex, unlike high-frequency stimuli with a fixed interval of 4s and 50ms (Figure 3). For model calculations, besides to setting the total duration to 1200s, we basically carry out the stimulation according to the experimental protocol.

2.7.2. *Inhibitory stimulus*

Hippocampal ripples, recognized for their pivotal role in memory consolidation and their profound impact on neocortical activity during sleep, are central to our investigation into real-time closed-loop stimulation [46, 47]. Our stimulation form was consistent with the experiment, with a distinct addition: brief stimulation bursts of 10 milliseconds are delivered at 10-millisecond intervals within 100-millisecond blocks, interspersed with 100-millisecond pause blocks to allow for no stimulation during these intervals (Figure 3). A preliminary 1-second ignition phase ensures system stability by dampening the effects of initial perturbations. The detection window is set at 200 milliseconds, reflecting the transient nature of ripple events, which do not exceed 200 milliseconds in duration. Upon ripple detection, a 6-second stimulation cycle on the cortex is initiated, proceeding without additional testing in a continuous sequence. Consistently, the closed-loop system modulates the intervals between stimuli based on the ripple events detected. Among them, the pause block was also detected, but the stimulus intensity was 0 (Figure 3).

It comprises a sequence of equidistant rectangular pulses, with each pulse lasting for $stitime$ and the interval between pulses being determined by the signal's frequency:

$$s[n] = \text{strength} \cdot 1_{\left[\left\lfloor \frac{n}{10h} \right\rfloor \cdot \frac{1}{\text{freq}}, \left\lfloor \frac{n}{10h} \right\rfloor \cdot \frac{1}{\text{freq}} + \frac{stitime}{h} \right)}(n) \quad (17)$$

where, freq is the frequency of the pulse (Unit:Hz) and strength is the amplitude of the pulse, h is the sampling interval (Unit:s) stitime is the duration of a single pulse (Unit:s), duration is the duration of the entire signal (Unit:s). $s[n]$ is the signal value at the n^{th} sampling point, n is the index of the sampling point, $n = 1:\text{floor}(1000/\text{freq}):N$, where $N = \text{duration}/h$ is the total number of sampling points. $1[a, b)$ is an indicator function, when $a \leq x < b$, $1[a, b)(x) = 1$, else $1[a, b)(x) = 0$. $\lfloor x \rfloor$ indicates the rounding down of x .

2.7.3. Transcranial magneto-acoustical stimulation (TMAS)

All the aforementioned stimulation methods are intracranial, therefore, we here introduce the non-intracranial magneto-acoustical stimulation (Figure 3) to search for the comparable effects of experimental intracranial closed-loop stimulation with the aim of providing the promising clinical stimulation therapy[32].

The principle of TMAS is that the action of a focused ultrasonic wave moves charged ions in the nerve tissue. Because a magnetostatic field is perpendicular to the movement direction of the charged ions, the Lorentz force on the ions can be induced in the tissue. The Lorentz force separates the positive and negative ions in opposite directions, thereby forming the electric current I_{ext} to stimulate neurons. The TMAS current can be finally expressed as follows (see the detailed derivation from the supplementary materials):

$$J_y \approx \sigma B_x \sqrt{\frac{2\Gamma}{\rho c_0}} \sin(2\pi f t + bias) \quad (18)$$

We added a bias on this basis, where in order to generate an action potential, the ultrasonic wave needs to be a sine wave with bias. Thus, during the magnetoacoustic stimulation, we can intermittently switch the magnetic field stimulation, so that the pulse ultrasound can simulate the pulse current in DBS, which can be modeled as:

$$x(t) = \begin{cases} 1 & (n-1)\frac{1}{RF} < t \leq [(n-1) + DC]\frac{1}{RF}, n = 1, 2, 3 \dots \\ 0 & \text{Others} \end{cases} \quad (19)$$

where RF is the repetition frequency and DC is the duty cycle. So the experimental stimulation process can be submitted by the TMAS stimulation,

i.e.:

$$S_{TMAS} = J_y \times x(t) \quad (20)$$

3. RESULTS

3.1. *Reproduction of the Experimental DBS*

3.1.1. *Dynamic explanation of memory consolidation enhancement*

Memory consolidation is intricately connected to the dynamics of the brain. To gain deeper insights into the kinetic mechanisms that drive changes in memory consolidation, we meticulously calculated the mean firing rate (MFR) of neurons nuclei within the HTC network. By adjusting the strength of the connections between the hippocampus and cortex, we unveiled the pivotal role of excitatory interactions from the cortex to the hippocampus in regulating neuronal firing rates and the dynamics of memory consolidation.

Under conditions that enhance excitatory connectivity from the cortex to the hippocampus, there were significant alterations in nuclear firing rates, particularly a marked increase in the MFR of excitatory neurons in the CA1 region(Figure 4a). This discovery highlights the system’s acute sensitivity to these connections. In contrast, modifications to the strength of other connections had a negligible impact on the firing rates of the network (see Figure S2). Naturally, since the changes pertain to the strength of connections between the hippocampus and neocortex, they do not substantially affect the firing rates of neurons in the thalamic nuclei (see Figure 5). We found that nuclear firing rates with significant changes had a positive effect on the promotion of memory consolidation (Figure 4b). Employing an experimental stimulation method with an intensity of 3200mV, the outcomes qualitatively align with experimental results (Reference [19], Figure 1f). That is, closed-loop stimulation promotes synchronization between the hippocampus and cortex, increasing spindle waves events and slow oscillations events while concurrently reducing hippocampal ripples.Stimuli that lack precise temporal control do not significantly affect memory consolidation. A general decline in the synchronization of thalamocortical spindles and hippocampal ripples, coupled with a significant decrease in the number of cortical slow oscillations, may lead to a decline in the function of memory consolidation. However, the synchronization of cortical slow oscillations with hippocampal ripples and an overall increase in the number of spindles may counteract the adverse effects of the aforementioned indicators’ decline, ultimately yielding

results consistent with experimental qualitative analysis (Figure 4c). However, parameters that have little effect on nuclear firing rates do not promote memory consolidation (see Figure S3).

To further demonstrate that altering the strength of cortical-hippocampal excitatory connections can change the entire system’s modality, we calculated the variation in nuclear neuron firing rates as a function of stimulation intensity. Under experimental settings with fixed connection strength, the analysis of nuclear firing rates in response to varying stimulus intensities showed no significant changes, further underscoring the importance of the strength of cortical-hippocampal excitatory connections in memory consolidation (see Figure 6).

3.1.2. Stimulation results in the case of the experimental

According to the experimental parameter settings (stimulation current range of 0.5mA to 1.5mA, resistance range of 1-4 k Ω), we set a voltage range of 2500mV to 3500mV in the model to match the stimulation current size in the experiment as much as possible. Each stimulus intensity and no stimulus state were calculated at the same initial value, and we counted the results of 12 different random initial values to ensure the reliability and scientificity of the results. Given the importance of the temporal coupling between cortical slow oscillations and cortical thalamic spindles, as well as hippocampal ripples, in memory consolidation, we specifically explored slow oscillations (0.5Hz-2Hz) in the cortex rather than slow waves (0.16Hz-1.25Hz) in the model. In addition, we replace the phase locking ratio of neurons with the phase locking value between waveforms. Our numerical simulation results can be qualitatively compared with the "Results" section in reference [19]. Real-time closed-loop stimulation can improve the synchronization between cortical thalamic spindles and hippocampal ripples within a certain stimulation intensity (Wilcox-test) (Figure 7b(i)); It also improved the synchronization between cortical slow oscillations and hippocampal ripples (Wilcox-test) (Figure 7b(ii)). The observed increase in the number of spindle waves is consistent with experimental data, and the number of spindle waves significantly increases at specific stimulus intensities($p = 0.0266$, $p = 0.0132$, $p = 0.0515$, $p = 0.0627$, representing stimulation intensities of 2500 mV, 2700 mV, 2800 mV, 3300 mV, respectively, Wilcox-test)(Figure 7b(iii)) ; The slow oscillation of the cortex also generally increased (Figure 7b(iv)); And the number of hippocampal ripple events decreased significantly under specific stimulus intensities, especially under high-intensity stimuli($p = 0.00728$, $p = 0.0117$,

$p = 0.00699$, $p = 0.103$, $p = 0.0272$, $p = 0.00295$, representing stimulation intensities of 2600 mV, 3000 mV, 3200 mV, 3300 mV, 3400 mV, 3500mV, wilcox-test, respectively) (Figure 7b(v)). The results and changes of the above closed-loop events are significantly consistent with the experimental results, thus verifying the effectiveness of the model in reflecting the complex dynamics of memory consolidation processes.

For stimuli that were not precisely timing-locked (Figure 7a), qualitative results were also obtained with the model. This form of stimulation enhanced the synchronization between hippocampal ripples and cortical slow oscillations (Figure 7a(ii)). Notably, this effect was pronounced at specific stimulus intensities(p values of 0.00466, 0.0281, 0.0148, and 0.00295 corresponding to 2700 mV, 2800 mV, 3200 mV, and 3500 mV, respectively Wilcox-test), as well as the number of spindle events (Figure 7a(iii)). However, there was a general decline in the synchronization between hippocampal ripples and thalamocortical spindles (Figure 7a(i)). Particularly concerning the cortical slow oscillations, a significant reduction was observed across all stimulus intensities, indicating a detrimental effect on memory consolidation (Figure 7a(iv)) (mean p value of 0.00276 Wilcox-test). The number of individual ripple events also decreased, consistent with the experimental results, suggesting that this form of stimulation leads to a general reduction in hippocampal ripples (Figure 7a(v)). These results reflect the nuanced impact of open-loop stimulation on memory consolidation. The observed decrease in synchronization between hippocampal ripples and thalamocortical spindles, along with a significant reduction in the number of cortical slow oscillations, directly contributes to the weakening of memory consolidation function. However, the increased synchronization between hippocampal ripples and cortical slow oscillations, coupled with a significant rise in spindle events, may counteract these effects, resulting in no significant overall change in the outcome of stimulation.

3.1.3. *Experimental two-parameter prediction*

For the experiment, the stimulus intensity was varied from 0.5mA to 1.5mA, while the frequency was consistently set at 100Hz, a parameter likely determined through meticulous tuning as referenced in study [19]. Our computational simulations qualitatively reproduced the experimental outcomes, indicating that an optimal stimulation intensity at the fixed 100Hz frequency was not discernible. To numerically validate the experimental frequency and explore potential superior frequencies, the stimulation frequency was sys-

tematically altered to 40Hz, 100Hz, 200Hz, 300Hz, 400Hz, and 500Hz, with constant voltage and consistent methodology. The total simulation time is 1200s. Given the challenge of using the diminishing count of ripple events as an indicator of memory consolidation, we focused on four alternative metrics. A heatmap in Figure 8, except for the number of So, which did not show significant improvement, all other indicators showed clear advantages, so we can consider that the 100Hz frequency is indeed more favorable. This finding from our numerical simulations corroborates the rationality of the frequency selection in the original experiments.

3.2. Improvement for the Experimental DBS

3.2.1. Inhibitive stimulation

During sleep, extensive interactions occur between the hippocampus and the neocortex, and active intracranial interventions can promote memory consolidation to a certain extent. In this study, we designed a real-time closed-loop inhibitory electrical stimulation scheme, incorporating seven indicators related to memory consolidation to assess the efficacy of the stimulation protocol. The stimulation was set to low voltage (50 mV to 250 mV) and high frequency (500 Hz) inhibitory stimulation, which is well below the safe maximum values for both long-term and short-term stimulation [48], with a total simulation duration of 600 seconds. To facilitate the observation of changes in indicator values, we made some proportional adjustments.

Our results indicate that regardless of the magnitude of inhibitory stimulation added, the PLV values of spindle waves and ripples are increased. The PLV values between So and spindle waves, as well as between So and ripples, are universally enhanced. However, other indicators, not limited to the number of events, including percentages, the amplitude of events (spindle), and the duration of events (spindle and ripple), generally decrease under intermediate stimulation intensities, with some showing significant declines (Figure 9b, Figure S4). To further select the optimal stimulation intensity, each stimulation intensity was compared with the results under no stimulation conditions. For closed-loop stimulation, two stimulation intensities (90 mV, 70 mV) were identified, where all indicators showed universal improvement, with most showing significant enhancement. At a stimulation intensity of 90 mV, the synchronization values among the three, the number of spindle events, the number of ripple events, the average amplitude of spindle events, the total duration of ripple events, and the percentage of all co-occurrences were all significantly increased ($p < 0.001$, mean: $p = 0.00013$, Wilcoxon-test),

with no significant difference in other indicators. At 70 mV, similar improvements were observed, with significant increases in PLV values, the number of So and ripple events, the average amplitude of spindle events, and the percentage of co-occurrence between So and ripples ($p < 0.001$, mean: $p = 0.00002$, Wilcoxon-test), again with no significant difference in other indicators (Figure 9d).

In open-loop stimulation, there is no need to detect hippocampal ripples; instead, the same stimulation is directly applied to the cerebral cortex (Figure 3). Similar to closed-loop stimulation, the PLV values of spindle waves and ripples are increased, and the PLV values between So and spindle waves, as well as between So and ripples, are generally improved. However, other values, including the number of events, percentages, event amplitude (spindle waves), and duration (spindle waves and ripples), are usually reduced under moderate stimulation intensities, with some even showing significant decreases (Figure 9a). Similarly, three optimal stimulation intensities were selected for comparison (130 mV, 110 mV, and 90 mV). Compared to the no-stimulation condition, there was a general improvement in indicator values. At stimulation intensities of 130 mV and 110 mV, the PLV values, the number of spindle events, the number of So and ripple events, the average amplitude and total duration of spindle events, and the percentage of all co-occurrences were significantly increased ($p < 0.001$, mean: $p = 0.0004$ for 130 mV, and $p = 0.0007$ for 110 mV, Wilcoxon-test). At a stimulation intensity of 90 mV, similar improvements were noted, with significant increases in PLV values, the number of So and ripple events, the average amplitude and total duration of spindle events, and the percentage of co-occurrence between So and ripples ($p < 0.001$, mean: $p = 0.0009$, Wilcoxon-test)(Figure 9c).

To evaluate the comparative efficacy of open-loop and closed-loop stimulation on memory consolidation, we calculated the percentage increase in various indicators compared to the no-stimulation condition at three open-loop and two closed-loop stimulation intensities (Figure 9e, Left). The analysis revealed that the optimal intensity for open-loop stimulation was 110 mV, while the most effective intensity for closed-loop stimulation was 90 mV. A direct comparison between the most effective open-loop (110 mV) and closed-loop (90 mV) stimulation intensities indicated that closed-loop stimulation achieved superior results (Figure 9e, Right). This suggests that closed-loop stimulation is more effective in enhancing memory consolidation even at lower stimulation intensities, highlighting its advantages and aligning with the experimental conditions.

Furthermore, a numerical comparison with experimental data showed that the maximum increase in the phase-locking value (PLV) between So and ripples in experiment [19] was 14.19%, and the maximum increase in the PLV between spindle waves and ripples was 19.54%. The maximum increase in the number of spindle events was 11.14%, and the maximum increase in the number of SO events was 6.04%. Clearly, our inhibitory stimulation protocol achieved a greater enhancement compared to the experimental results (Figure 9e).

3.2.2. Two-parameter prediction of inhibitory stimulation

To delve deeper into the impact of stimulus frequency on memory consolidation, we selected a range of stimulus frequencies (100Hz, 200Hz, 250Hz, 400Hz, and 500Hz), based on the outcomes of inhibitory stimuli, selected low stimulation intensities (below 150 mV) for both open-loop and closed-loop experiments. Aligning with experimental benchmarks, we analyzed changes in the number of events and the synchronization between the cortex and hippocampus. The total simulation time is 600s. Simulation results revealed that, regardless of the stimulation intensity or frequency, stimulation at 90mV to 150 mV consistently outperformed the no-stimulation condition (Figure 10a). Furthermore, the overall performance of closed-loop stimulation was superior to that of open-loop stimulation. Additional analyses of the impact of stimulation frequency at average stimulation intensities indicated that, except for the minimal number of So events at the high frequency of 500Hz, other indicators generally increased with increasing stimulation frequency (Figure 10b). These findings reaffirm the rationality of our chosen stimulation frequencies.

3.3. Comparable effect of non-invasive Transcranial Stimulation

In this study, we investigated the feasibility of enhancing memory consolidation using a composite magnetic and ultrasonic stimulation. Given that the induced current is a product of the magnetic field and ultrasonic waves, the primary resistance in our model is attributed to the cerebral cortex. Previous studies have shown that the resistance of the cerebral cortex is approximately between several thousand to tens of thousands of ohms, therefore, to better align with the resistance provided by the cortex, the resistance was set to a high value (15 k Ω) in our simulations. Through iterative testing, we identified a set of optimal parameters (see Table S2). With these parameters held constant, adjusting the bias range from 1 to 4 yielded favorable outcomes

for memory consolidation (Figure 11a), particularly in the number of ripple events, which corresponded with the results from experimental closed-loop intracranial stimulation (Figure 11a(ii)). To further assess the effectiveness of magneto-ultrasonic stimulation in enhancing memory consolidation, we compared it with the results from closed-loop intracranial experiments, with a simulation duration set to 20 minutes.

Numerical simulation results demonstrate that both stimulation methods are equally effective in promoting memory consolidation. To ensure a fair comparison, we performed a differential analysis of five indicators under various initial conditions in the absence of stimulation, revealing that the experimental outcomes are largely independent of initial values (Wilcox-test) (Figure 11b). Subsequently, we compared the outcomes of the two stimulation methods and conducted a significant difference analysis. In magneto-ultrasonic stimulation, only the bias was varied (1-4). For closed-loop intracranial stimulation, parameters remained consistent, with adjustments made to the voltage range (2500mV-3500mV). The synchronization gain between thalamocortical spindles and hippocampal ripples, along with the increase in the number of cortical slow oscillation events, did not exhibit significant differences ($p=0.7646484$ for spindle-ripple PLV, $p=0.0673828$ for the number of So events, Wilcox-test) (Figure 11c(iii,iv)). Furthermore, the reduction in the number of ripple events was found to be largely consistent between magneto-ultrasonic stimulation and closed-loop intracranial electrical stimulation ($p=0.2783203$, Wilcox-test) (Figure 11c(ii)). However, the increase in the number of spindle events was significantly lower with magneto-ultrasonic stimulation compared to closed-loop intracranial stimulation ($p=0.0097284$, Wilcox-test) (Figure 11c(i)). In contrast, the enhancement of synchronization values between cortical slow oscillations and hippocampal ripples was markedly higher with magneto-ultrasonic stimulation than with closed-loop intracranial electrical stimulation ($p=0.0048828$, Wilcox-test) (Figure 11c(v)). Although this improvement may offset the deficiency in the number of spindle events, the actual effects necessitate further experimental confirmation. We do not assert that the selected parameters are the best possible, but we propose that TMAS, under conditions of comparable efficacy, has the potential to serve as a potent non-invasive method for disrupting brain rhythms, with implications for both diagnostic and therapeutic applications. The substitution of magneto-ultrasonic stimulation for closed-loop intracranial stimulation could be advantageous for patient care and cost considerations.

4. Conclusion and Discussion

Existing research indicates that physiological experiments including closed-loop auditory, electrical, magnetic, and transcranial electrical stimulation can enhance memory [13, 19, 35, 49]. Yet, research into the dynamics of external stimuli in regulating memory consolidation within the HTC network during sleep is relatively scarce [34, 36]. This study employed the HTC network model to explore the generation and coupling mechanisms of slow-wave sleep rhythms [50, 51, 52, 53]. The existence of a two-way communication between the PFC (anterior cingulate cortex) and hippocampus has been reported previously [54]. Hence similar to a recent modeling study [55] in the full model consisting of CA3-CA1 networks and the thalamocortical networks, the cortical networks are recurrently connected to CA3-CA1 network so that all the anatomical connections from the thalamocortical network to the hippocampus are modeled by one projection from the cortex to the hippocampus. Our computational approach unveiled the intrinsic regulatory mechanisms of memory consolidation under external stimuli and introduced a novel inhibitory intracranial stimulation protocol to bolster memory consolidation. We identified seven markers linked to memory consolidation based on experimental findings, and quantified how various stimulus intensities and frequencies impact memory consolidation using a model of the HTC network, allowing for concurrent observation of multiple marker changes.

Earlier studies have demonstrated an association between increased spindle wave frequency during NREM in older subjects and memory impairment [43], as well as an inverse correlation between spindle wave frequency and cognitive ability in children [46, 47, 48]. Consequently, spindle wave frequency should be incorporated into subsequent research. Similarly, we will consider an increasing array of indicators for memory consolidation in the future to enhance the precision of our stimulation protocols. We have successfully replicated the effects of prior experimental techniques using this model. Hence, going forward, we will employ this model to replicate existing experiments, devise diverse and reliable electrical stimulation protocols. Furthermore, we will apply varying or identical stimuli to distinct brain regions simultaneously, continually adapting stimulation protocols to predict experimental outcomes. We can also observe the impact of external stimuli on the network manifold structure, among other effects.

Several features of our experimental design enhance its rationality. These include: (i) incorporating electrical stimulation to the cortex, based on the

detection of hippocampal ripples, to influence the hippocampal-neocortical pathway; (ii) synchronizing electrical stimulation with the hippocampal ripples to synchronize more ripples; (iii) given that nerve damage appears closely related to excessive fiber activity, we developed an intermittent stimulation strategy. Additionally, considering the comfort and safety of electrical stimulation, this strategy features low stimulation intensity, high-frequency inhibition, and brief stimulation duration; (iv) our setup allows for continuous changes in stimulation amplitude and frequency to explore more effective, comfortable, and safe stimulation protocols; However, we do not assert that the specific timing and stimulation parameters in this paper are definitively optimal. Future research should investigate whether simultaneous refinement of stimulation timing and other parameters can further enhance memory consolidation.

In summary, our research transcends traditional models, employing a comprehensive hippocampal-cortical-thalamic model to explore how external stimuli influence the dynamics of slow oscillations, spindle waves, and ripples—key to memory consolidation. On the basis of accurately reproducing existing experimental results using this model, we ensured the scientific and accurate nature of the model, induct the concept of using inhibitory intracranial stimulation during sleep to enhance memory, challenge the norm of excitatory stimulation. showing that carefully designed inhibitory stimuli can also bolster memory. And the effect is better. In addition, we also explored an extracranial stimulation method using transcranial magnetic ultrasound stimulation to promote memory consolidation, and conducted in-depth research on the effects of connections between different neurons on memory consolidation. Our results enrich the knowledge basis of memory consolidation and may provide new paths and ideas for solving memory disorders or experimental findings [56, 57].

References

- [1] Helfrich, R.F., Mander, B.A., Jagust, W.J., et al.: Old Brains Come Uncoupled in Sleep: Slow Wave-Spindle Synchrony, Brain Atrophy, and Forgetting. *Neuron*. **97**, 221-230.e4 (2018)
- [2] Latchoumane, C.F.V., Ngo, H.V.V., Born, J., et al.: Thalamic Spindles Promote Memory Formation during Sleep through Triple Phase-Locking of Cortical, Thalamic, and Hippocampal Rhythms. *Neuron*. **95**, 424-435.e6 (2017)

- [3] Maingret, N., Girardeau, G., Todorova, R., et al.: Hippocampo-cortical coupling mediates memory consolidation during sleep. *Nat Neurosci.* **19**, 959–964 (2016)
- [4] Niknazar, M., Krishnan, G.P., Bazhenov, M., et al.: Coupling of Thalamocortical Sleep Oscillations Are Important for Memory Consolidation in Humans. *PLOS ONE.* **10**, e0144720 (2015)
- [5] Maquet, P.: The Role of Sleep in Learning and Memory. *Science.* **294**, 1048–1052 (2001)
- [6] Hruska, M., Cain, R.E., Dalva, M.B.: Nanoscale rules governing the organization of glutamate receptors in spine synapses are subunit specific. *Nat Commun.* **13**, 920 (2022)
- [7] Sekeres, M.J., Winocur, G., Moscovitch, M.: The hippocampus and related neocortical structures in memory transformation. *Neuroscience Letters.* **680**, 39–53 (2018)
- [8] Vaz, A.P., Inati, S.K., Brunel, N., et al.: Coupled ripple oscillations between the medial temporal lobe and neocortex retrieve human memory. *Science.* **363**, 975–978 (2019)
- [9] Azimi, A., Alizadeh, Z., Ghorbani, M.: The essential role of hippocampo-cortical connections in temporal coordination of spindles and ripples. *NeuroImage.* **243**, 118485 (2021)
- [10] Alizadeh, Z., Azimi, A., Ghorbani, M.: Enhancement of Hippocampal-Thalamocortical Temporal Coordination during Slow-Frequency Long-Duration Anterior Thalamic Spindles. *J. Neurosci.* **42**, 7222–7243 (2022)
- [11] Klinzing, J.G., Mölle, M., Weber, F., et al.: Spindle activity phase-locked to sleep slow oscillations. *NeuroImage.* **134**, 607–616 (2016)
- [12] Binder, S., Mölle, M., Lippert, M., et al.: Monosynaptic Hippocampal-Prefrontal Projections Contribute to Spatial Memory Consolidation in Mice. *J. Neurosci.* **39**, 6978–6991 (2019)
- [13] Yu, Y., Wang, H., Liu, X., et al.: Closed-loop transcranial electrical stimulation for inhibiting epileptic activity propagation: a whole-brain model study. *Nonlinear Dyn.* **112**, 21369–21387 (2024).

- [14] Wang, X., Yu, Y., Han, F., et al.: Dynamical mechanism of parkinsonian beta oscillation in a heterogenous subthalamopallidal network. *Nonlinear Dyn.* **111**, 10505–10527 (2023).
- [15] Hou, S., Fan, D., Wang, Q.: Novel perturbation mechanism underlying the network fragility evolution. *EPL.* **144**, 32002 (2023).
- [16] Yang, H., Han, F., Wang, Q.: A large-scale neuronal network modelling study: Stimulus size modulates gamma oscillations in the primary visual cortex by long-range connections. *European Journal of Neuroscience.* **60**, 4224–4243 (2024).
- [17] Leminen, M.M., Virkkala, J., Saure, E., et al.: Enhanced Memory Consolidation Via Automatic Sound Stimulation During Non-REM Sleep. *Sleep.* **40**, zsx003 (2017).
- [18] Ong, J.L., Lo, J.C., Chee, N.I.Y.N., et al.: Effects of phase-locked acoustic stimulation during a nap on EEG spectra and declarative memory consolidation. *Sleep Medicine.* **20**, 88–97 (2016)
- [19] Geva-Sagiv, M., Mankin, E.A., Eliashiv, D., et al.: Augmenting hippocampal–prefrontal neuronal synchrony during sleep enhances memory consolidation in humans. *Nat Neurosci.* **26**, 1100–1110 (2023)
- [20] Nikolin, S., Martin, D., Loo, C.K., et al.: Effects of TDCS dosage on working memory in healthy participants. *Brain Stimulation.* **11**, 518–527 (2018)
- [21] Coffman, B.A., Clark, V.P., Parasuraman, R.: Battery powered thought: Enhancement of attention, learning, and memory in healthy adults using transcranial direct current stimulation. *NeuroImage.* **85**, 895–908 (2014).
- [22] Zakary, O., Rachik, M., Elmouki, I.: On the analysis of a multi-regions discrete SIR epidemic model: an optimal control approach[J]. *International Journal of Dynamics and Control.* **5**, 917-930 (2017).
- [23] Horikawa, Y.: Bifurcations and chaos in a minimal neural network: Forced coupled neurons[J]. *International Journal of Bifurcation and Chaos.* **31**, 2150147 (2021).

- [24] Mehmood, S., Singh, J P.: A memristor-based magnetized Hopfield neural network for hidden scroll chaotic attractors and control analysis with reduced input[J]. *International Journal of Dynamics and Control*. 1-12(2024).
- [25] Stocco, A., Rice, P., Thomson, R. et al.: An Integrated Computational Framework for the Neurobiology of Memory Based on the ACT-R Declarative Memory System. *Comput Brain Behav* **7** 129–149 (2024).
- [26] Zhao, J., Yu, Y., Han, F., et al.: Regulating epileptiform discharges by heterogeneous interneurons in thalamocortical model. *Chaos: An Interdisciplinary Journal of Nonlinear Science*. **33**, 083128 (2023).
- [27] Fan, D., Wang, Y., Wu, J., et al.: The preview control of a corticothalamic model with disturbance. *era*. **32**, 812–835 (2024).
- [28] Yin, L., Han, F., Yu, Y., et al.: A computational network dynamical modeling for abnormal oscillation and deep brain stimulation control of obsessive–compulsive disorder. *Cogn Neurodyn*. **17**, 1167–1184 (2023).
- [29] Gosak, M., Milojević, M., Duh, M., et al.: Networks behind the morphology and structural design of living systems. *Physics of Life Reviews*. **41**, 1-21 (2022).
- [30] Gosak, M., Markovič, R., Dolenšek, J., et al.: Network science of biological systems at different scales: A review. *Physics of life reviews*. **24**,118-135(2018).
- [31] Hashemi, N.S., Dehnavi, F., Moghimi, S., et al.: Slow spindles are associated with cortical high frequency activity. *NeuroImage*. **189**, 71–84 (2019)
- [32] Yuan, Y., Chen, Y., Li, X.: Theoretical Analysis of Transcranial Magneto-Acoustical Stimulation with Hodgkin-Huxley Neuron Model. *Front. Comput. Neurosci*. **10**(2016).
- [33] Klinzing, J.G., Niethard, N., Born, J.: Mechanisms of systems memory consolidation during sleep. *Nat Neurosci*. **22**, 1598–1610 (2019).
- [34] Helfrich, R.F., Mander, B.A., Jagust, W.J., et al.: Old Brains Come Uncoupled in Sleep: Slow Wave-Spindle Synchrony, Brain Atrophy, and Forgetting. *Neuron*. **97**, 221-230.e4 (2018).

- [35] Ladenbauer, J., Ladenbauer, J., Külzow, N., et al.: Promoting Sleep Oscillations and Their Functional Coupling by Transcranial Stimulation Enhances Memory Consolidation in Mild Cognitive Impairment. *J. Neurosci.* **37**, 7111–7124 (2017).
- [36] Staresina, B.P., Bergmann, T.O., Bonnefond, M., et al.: Hierarchical nesting of slow oscillations, spindles and ripples in the human hippocampus during sleep. *Nat Neurosci.* **18**, 1679–1686 (2015).
- [37] Levenstein, D., Buzsáki, G., Rinzl, J.: NREM sleep in the rodent neocortex and hippocampus reflects excitable dynamics. *Nat Commun.* **10**, 2478 (2019).
- [38] Staresina, B.P., Bergmann, T.O., Bonnefond, M., et al.: Hierarchical nesting of slow oscillations, spindles and ripples in the human hippocampus during sleep. *Nat Neurosci.* **18**, 1679–1686 (2015).
- [39] Adamantidis, A.R., Gutierrez Herrera, C., Gent, T.C.: Oscillating circuitries in the sleeping brain. *Nat Rev Neurosci.* **20**, 746–762 (2019).
- [40] Varela, C., Wilson, M.A.: mPFC spindle cycles organize sparse thalamic activation and recently active CA1 cells during non-REM sleep. *eLife.* **9**, e48881 (2020).
- [41] Diekelmann, S., Born, J.: The memory function of sleep. *Nat Rev Neurosci.* **11**, 114–126 (2010).
- [42] Fernández-Ruiz, A., Oliva, A., Fermino de Oliveira, E., et al.: Long-duration hippocampal sharp wave ripples improve memory. *Science.* 364, 1082–1086 (2019).
- [43] Fogel, S.M., Smith, C.T., Cote, K.A.: Dissociable learning-dependent changes in REM and non-REM sleep in declarative and procedural memory systems. *Behavioural Brain Research.* **180**, 48–61 (2007).
- [44] Ngo, H.-V.V., Martinetz, T., Born, J., et al.: Auditory Closed-Loop Stimulation of the Sleep Slow Oscillation Enhances Memory. *Neuron.* **78**, 545–553 (2013).

- [45] Nikolin, S., Loo, C.K., Bai, S., et al.: Focalised stimulation using high definition transcranial direct current stimulation (HD-tDCS) to investigate declarative verbal learning and memory functioning. *NeuroImage*. **117**, 11–19 (2015).
- [46] Logothetis, N.K., Eschenko, O., Murayama, Y., Augath, M., Steudel, T., Evrard, H.C., Besserve, M., Oeltermann, A.: Hippocampal–cortical interaction during periods of subcortical silence. *Nature*. **491**, 547–553 (2012).
- [47] Vaz, A.P., Inati, S.K., Brunel, N., Zaghloul, K.A.: Coupled ripple oscillations between the medial temporal lobe and neocortex retrieve human memory. *Science*. **363**, 975–978 (2019).
- [48] Gordon, B., Lesser, R.P., Rance, N.E., et al.: Parameters for direct cortical electrical stimulation in the human: histopathologic confirmation. *Electroencephalography and Clinical Neurophysiology*. **75**, 371–377 (1990).
- [49] Guskjolen, A., Cembrowski, M.S.: Engram neurons: Encoding, consolidation, retrieval, and forgetting of memory. *Mol Psychiatry*. **28**, 3207–3219 (2023).
- [50] Ngo, H.-V., Fell, J., Staresina, B.: Sleep spindles mediate hippocampal–neocortical coupling during long-duration ripples. *eLife*. **9**, e57011 (2020).
- [51] Phipps, C.J., Murman, D.L., Warren, D.E.: Stimulating Memory: Reviewing Interventions Using Repetitive Transcranial Magnetic Stimulation to Enhance or Restore Memory Abilities. *Brain Sciences*. **11**, 1283 (2021).
- [52] Traub, R.D., Whittington, M.A., Stanford, I.M., Jefferys, J.G.R.: A mechanism for generation of long-range synchronous fast oscillations in the cortex. *Nature*. **383**, 621–624 (1996).
- [53] Helfrich, R.F., Lendner, J.D., Mander, B.A., et al.: Bidirectional prefrontal–hippocampal dynamics organize information transfer during sleep in humans. *Nat Commun*. **10**, 3572 (2019).

- [54] Rajasethupathy, P., Sankaran, S., Marshel, et al.: Projections from neocortex mediate top-down control of memory retrieval. *Nature*. **526**, 653–659 (2015).
- [55] Sanda, P., Malerba, P., Jiang, X., et al.: Bidirectional interaction of hippocampal ripples and cortical slow waves leads to coordinated spiking activity during NREM sleep. *Cerebral Cortex*. **31**, 324-340(2021).
- [56] Li, Y., Briguglio, J. J., Romani, S., Magee, J. C.: Mechanisms of memory-supporting neuronal dynamics in hippocampal area CA3. *Cell*. **187**, 1-16(2024).
- [57] McHugh S.B., Lopes-Dos-Santos V., Castelli M., Gava G.P., Thompson S.E., Tam S.K.E., Hartwich K., Perry B., Toth R., Denison T., Sharott A., Dupret D.: Offline hippocampal reactivation during dentate spikes supports flexible memory. *Neuron*. **112**, 1-14(2024).

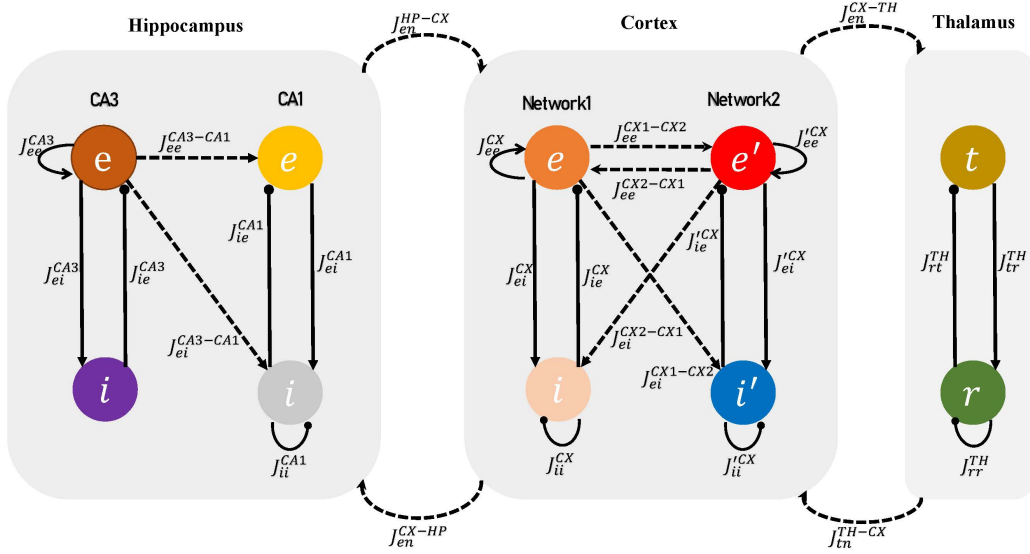


Figure 1: The structure of synaptic connections between neurons of the HTC network. This network model consists of three subnetworks: hippocampus, cortex, and thalamus. In the hippocampal subnetwork and the cortex subnetwork, the excitatory neurons (shown by “e”) and the inhibitory neurons (shown by “i”) in the CA1 and CA3 regions are connected using “J” synaptic strengths. The thalamocortical(TC) and the reticular(RE) neurons shown in the thalamus network are represented by “t” and “r”. Excitatory synaptic connections are indicated by arrows and inhibitory connections are shown as lines ending in a dot. Short-range connections are displayed with solid lines and long-range connections with dotted lines. “n” represents the receptor network.

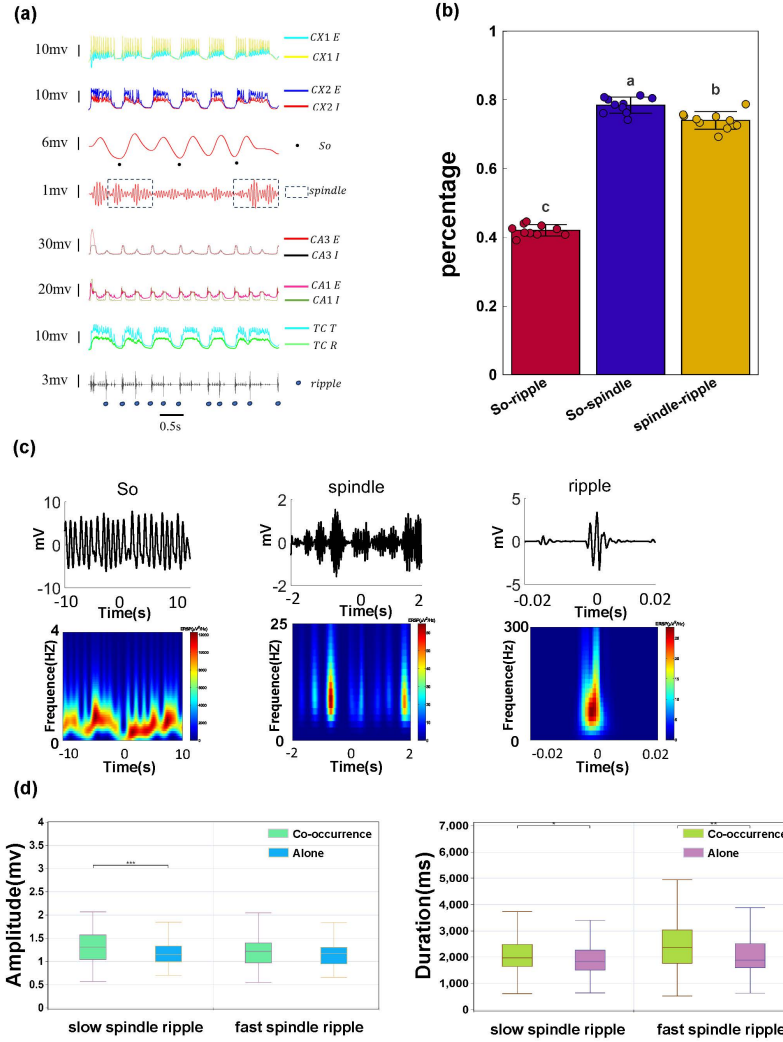


Figure 2: Generation of SOs, spindles, and ripple in the full hippocampo-cortico-thalamic model and their firing characteristics. **(a)** From top bottom respectively: Broadband traces of the membrane potential of the cortical networks 1 and 2, filtered traces of the membrane potential of the cortical network 2 excitatory neuron in the frequency range of So [0.5Hz–2Hz] and spindle [12Hz–16Hz] with detected SO troughs (filled circles) and spindles (dashed box), broadband traces of the membrane potential of CA3, CA1 and TC neurons, filtered [100Hz–250Hz] traces of the membrane potential of CA1 excitatory neurons with detected ripples (grey circles). **(b)** The percentage of the ripples co-occuring with spindles ($p=0.0000108$) and SOs ($p=0.0000108$), and spindles co-occuring with SOs ($p=0.00125$), respectively (Duncan’s Multiple Range Test; wilcox-test). The difference box diagram of the amplitude **(c)** From top to bottom, from left to right: Top, So, spindle events, one ripple event; Bottom, Corresponding spectrograms of the waveforms above. **(d)** and duration **(e)** of slow and fast spindles in conjunction with ripples and isolated spindles, respectively. The model duration was set to 10 minutes. Fast spindle: $p=0.01252$, $p=0.29371$, for duration and amplitude, respectively, Kruskal-Wallis test; mean duration=2.4323s and mean amplitude=1.1864mV, $n=143$ for spindles coupled with ripples; mean duration=2.0462s and mean amplitude=1.1435mV, $n=54$ for isolated spindles. Slow spindle: $p=0.09902$, $p=0.008306$, for duration and amplitude, respectively, Kruskal-Wallis test; mean duration=2.1620s and mean amplitude=1.3100mV, $n=197$ for spindles coupled to ripples; mean duration=1.9092s and mean amplitude=1.1514mV, $n=39$ for isolated spindles.

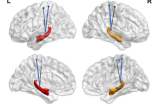
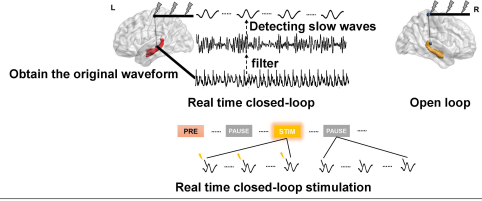
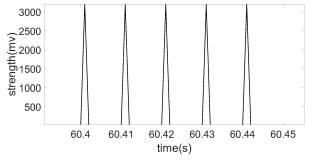
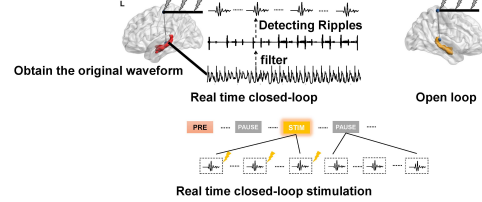
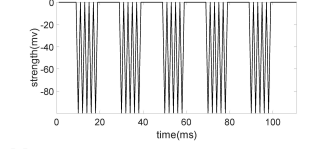
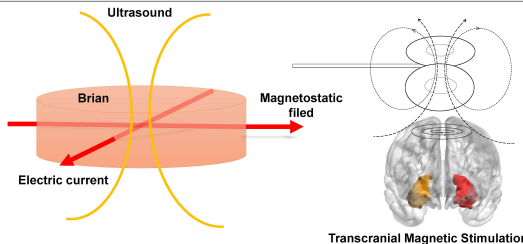
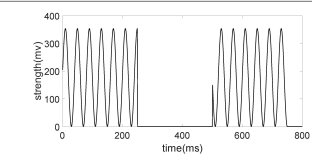
| Stimulation Protocol | Invasive (Yes/No) | Physical Principle | Stimulation Currents and Mathematical Expression |
|--|-------------------|---|---|
| Experimental Closed-loop Phase-locking Deep Brain Stimulation | Yes |  <p>— Sync-stimulation - cortex lobe — mixed-phase stimulation</p> | |
| Computational Closed-loop Phase-locking Excitable Stimulation | Yes |  <p>Real time closed-loop stimulation</p> |  |
| Computational Closed-loop Phase-locking Inhibitive Stimulation | Yes |  <p>Real time closed-loop stimulation</p> |  $s[n] = \text{strength} \cdot 1 \left(\left[\frac{n}{10h} \right] \cdot \frac{1}{\text{freq}} \cdot \left(\left[\frac{n}{10h} \right] \cdot \frac{1}{\text{freq}} + \frac{\text{stime}}{h} \right) \right) (n)$ |
| Magnetic ultrasonic stimulation | No |  <p>Transcranial Magnetic Stimulation</p> |  $x(t) \times (\sin(2\pi ft) + 1)$ $x(t) = \begin{cases} 1(n-1) \frac{1}{RF} & t \leq [(n-1) + DC] \frac{1}{RF} \\ 0 & \text{others} \end{cases}, n = 1, 2, 3, \dots$ |

Figure 3: Three type of invasive stimulus therapies and one type of non-invasive stimulation pattern (magnetic ultrasonic stimulation), and their performing process and physical mechanism, stimulation waveforms as well as mathematical expressions.

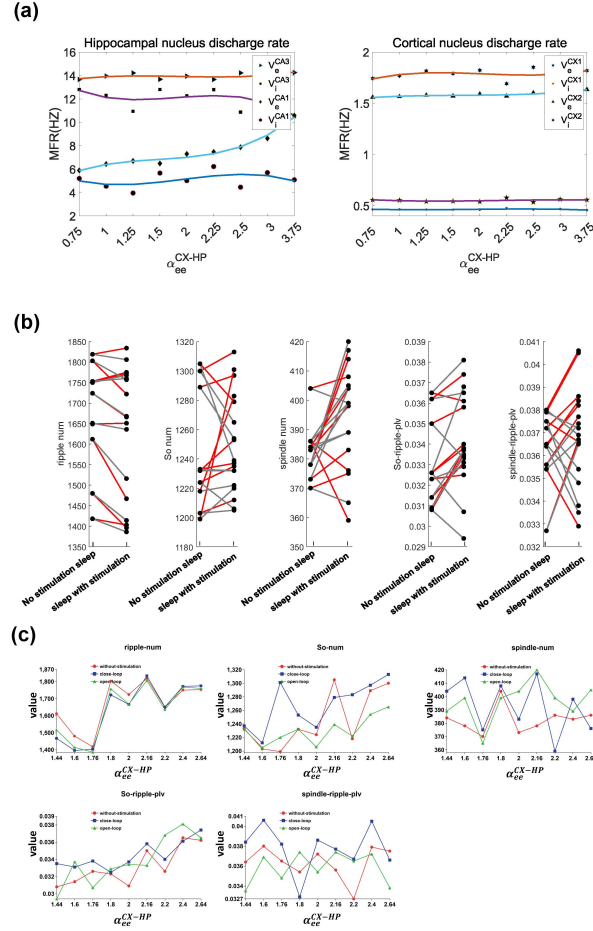


Figure 4: The impact of the strength of cortico-hippocampal excitatory connections on their firing rate and their facilitation effects to memory consolidation. It is shown that this excitatory connection has significant implications for the promotion of memory consolidation. **a** Left, Changes of cortical nucleus neuron firing rate with cortical hippocampal excitatory connection; Right, Changes in the firing rate of hippocampal nucleus neurons with cortical hippocampal excitatory connections (α_{ee}^{CX-HP} showing the factor multiplied to both J_{ee}^{CX-HP} and J'_{ee}^{CX-HP}). **b** The stimulation intensity was fixed (3200mV), and the corticohippocampal excitatory connection intensity parameters (α_{ee}^{CX-HP} showing the factor multiplied to both J_{ee}^{CX-HP} and J'_{ee}^{CX-HP}) were changed with reference to the experimental stimulation scheme, and the changes in five indicators of memory consolidation were observed (the number of ripple, the number of So, the number of spindle, the synchronization value of So and ripple, and the synchronization value of spindle and ripple). The black dots represent different connection strengths, the red lines represent closed loops, and the gray lines represent open loops. **c** Change of cortical-hippocampal excitatory connection strength parameters, specific numerical changes of the five index values, black dots represent different connection strength, red line represents no stimulus, blue line represents closed-loop stimulus, and green line represents open-loop stimulus

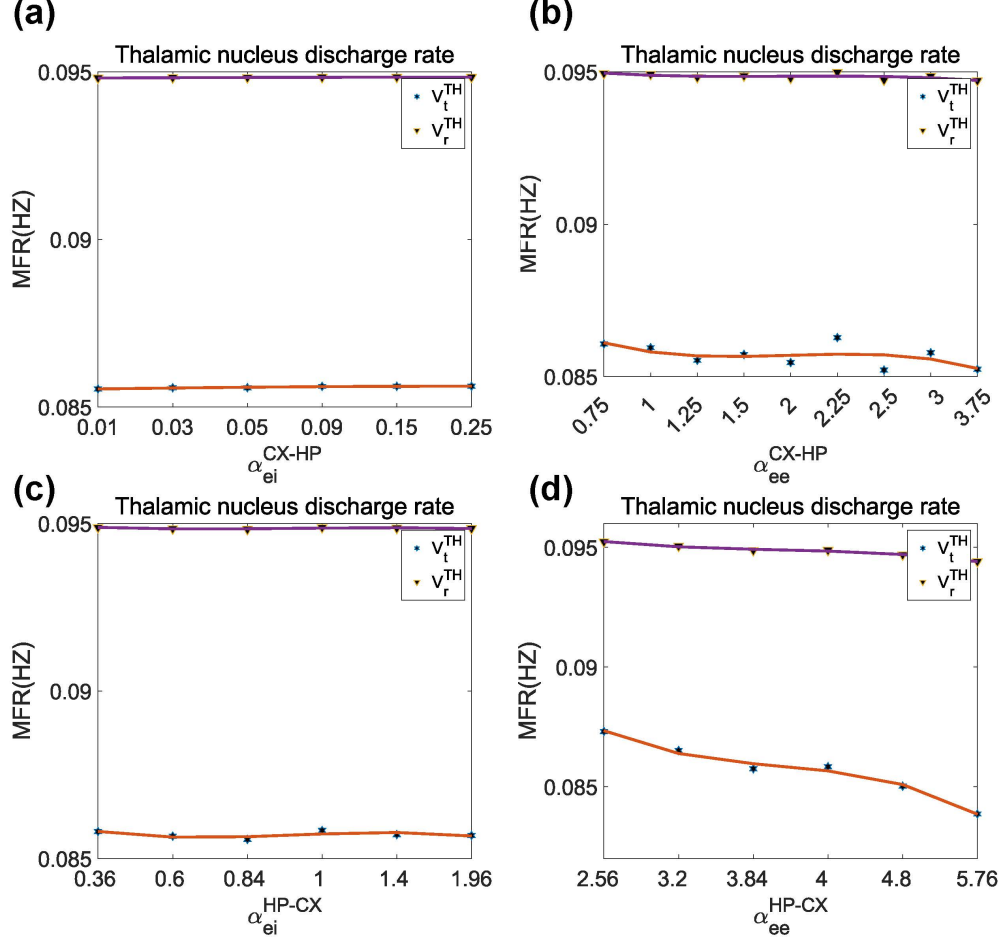


Figure 5: The impact of varying connection strengths on the firing rate of thalamic neurons. Under varying connection strengths among different neurons, there is almost no effect on the firing rate of thalamic neurons. **a** The firing frequency of thalamic nucleus neurons varies with the strength of cortical hippocampal excitatory inhibitory connections (α_{ei}^{CX-HP} showing the factor multiplied to both J_{ei}^{CX-HP} and J'_{ei}^{CX-HP}). **b** The firing frequency of thalamic nucleus neurons varies with the strength of cortical hippocampal excitatory connections (α_{ee}^{CX-HP} showing the factor multiplied to both J_{ee}^{CX-HP} and J'_{ee}^{CX-HP}). **c** The firing frequency of thalamic nucleus neurons varies with the strength of hippocampal cortical excitatory inhibitory connections (α_{ei}^{HP-CX} showing the factor multiplied to both J_{ei}^{HP-CX} and J'_{ei}^{HP-CX}). **d** The firing frequency of thalamic nucleus neurons varies with the strength of hippocampal cortical excitatory connections (α_{ee}^{HP-CX} showing the factor multiplied to both J_{ee}^{HP-CX} and J'_{ee}^{HP-CX}).

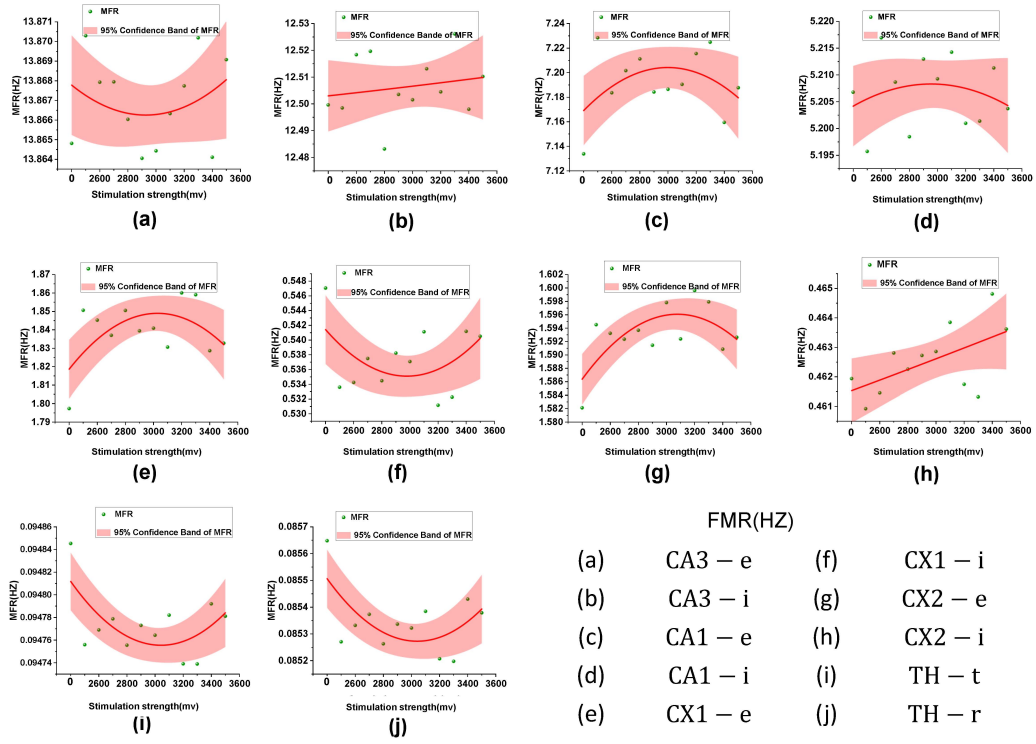


Figure 6: According to the experimental stimulus scheme [19], the effect of changing the stimulus intensity on the firing rate of neurons in HTC network was studied. Under a fixed connection strength, changing the stimulus intensity has little effect on the discharge rate of the nucleus, further explaining the important role of excitatory connections in the cortical-hippocampal neurons in promoting memory consolidation.

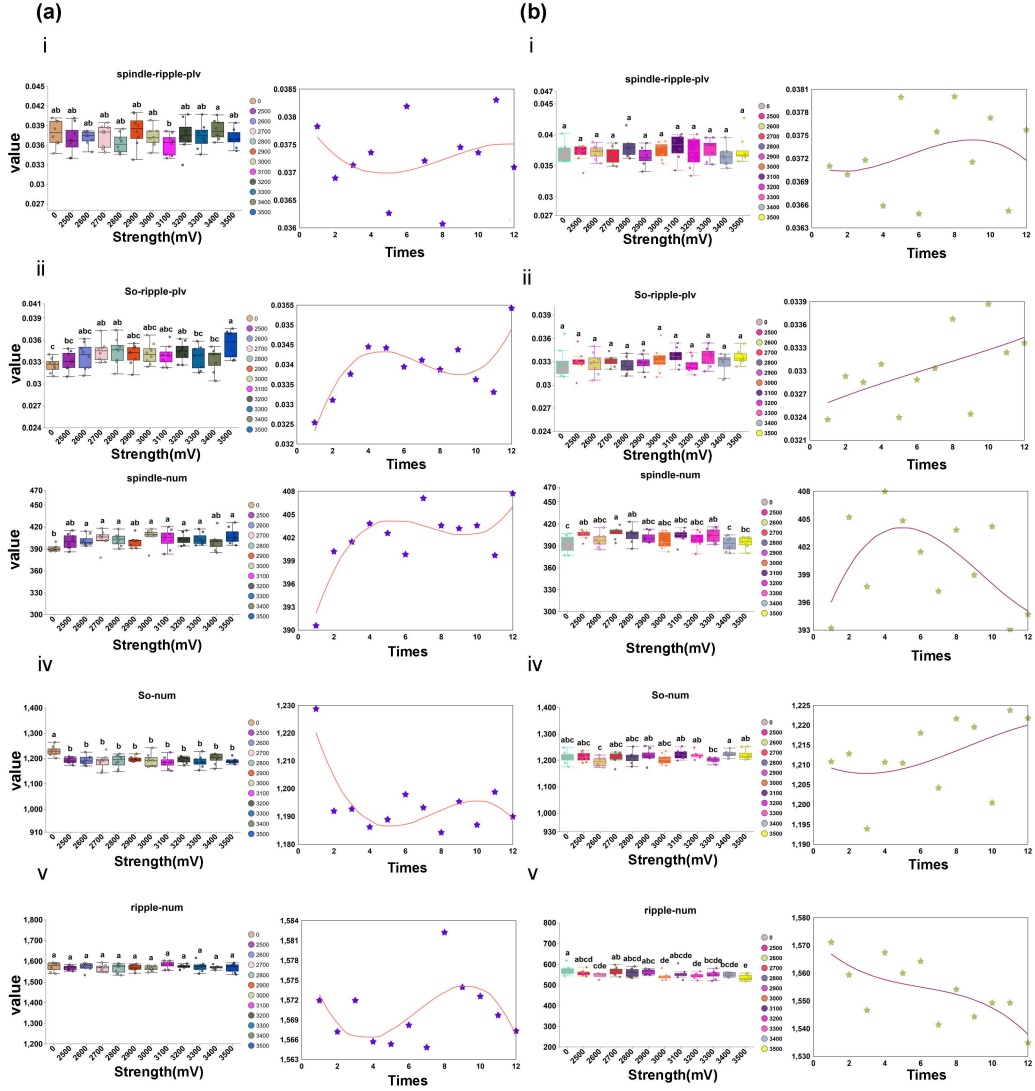


Figure 7: Numerical simulations reproduce the experimental results, namely that under real-time closed-loop stimulation, synchronization increases and the number of ripple events decreases, while the number of other events increases; without precise temporal stimulation, the results are qualitatively consistent with the experimental findings. **a** The difference boxplot (Left) and the corresponding scatter fitting curve (Right) of five indices (i, spindle-ripple-plv; ii, So-ripple-plv; iii, spindle number; iv, So number; V, ripple number) were obtained by open-loop stimulation. **b** The difference boxplot (Left) and the corresponding scatter fitting curve (Right) of five indexes (i, spindle-ripple-plv; ii, So-ripple-plv; iii, spindle number; iv, So number; V, ripple number) by the closed-loop stimulation were studied.

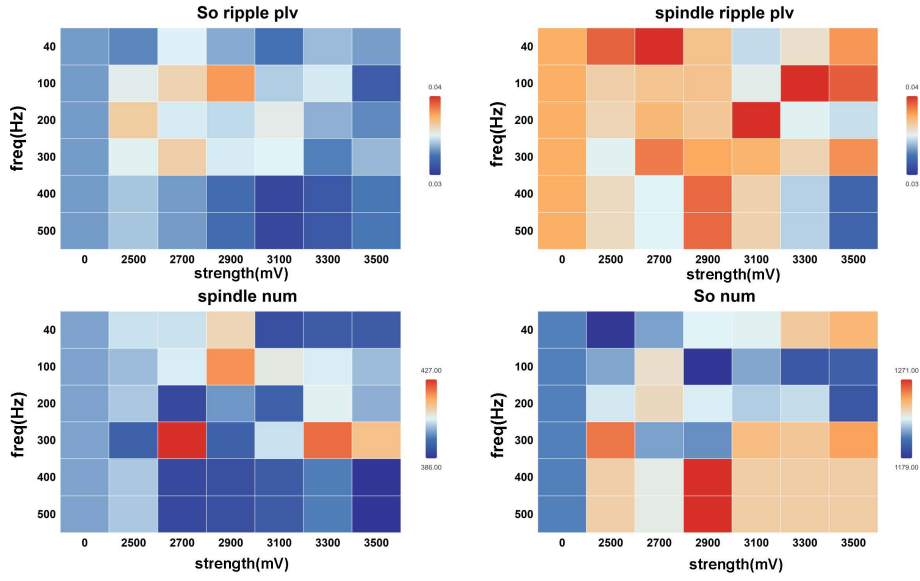


Figure 8: Heatmap of exponential changes under dual-parameter experimental stimulation. This further affirms the rationality of the experimental stimulation frequency (100Hz) chosen in the numerical simulations. From left to right, from top to bottom, the plv values of So and ripple, the plv values of spindle and ripple, the number of spindle and the number of So, and the abscordinate is the stimulus intensity. Each color depth represents the value, the bluer represents the larger value, and the reder represents the smaller value

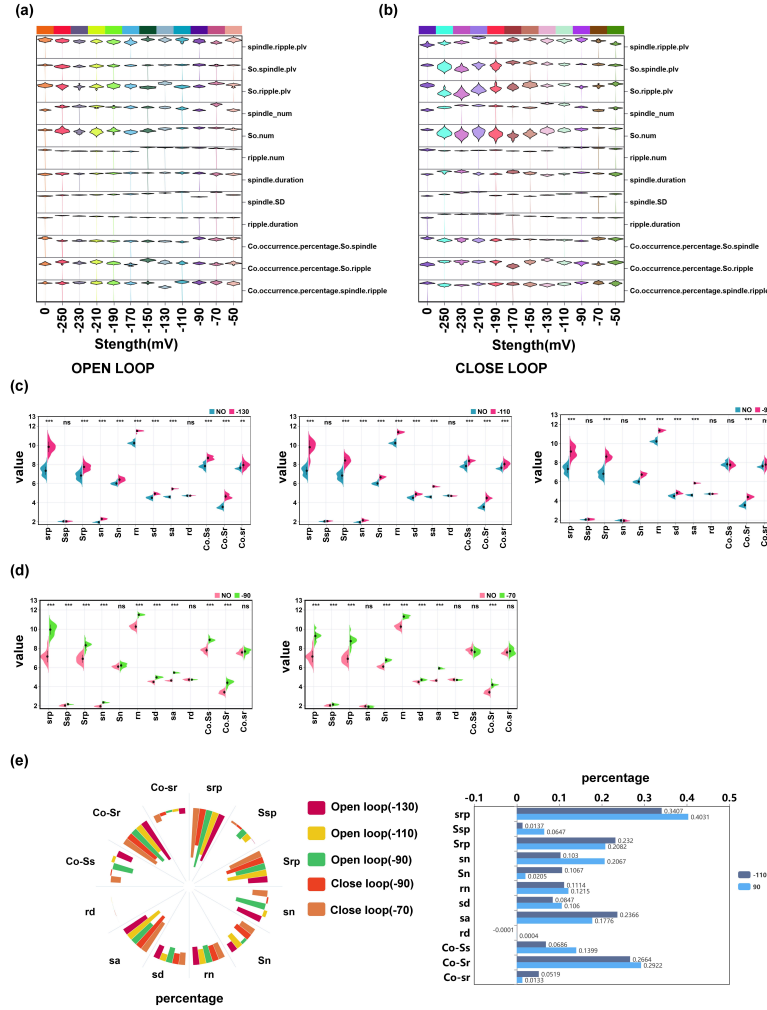
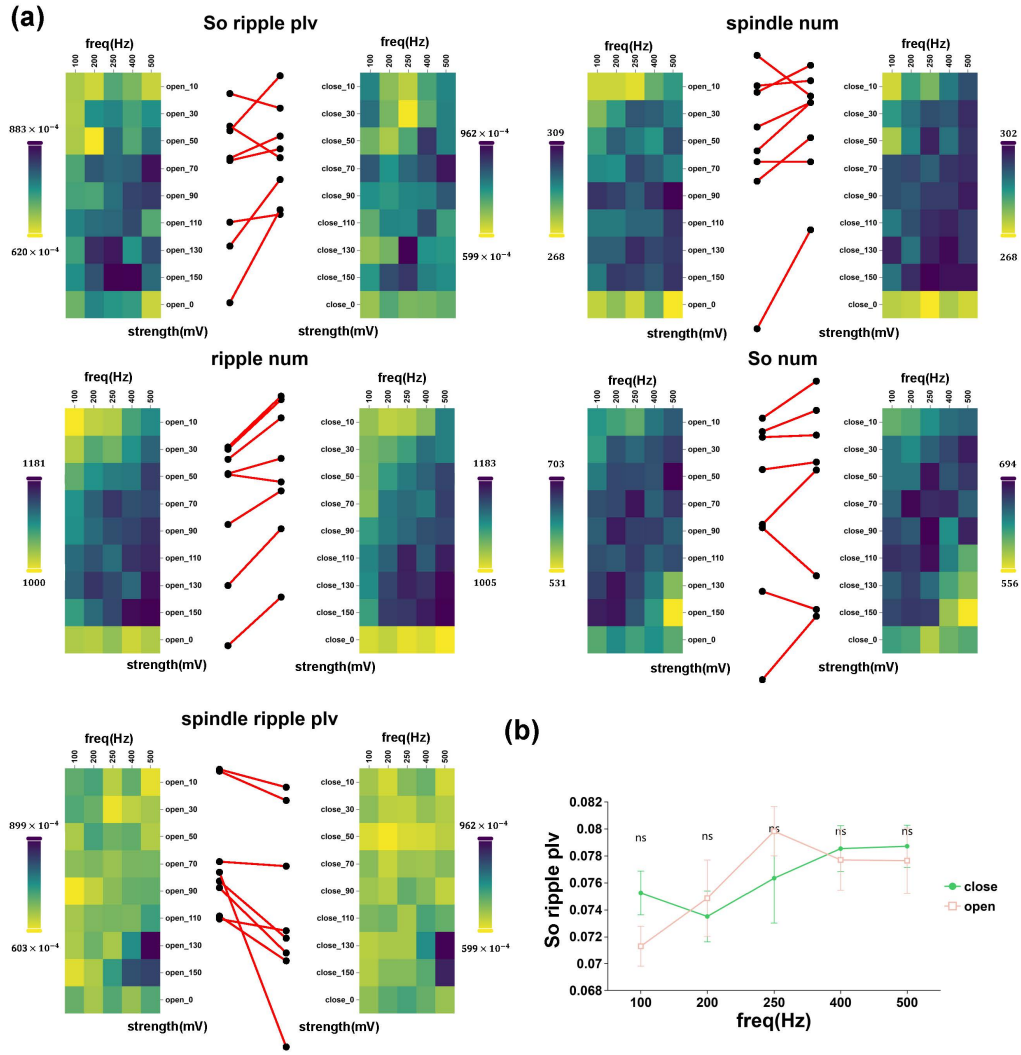


Figure 9: Results of the inhibitory stimulation protocol. The low-current inhibitory stimulation scheme is more effective than the existing experiments (with significant increases in synchronization values as well as the number and characteristics of events), further demonstrating the rationality and superiority of real-time closed-loop stimulation. **a** Violin diagram of inhibitory open-loop stimulus matrix, the horizontal coordinate is the stimulus intensity (negative sign represents the inhibitory stimulus), and the vertical coordinate represents each index value. **b** Like **d**, violin diagram of inhibitory closed loop matrix. **c** The intensity of open-loop inhibitory stimulation was 130 mV (left), 110 mV (middle), 90 mV (right) violin plots showing the index in the relatively unstimulated case. Difference analysis (***) indicates $p < 0.001$, ** indicates $p < 0.01$, * indicates $p < 0.05$, and ns indicates no significant difference). **srp** represents the plv value of spindle and ripple, **Ssp** represents the plv value of So and spindle, **Srp** represents the plv value of So and ripple, **sn** represents the number of spindle events, **Sn** represents the number of So events, **rn** represents the number of ripple events. **sd** represents the duration of spindle, **sa** represents the average amplitude of spindle, **rd** represents the duration of ripple, **Co. Ss** represents the percentage of So and spindle occurring together, **Co. Sr** represents the percentage of So co-occurring with ripple and **Co. sr** represents the percentage of spindle co-occurring with ripple. **d** The closed-loop inhibitory stimulus intensity was 90 mV (left), 70 mV (right), violin plot showing the index in the relatively unstimulated case. Difference analysis (***) indicates $p < 0.001$, ** indicates $p < 0.01$, * indicates $p < 0.05$, and ns indicates no significant difference. **e** left: The above polar graph shows the percentage (mean) increase of stimulus intensity relative to each index of non-stimulus; right: The percentage increase in each index relative to no stimulation was best for closed-loop stimulation inten-



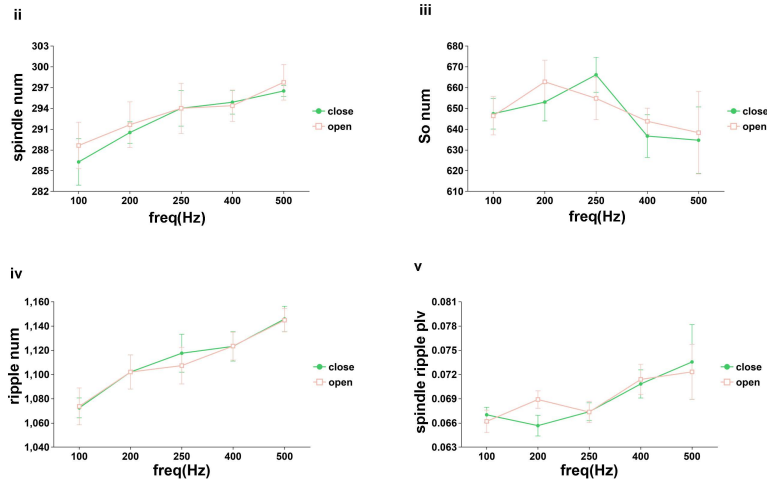


Figure 10: Dual-parameter inhibitory stimulation. Similarly, it also further confirms the rationality and superiority of our chosen stimulation frequency (500Hz). **a** Combined heat maps, the left side of each subgraph represents the open loop heat map results; On the right is the closed-loop thermal map result; Each point in the middle plot represents a different stimulus intensity, and the average stimulus frequency indicator is based on the percentage increase in no stimulus, with the left side being open loop and the right side being closed loop; i, ii, iii, iv, and v represent respectively the plv of So and ripple, the number of spindle events, the number of ripple events, the number of So events, and the plv of spindle and ripple. **b** Compare the open-loop (pink) and closed-loop (green) results

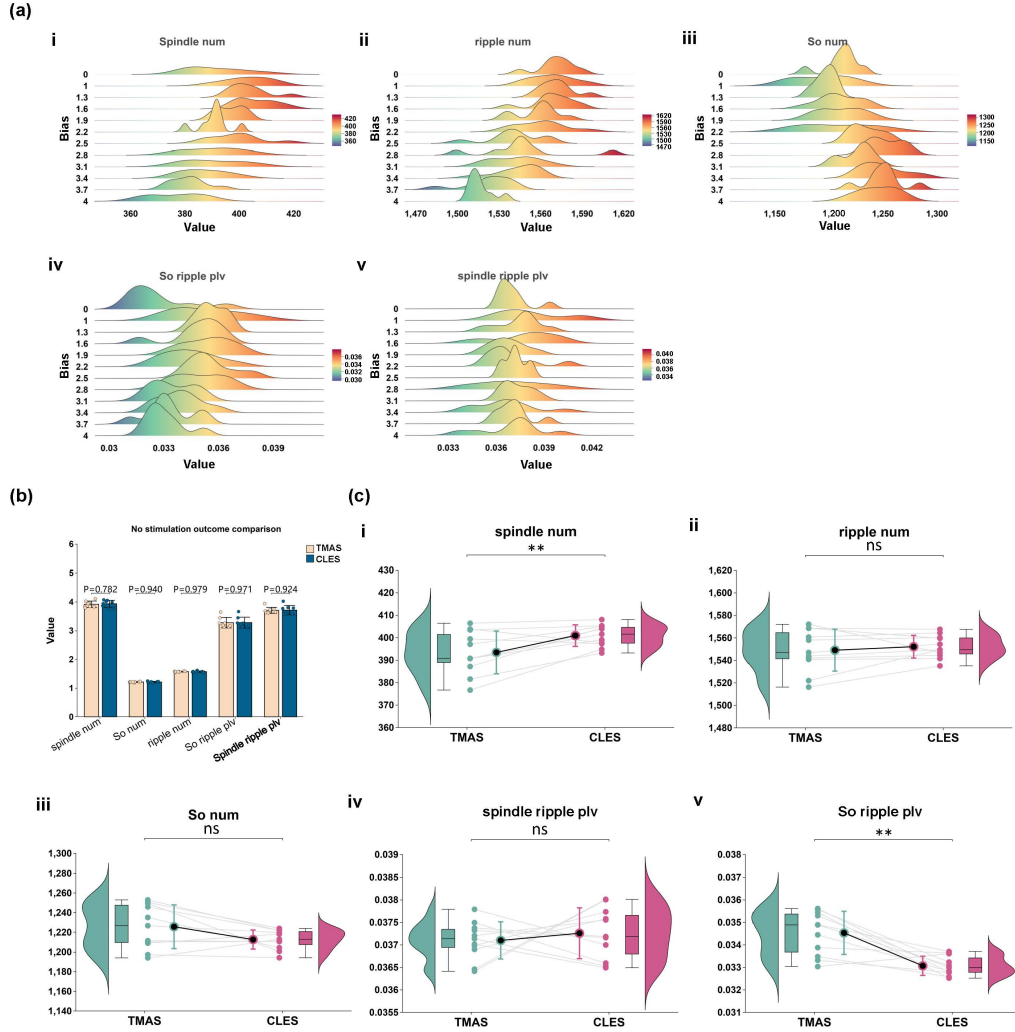
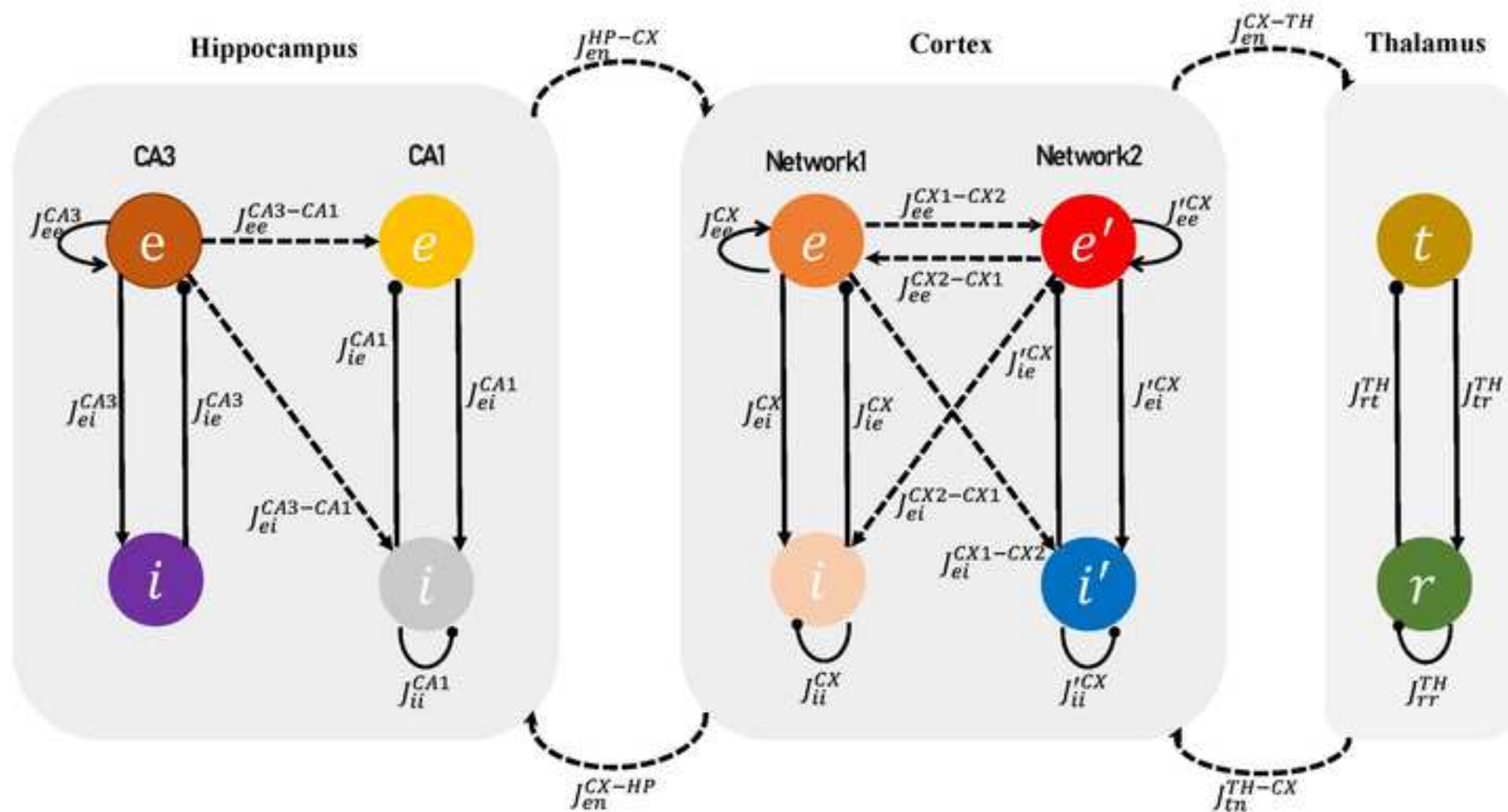
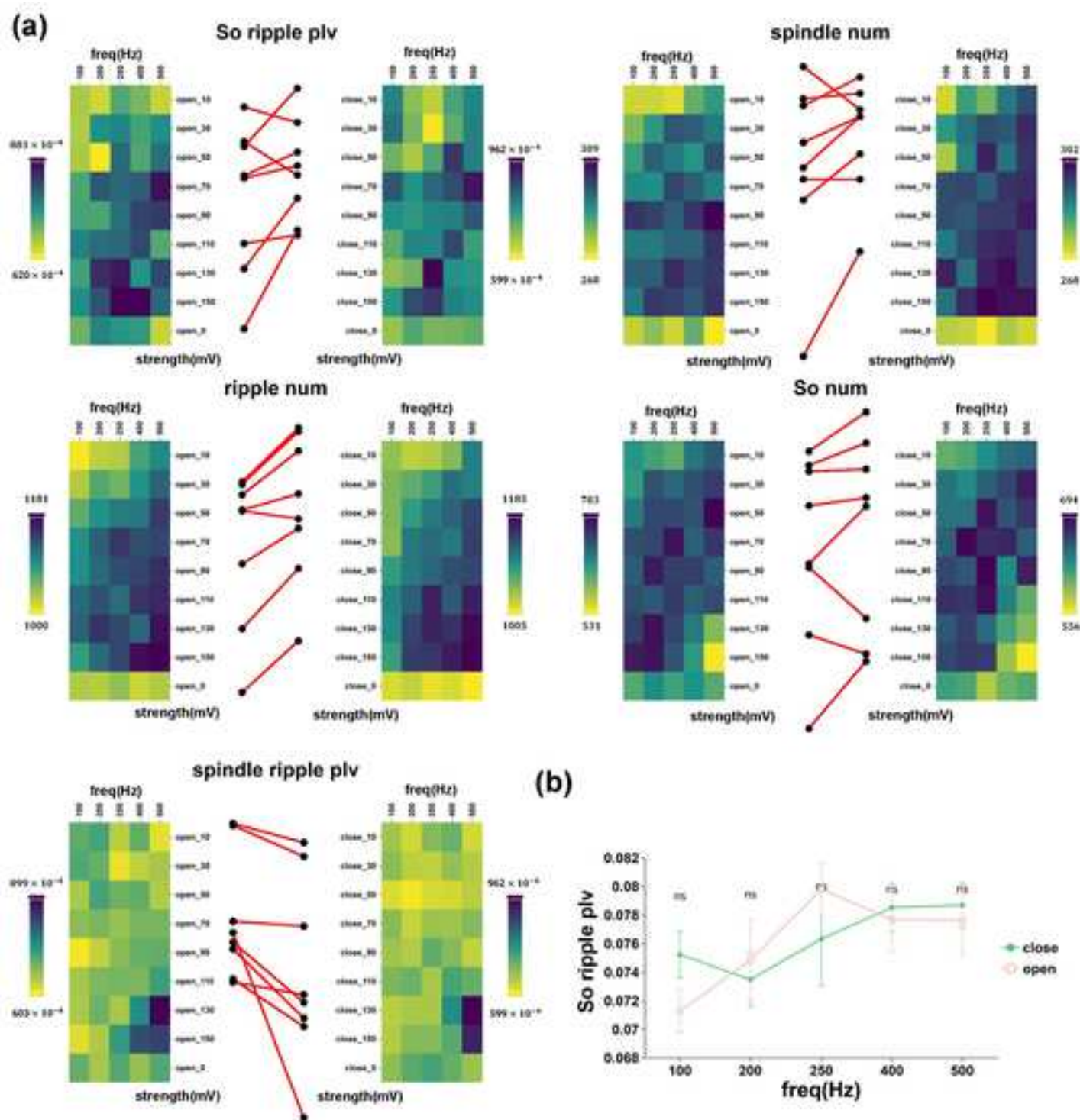


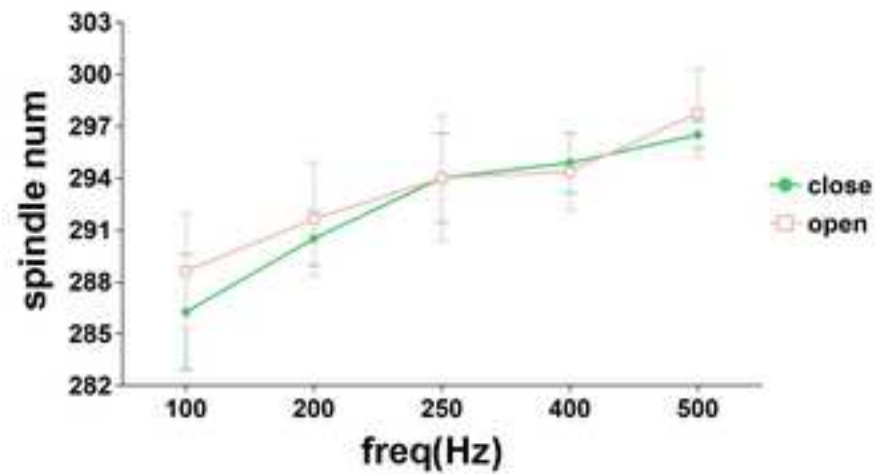
Figure 11: Results of magneto-ultrasound stimulation, compared with the effects of experimental closed-loop intracranial stimulation. It indicates that the effects of magneto-ultrasound stimulation are comparable to those of experimental closed-loop intracranial stimulation. That is, the synchronization gain of thalamo-cortical spindle waves with hippocampal ripples and the increase in the number of cortical slow oscillation events show no significant difference, and the reduction in the number of ripple events is roughly consistent. The increase in spindle events under magneto-ultrasound stimulation is slightly inferior, but in comparison, the enhancement of cortical slow oscillation and hippocampal ripple synchronization under magneto-ultrasound stimulation is significantly higher than that under closed-loop intracranial electrical stimulation. This improvement may offset the insufficiency in the number of spindle events. **a** Changes of magnetic ultrasound stimulation compared with no stimulation. **b** Comparison of index changes under different initial values. **c** Comparison of results between magnetic ultrasound stimulation and experimental closed-loop stimulation.

Figure1

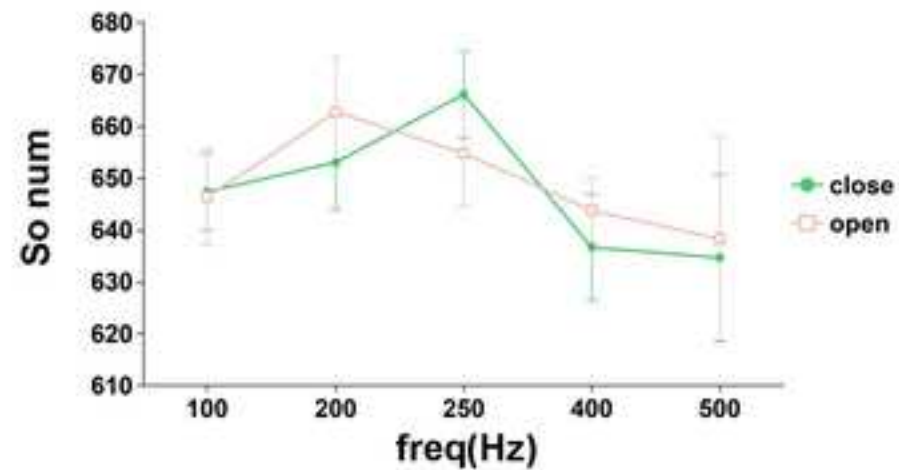




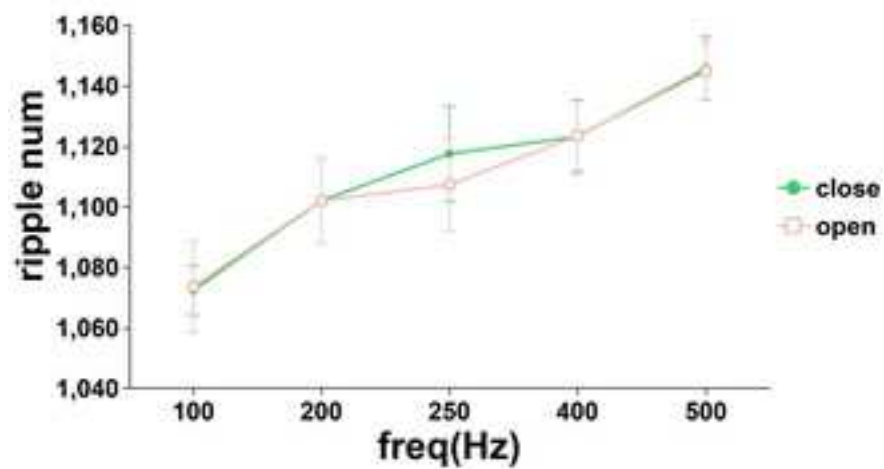
ii



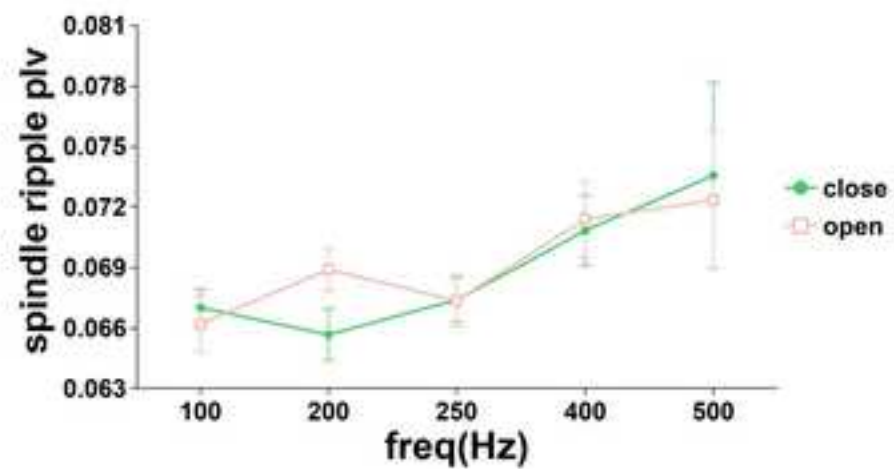
iii

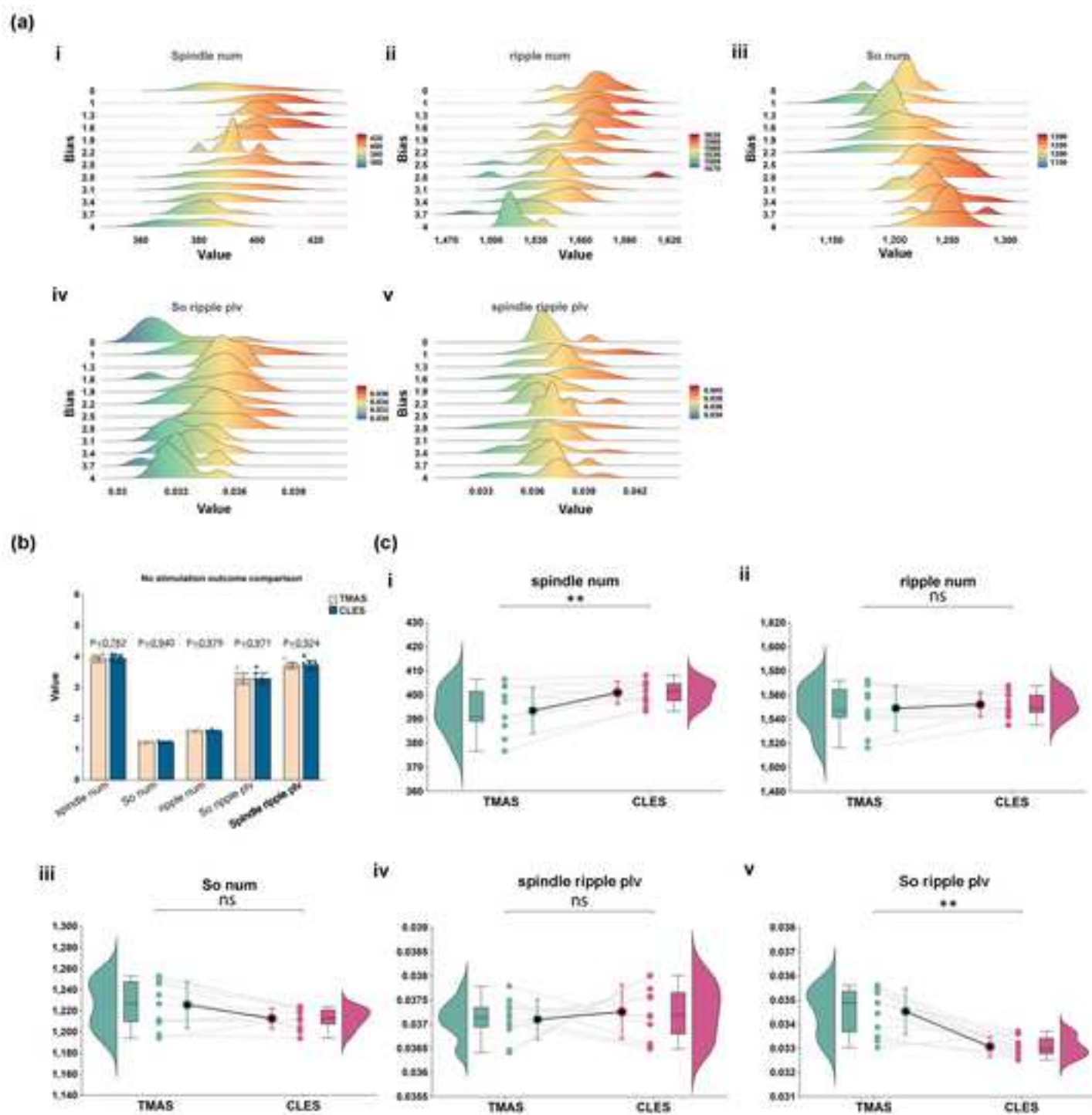


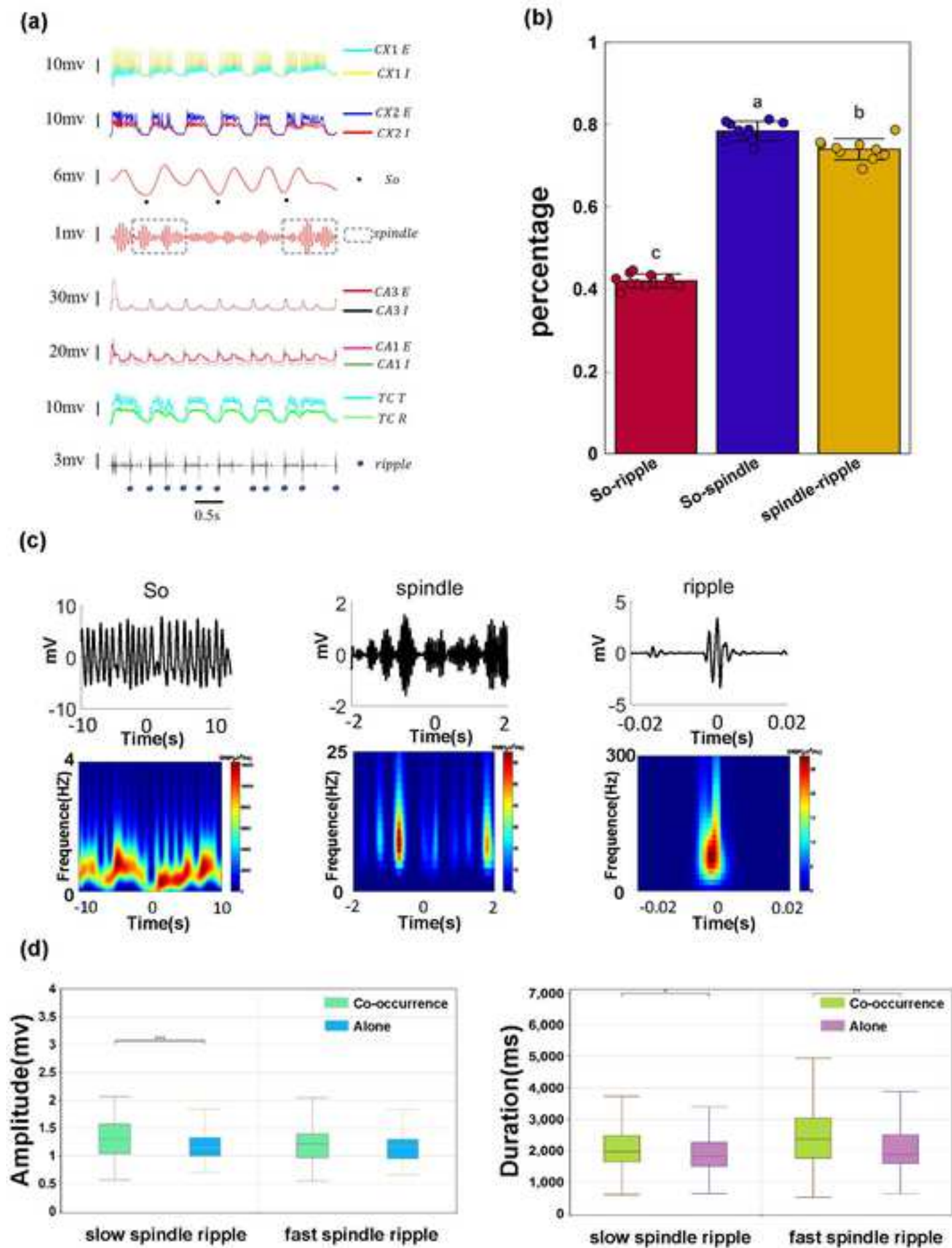
iv

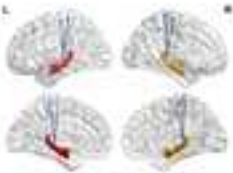
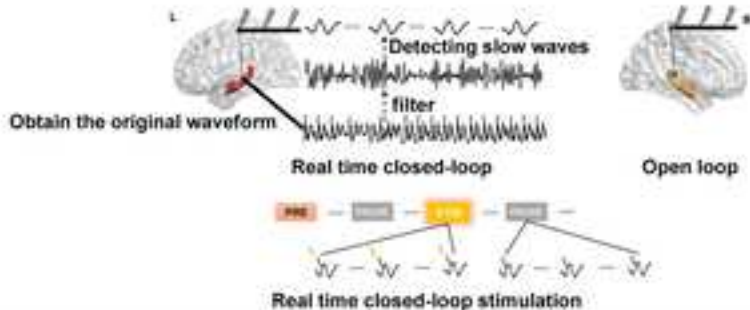
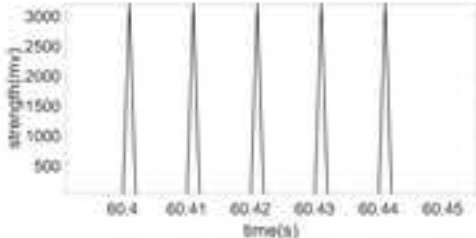
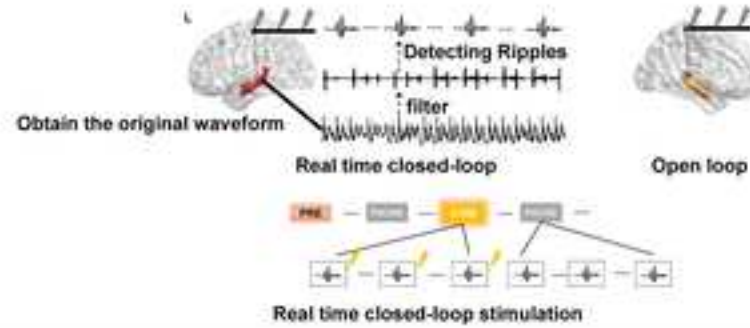
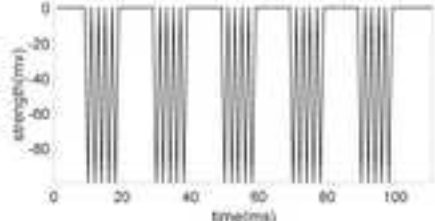
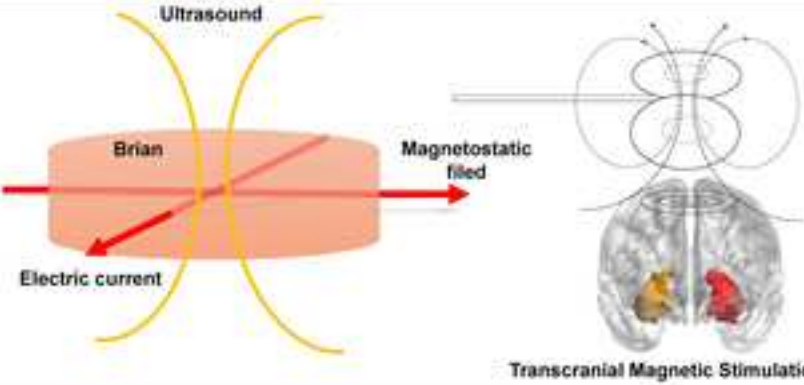
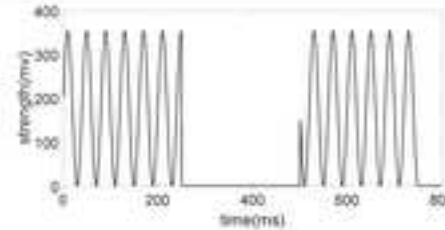


v

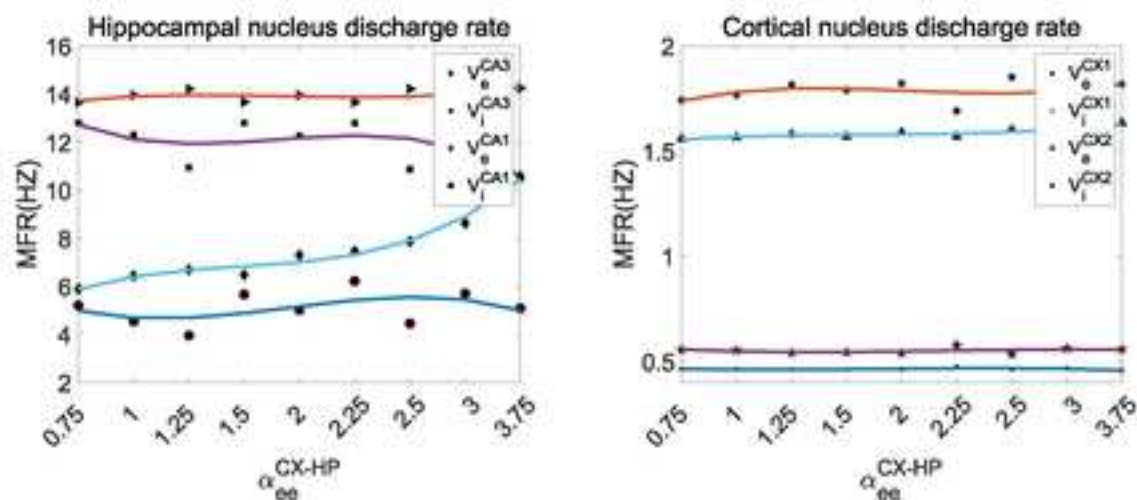




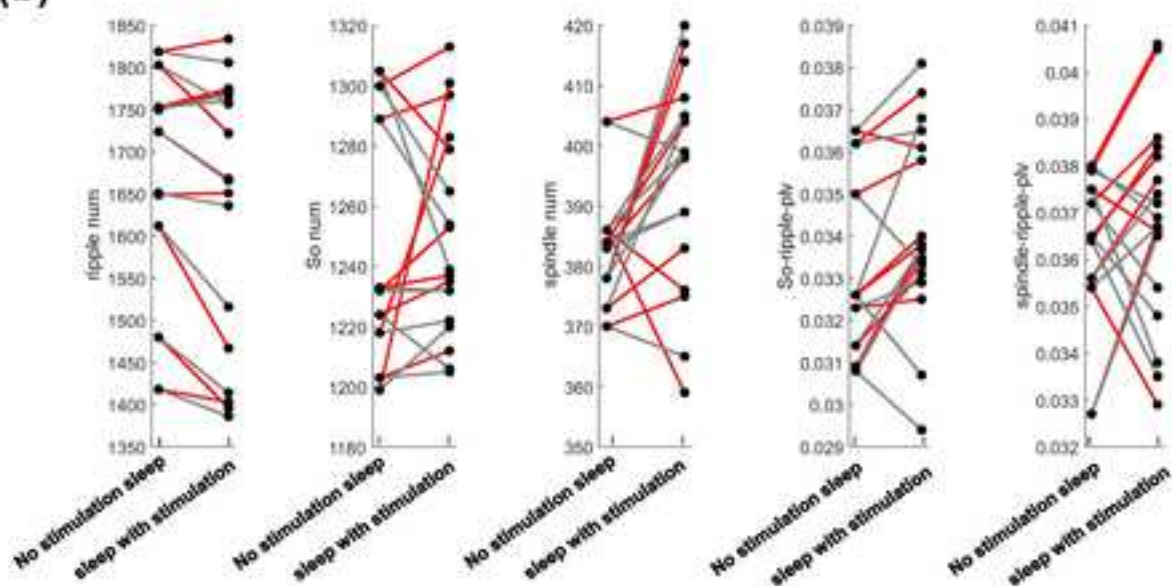


| Stimulation Protocol | Invasive (Yes/No) | Physical Principle | Stimulation Currents and Mathematical Expression |
|--|-------------------|---|--|
| Experimental Closed-loop Phase-locking Deep Brain Stimulation | Yes |  <p>— Sync-stimulation - cortex lobe — mixed-phase stimulation</p> | |
| Computational Closed-loop Phase-locking Excitable Stimulation | Yes |  <p>Obtain the original waveform</p> <p>Real time closed-loop stimulation</p> <p>Open loop</p> |  |
| Computational Closed-loop Phase-locking Inhibitive Stimulation | Yes |  <p>Obtain the original waveform</p> <p>Real time closed-loop stimulation</p> <p>Open loop</p> |  $s[n] = \text{strength} \cdot 1_{\left[\left\lfloor \frac{n}{10h} \right\rfloor \cdot \frac{1}{\text{freq}} - \left\lfloor \frac{n}{10h} \right\rfloor \cdot \frac{1}{\text{freq}} + \frac{\text{sttime}}{h} \right]}(n)$ |
| Magnetic ultrasonic stimulation | No |  <p>Ultrasound</p> <p>Brain</p> <p>Magnetostatic field</p> <p>Electric current</p> <p>Transcranial Magnetic Stimulation</p> |  $x(t) \times (\sin(2\pi ft) + 1)$ $x(t) = \begin{cases} 1(n-1) \frac{1}{RF} < t \leq [(n-1) + DC] \frac{1}{RF}, n = 1, 2, 3, \dots \\ 0 & \text{others} \end{cases}$ |

(a)



(b)



(c)

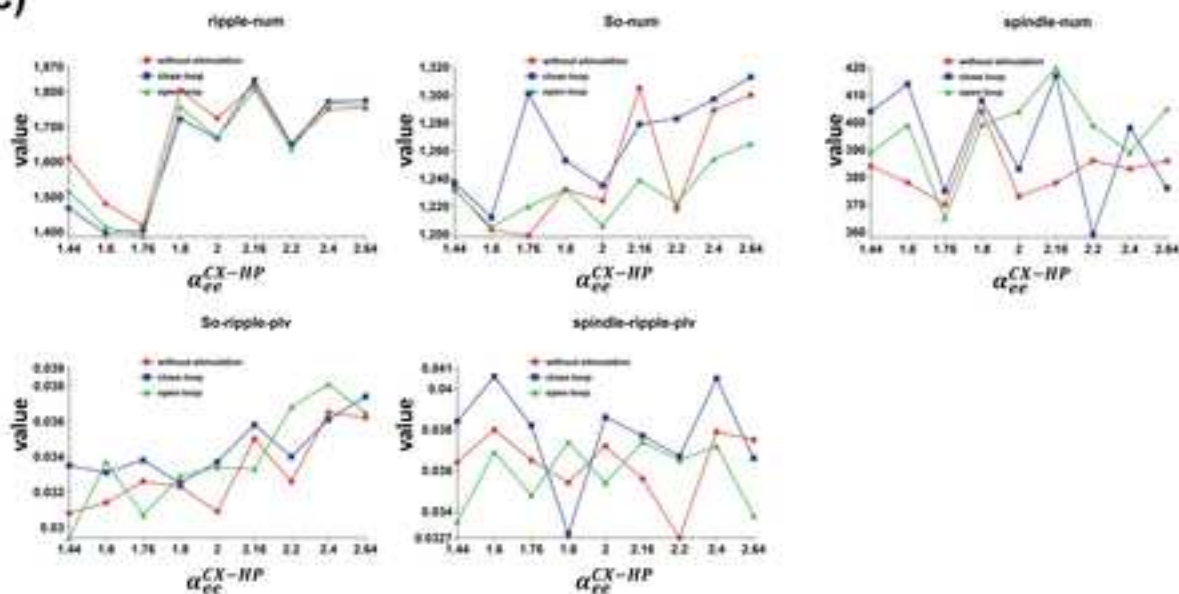


Figure5

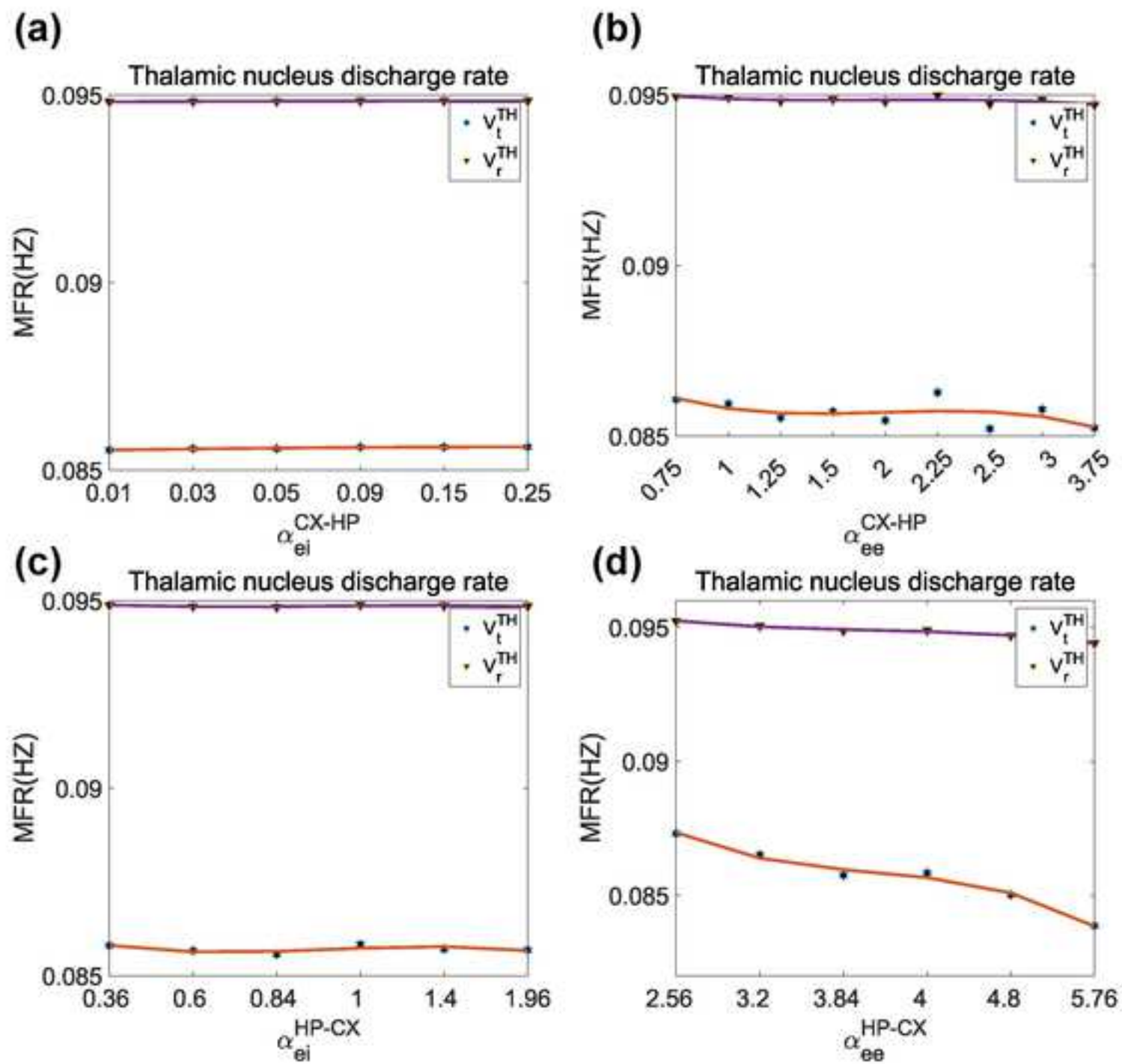
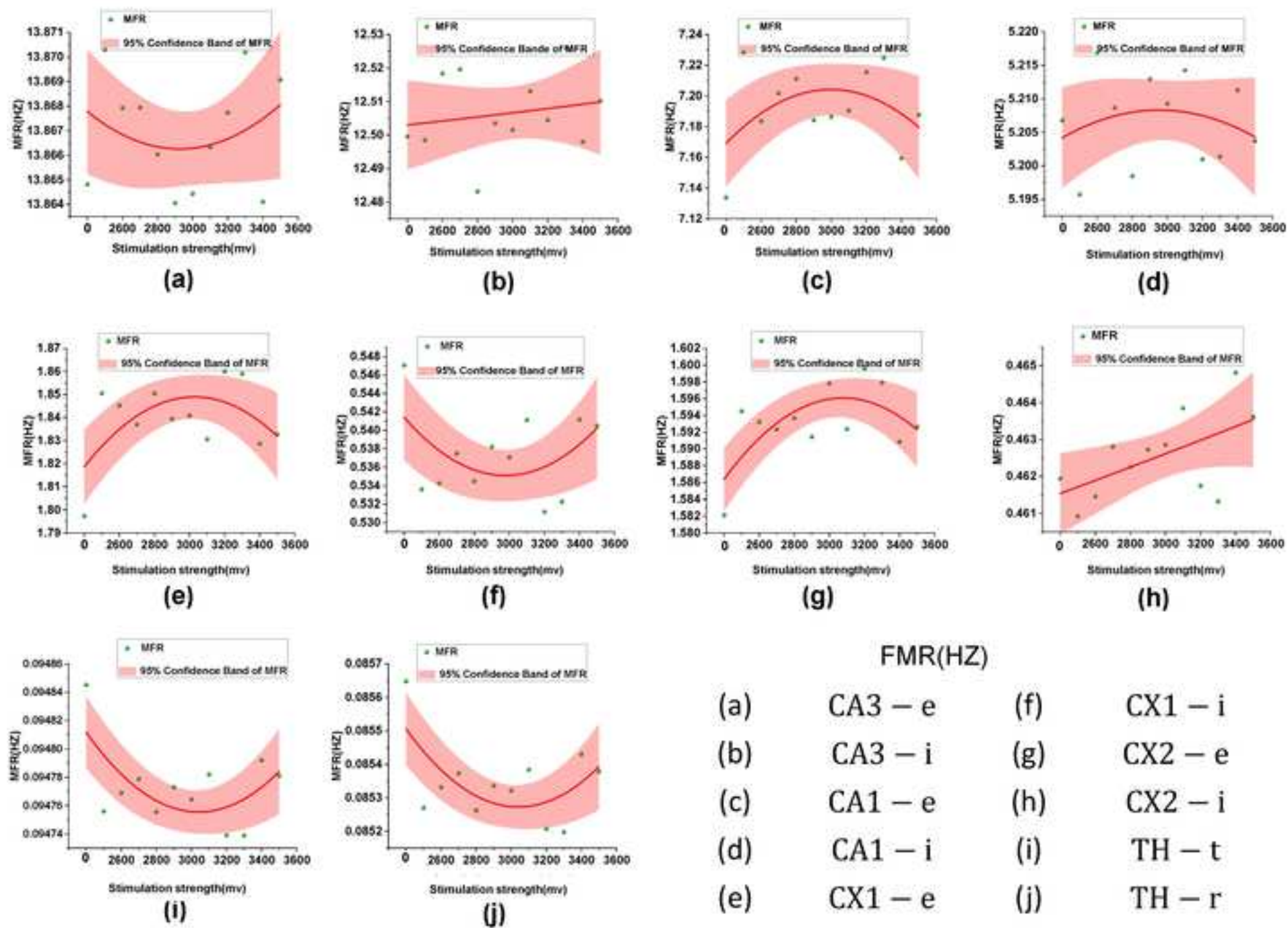


Figure6



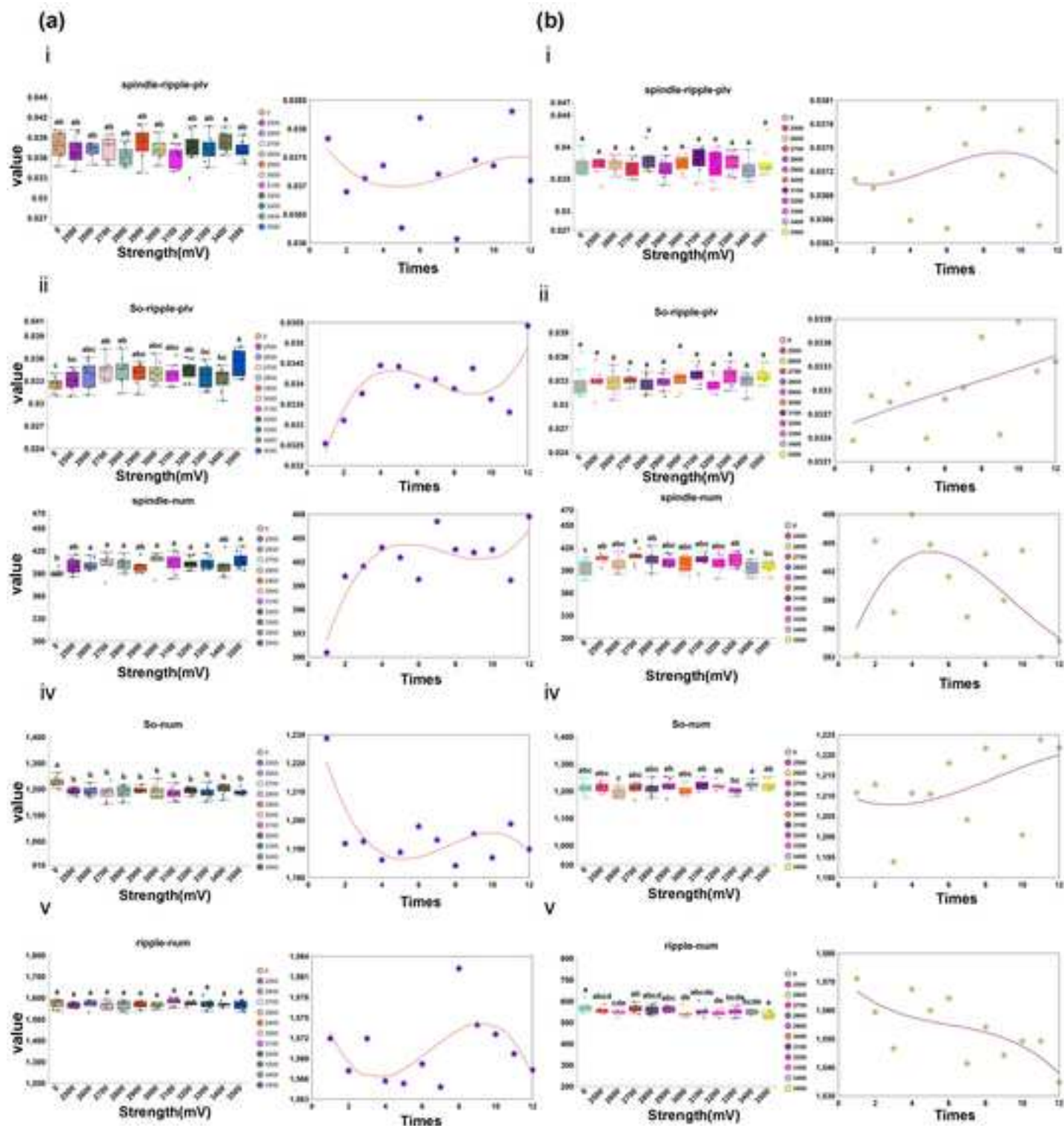
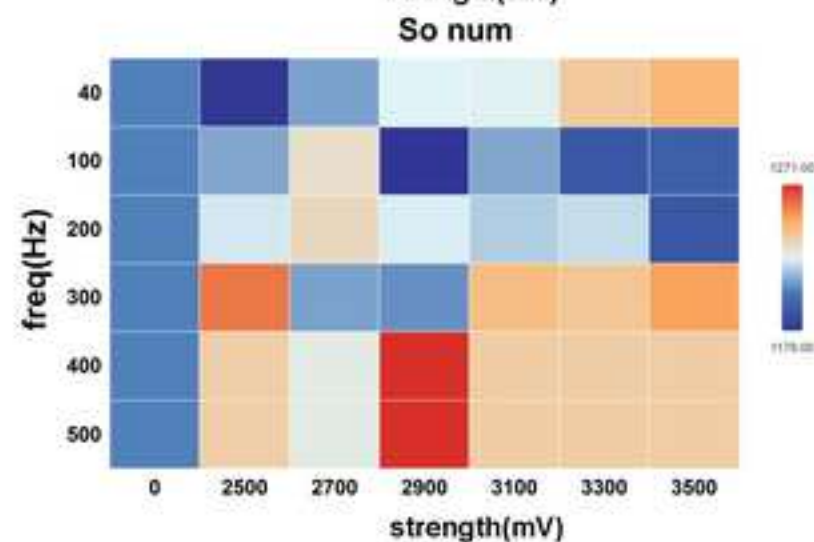
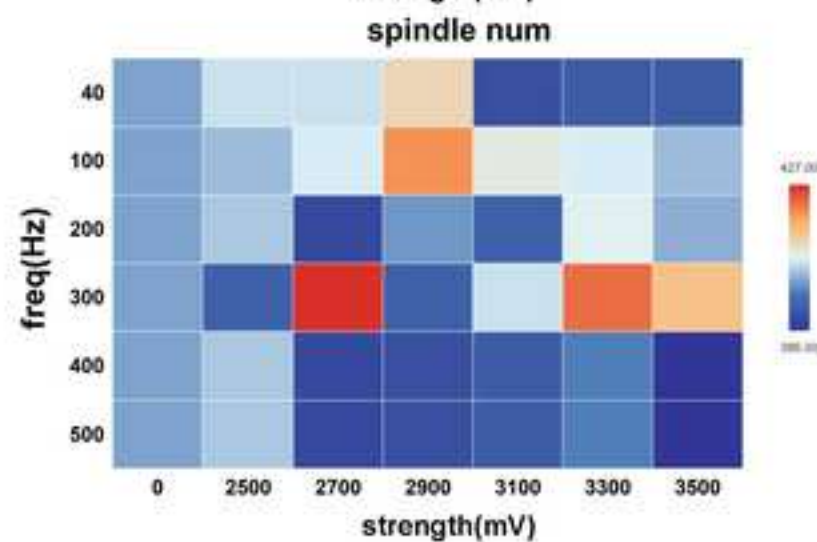
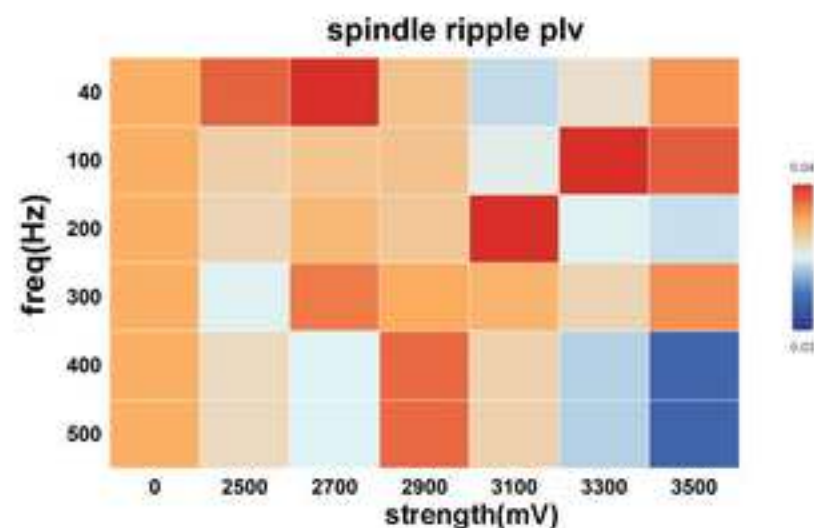
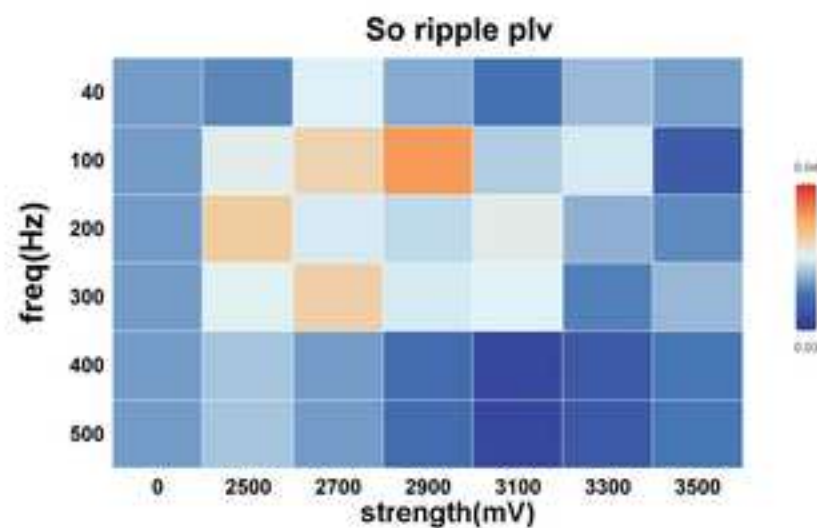
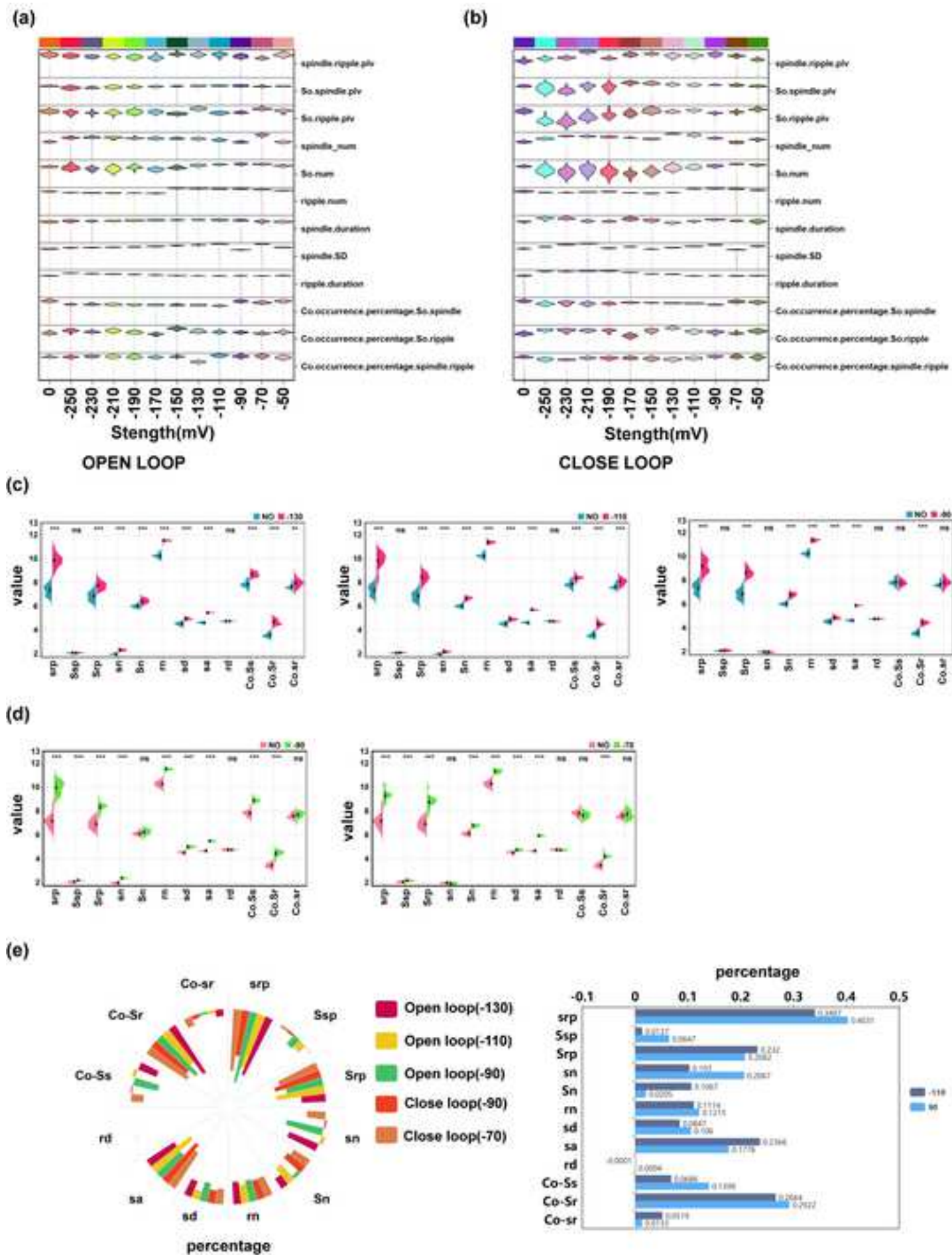
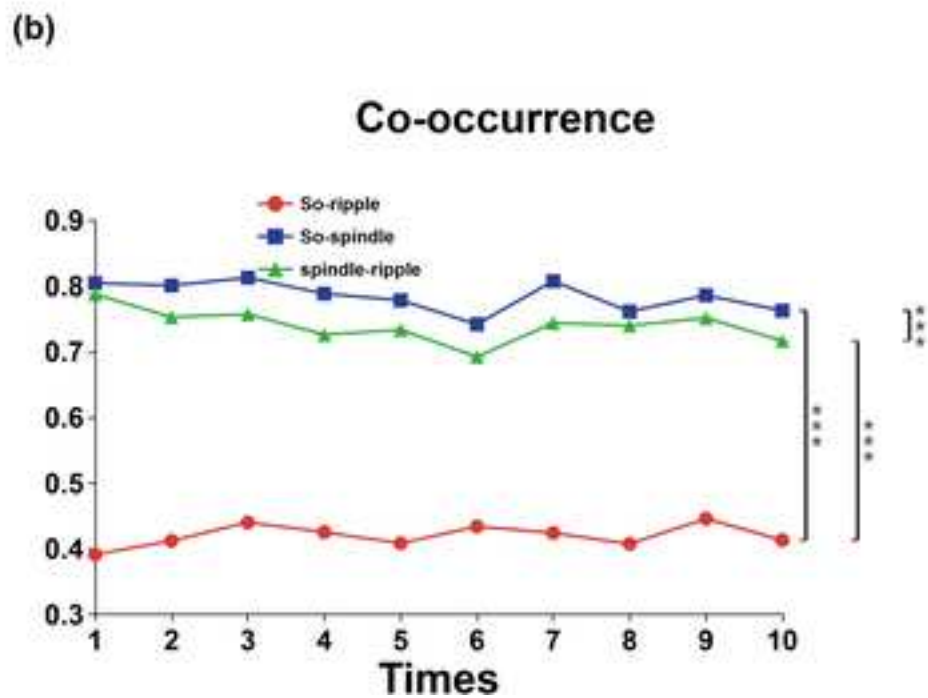
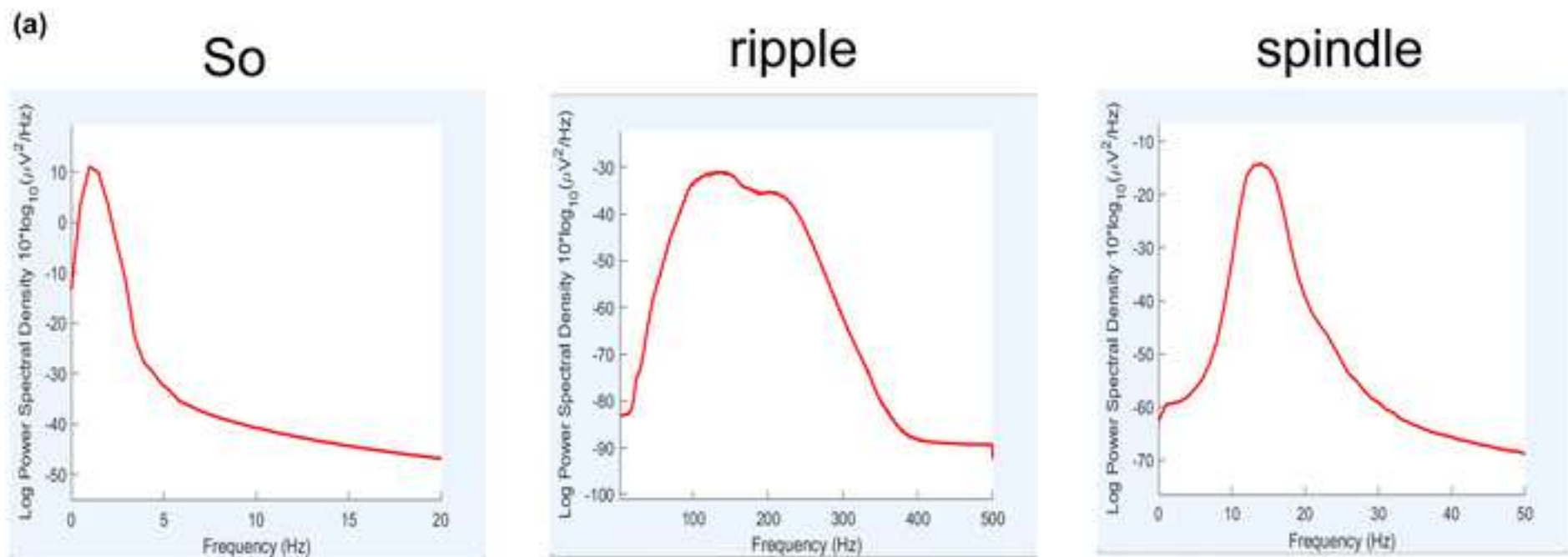
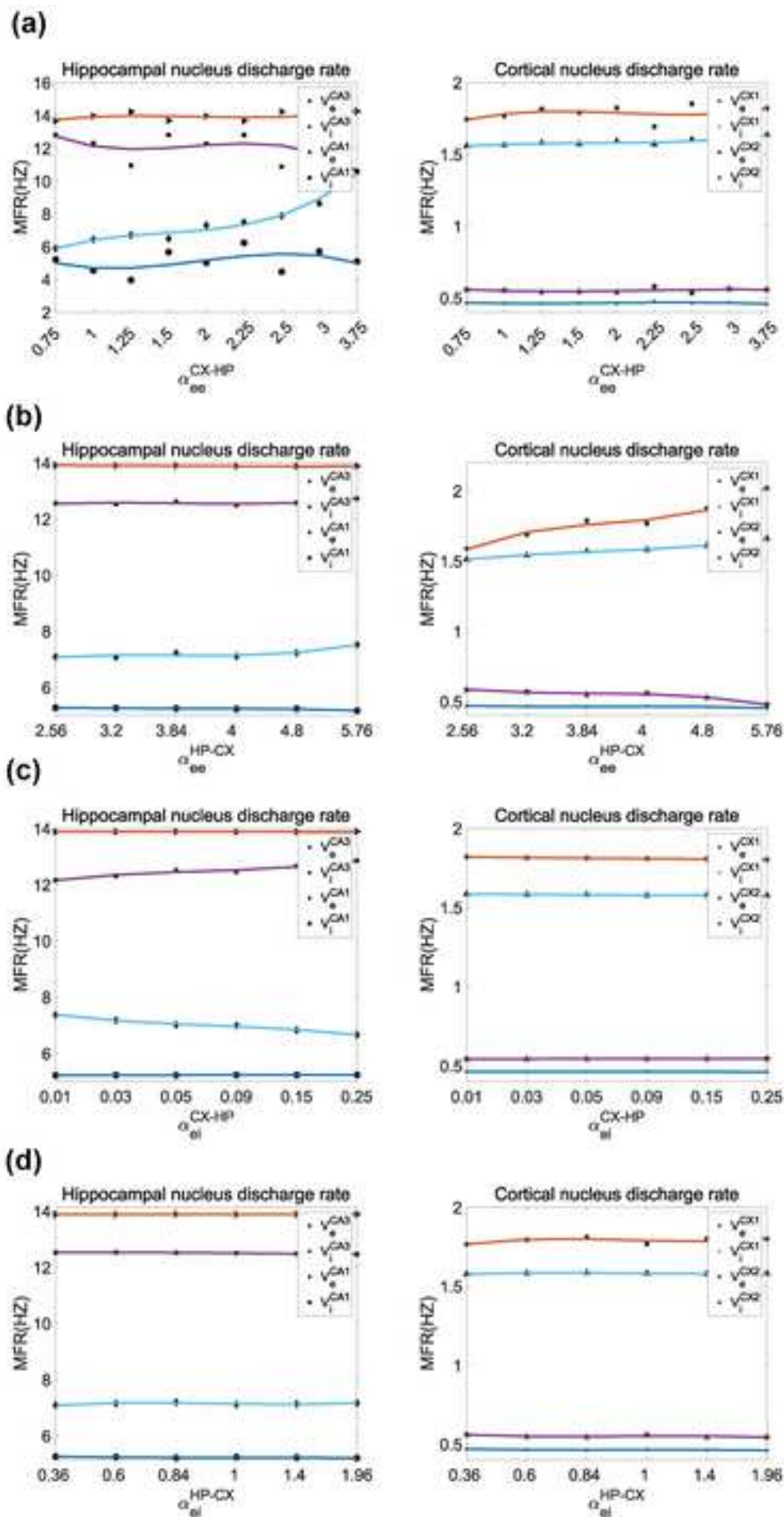


Figure8

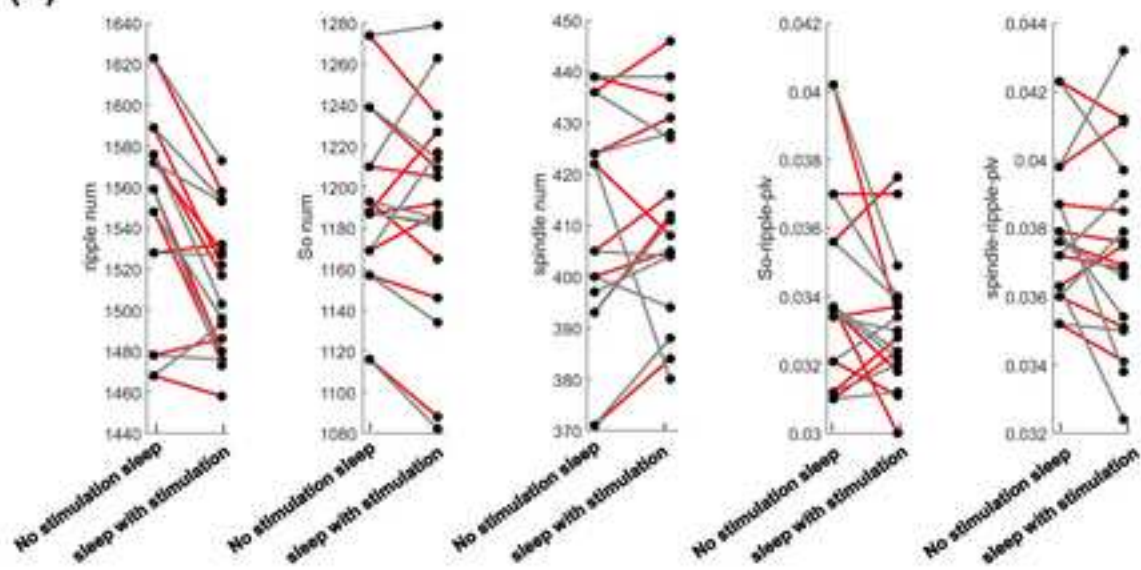




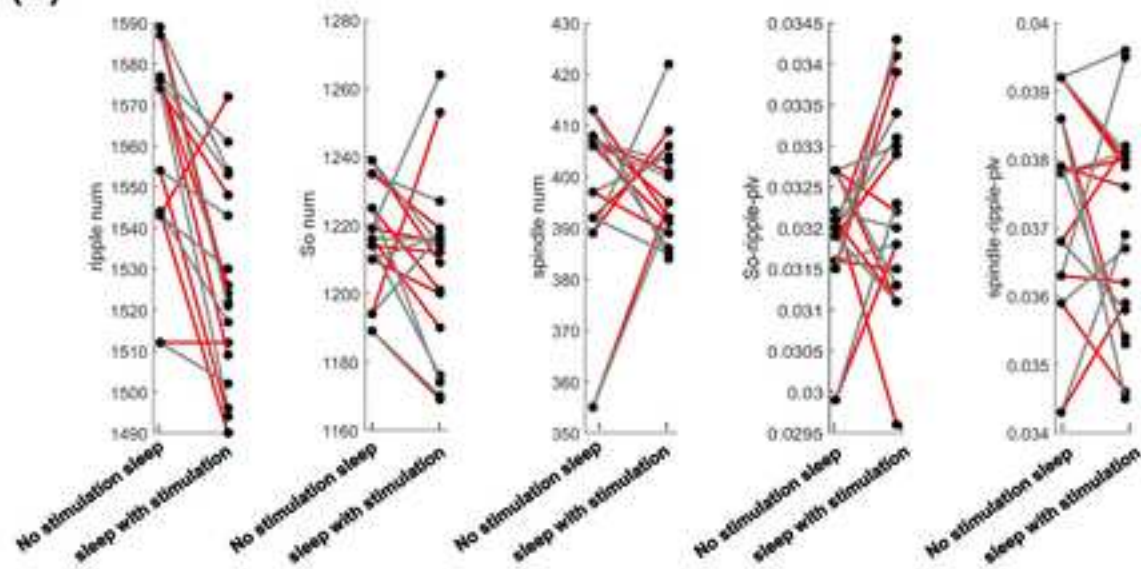




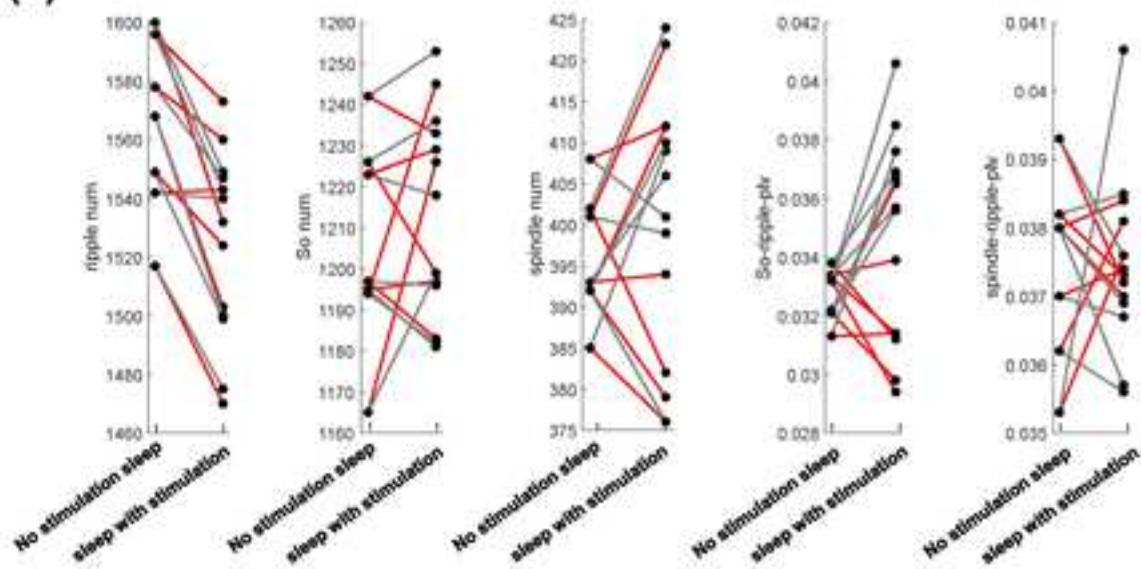
(a)

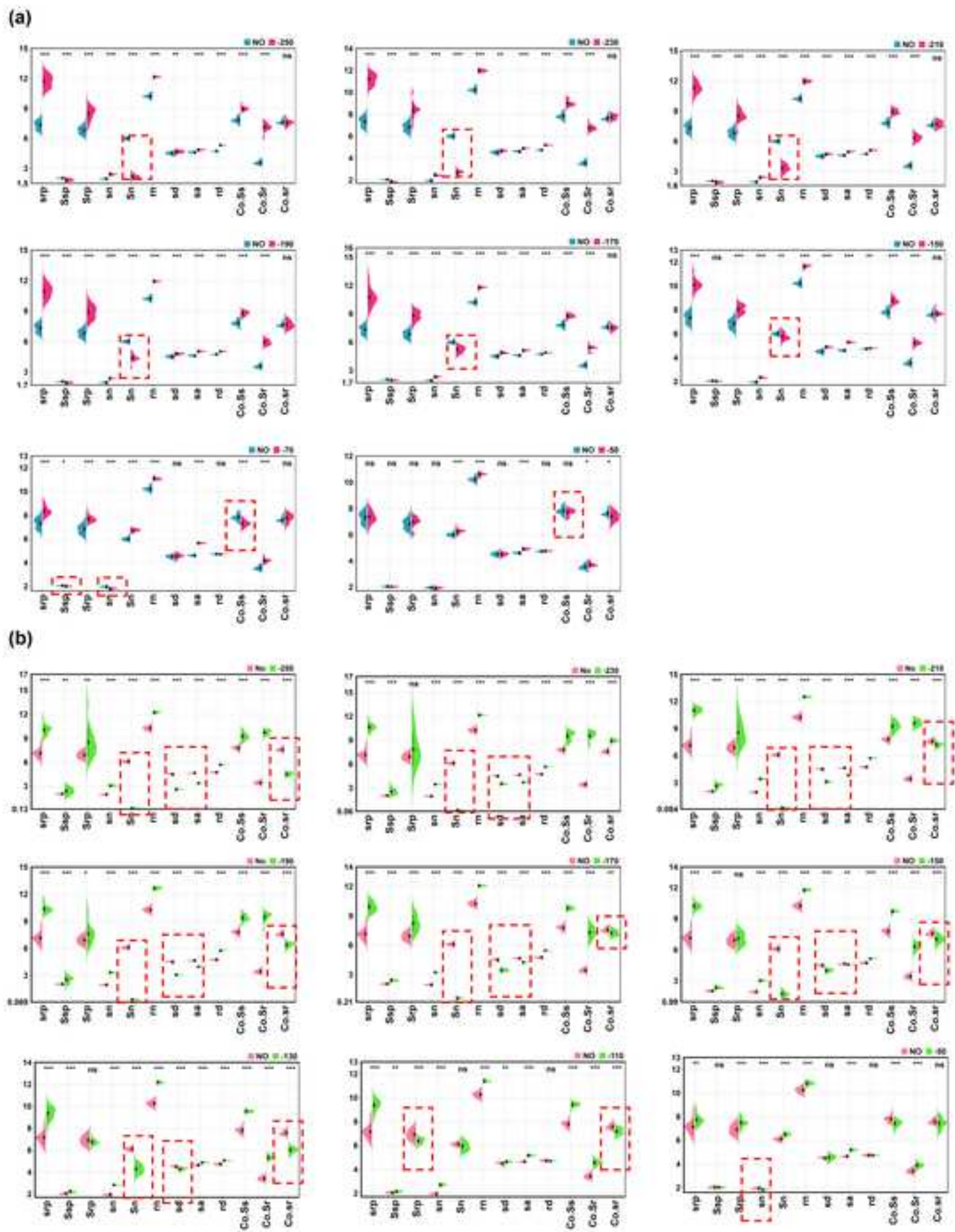


(b)



(c)

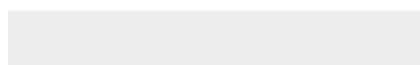
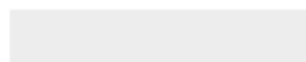






[Click here to access/download](#)

Supplementary Material for on-line publication only
SM-clean.pdf





[Click here to access/download](#)

Supplementary Material for on-line publication only
SM-marked.pdf





Declaration of Interest Statement

All authors declare that there are no conflicts of interest in relation to the manuscript titled "From experimental phenomena to computational models: Exploring the synchronization mechanisms of phase-locked stimulation in the hippocampal-thalamic-cortical circuit for memory consolidation" submitted to Chaos, Solitons and Fractals. I confirm that the results and interpretations reported in the manuscript are original and have not been plagiarized.

Authors' Response to the Comments

Thank you to the reviewers for their pertinent comments, which have greatly assisted us in improving the paper. We have carefully reviewed all the comments and made the necessary modifications in the corresponding sections of the paper. The changes made are highlighted in a light color in the main manuscript.

We also extend our special thanks to Editor for all the efforts made to improve this paper.

Response to Reviewer 1:

Reviewer #1: Closed-loop phase-locking stimulation has been shown in experiments to help strengthen memory consolidation, a process that relies on the coordinated interactions between slow waves in the cortex, thalamocortical sleep spindles, and hippocampal ripples. However, the ways in which this stimulation aids memory consolidation are not yet fully understood. To investigate, this study uses computational modeling to examine synchronization mechanisms within the hippocampal-thalamocortical loop and simulates the effects of stimulation on memory consolidation based on experimental findings.

The results reveal that excitatory connections between the cortex and hippocampus are essential for effective memory consolidation. An improved protocol for inhibitory closed-loop phase-locking stimulation was also tested, demonstrating even greater benefits for memory consolidation than previously established stimulation methods. Notably, non-invasive stimulation methods present fewer side effects, lower costs, and easier implementation compared to invasive approaches.

Further experiments were conducted using a non-invasive magnetic-acoustic stimulation protocol, which achieved effects similar to invasive deep brain stimulation techniques. These findings not only provide insights into the neural mechanisms behind memory processing but also lay a theoretical foundation for developing innovative, non-invasive therapies for enhancing memory consolidation.

I have very much enjoyed reading this review, and I believe it covers an important subject in an innovative and comprehensive way. There are, however, some minor aspects of the work that could be further improved. I would recommend addressing the following comments.

Thank you very much for your positive feedback on our work and valuable evaluation as well as suggestions on our manuscript. Based on your suggestions, we have made the following revisions to the manuscript.

(1) I would like to note recent research that would fit well to the introduction, namely Networks behind the morphology and structural design of living systems, Marko Gosak, et al., Phys. Life Rev. 41, 1-21 (2022) and Network science of biological systems at different scales: A review, Marko Gosak, et al., Phys. Life Rev. 24, 118-135 (2018). This would also help showcase the full breadth of research along these lines, beyond phase-locked stimulation in the hippocampal-thalamic-cortical circuit.

Response: We sincerely appreciate your suggestions regarding Networks behind the morphology and structural design of living systems and Network science of biological systems at different scales. We have cited the two references you recommended (references 29 and 30) in the manuscript, which provide important theoretical support by revealing the complex network behaviour. In addition, we also added two new references (references 56 and 57) about mechanisms of memory-supporting neuronal dynamics. These references will guide future improvements in the network science for brain cognitive and memory states.

[29] Gosak, M., Milojević, M., Duh, M., et al.: Networks behind the morphology and structural design of living systems. Physics of Life Reviews. 41, 1-21 (2022).

[30] Gosak, M., Markovič, R., Dolenšek, J., et al.: Network science of biological systems at different scales: A review. Physics of life reviews. 24, 118-135 (2018).

[56] Li, Y., Briguglio, J. J., Romani, S., Magee, J. C.: Mechanisms of memory-supporting neuronal dynamics in hippocampal area CA3. Cell. 187, 1-16 (2024).

[57] McHugh S.B., Lopes-Dos-Santos V., Castelli M., Gava G.P., Thompson S.E., Tam S.K.E., Hartwich K., Perry B., Toth R., Denison T., Sharott A., Dupret D.: Offline hippocampal reactivation during dentate spikes supports flexible memory. Neuron. 112, 1-14 (2024).

(2) It would also improve the paper if the figure captions would be made more self-contained. The authors should consider a sentence or two saying what is the main message of the presented results/data in each figure.

Response: Thank you very much for this comment. According to the reviewer's suggestion, in the following, we have added one sentence for each figure to show the main message of the presented results and data:

Figure 1: The structure of synaptic connections between neurons of the HTC network. This network model consists of three subnetworks: hippocampus, cortex, and thalamus.

Figure 2: Generation of SOs, spindles, and ripple in the full hippocampo-cortico-thalamic model and their firing characteristics.

Figure 3: Three type of invasive stimulus therapies and one type of non-invasive stimulation pattern (magnetic ultrasonic stimulation), and their performing process and physical mechanism, stimulation waveforms as well as mathematical expressions.

Figure 4: The impact of the strength of cortico-hippocampal excitatory connections on their firing rate and their facilitation effects to memory consolidation. It is shown that this excitatory connection has significant implications for the promotion of memory consolidation.

Figure 5: The impact of varying connection strengths on the firing rate of thalamic neurons. Under varying connection strengths among different neurons, there is almost no effect on the firing rate of thalamic neurons.

Figure 6: Under a fixed connection strength, changing the stimulus intensity has little effect on the discharge rate of the nucleus, further explaining the important role of excitatory connections in the cortical-hippocampal nucleus neurons in promoting memory consolidation.

Figure 7: Numerical simulations reproduce the experimental results, namely that under real-time closed-loop stimulation, synchronization increases and the number of ripple events decreases, while the number of other events increases; without precise temporal stimulation, the results are qualitatively consistent with the experimental findings. The significant reduction in the number of slow oscillation events may counteract the decreased synchronization between hippocampal ripples and cortical slow oscillations, leading to no significant changes after stimulation or potentially being detrimental to memory consolidation.

Figure 8: Heatmap of exponential changes under dual-parameter experimental stimulation. This further affirms the rationality of the experimental stimulation frequency (100Hz) chosen in the numerical simulations.

Figure 9: Results of the inhibitory stimulation protocol. The low-current inhibitory stimulation scheme is more effective than the existing experiments (with significant increases in synchronization values as well as the number and characteristics of events), further demonstrating the rationality and superiority of real-time closed-loop stimulation.

Figure 10: Dual-parameter inhibitory stimulation. Similarly, it also further confirms the rationality and superiority of our chosen stimulation frequency (500Hz).

Figure 11: Results of magneto-ultrasound stimulation, compared with the effects of experimental closed-loop intracranial stimulation. It indicates that the effects of magneto-ultrasound stimulation are comparable to those of experimental closed-loop intracranial stimulation. That is, the synchronization gain of thalamo-cortical spindle waves with hippocampal ripples and the increase in the number of cortical slow oscillation events show no significant difference, and the reduction in the number of ripple events is roughly consistent. The increase in spindle events under magneto-ultrasound stimulation is slightly inferior, but in comparison, the enhancement of cortical slow oscillation and hippocampal ripple synchronization under magneto-ultrasound stimulation is significantly higher than that under closed-loop intracranial electrical stimulation. This improvement may offset the insufficiency in the number of spindle events.

Figure S1: The time-frequency plots of the three types of waves and the percentage of their co-occurrence (So and spindle have approximately 85% co-occurrence, spindle and ripple have approximately 75% co-occurrence, So and ripple have approximately 50% co-occurrence).

Figure S2: Discharge rates of hippocampal and cortical nucleus neurons under different connection strengths. (Apart from the change in cortical excitatory connections to the hippocampus affecting the discharge rate of neurons, there are almost no changes in the others).

Figure S3: Changes in memory consolidation-related indicators with altered connection strengths other than the excitatory connections from the cortex to the hippocampal neurons. It does not promote memory consolidation.

Figure S4: Changes in memory consolidation indicators under different inhibitory stimulation intensities. None of the above stimulation intensities can simultaneously increase all indicators of memory consolidation, and may even significantly impair memory consolidation.

(3) Apart from the above, I am happy to congratulate the authors on their excellent work.

Response: Thank you very much for your positive feedback on our work.

Graphical Abstract

From experimental phenomena to computational models: Exploring the synchronization mechanisms of phase-locked stimulation in the hippocampal-thalamic-cortical circuit for memory consolidation

Denggui Fan, Jin Chen, Songan Hou, Zhengyong Song, Gerold Baier, Qingyun Wang

Figure 1: The structure of synaptic connections between neurons of the HTC network. This network model consists of three subnetworks: hippocampus, cortex, and thalamus.

Figure 2: Generation of SOs, spindles, and ripple in the full hippocampo-cortico-thalamic model and their firing characteristics.

Figure 3: Three type of invasive stimulus therapies and one type of non-invasive stimulation pattern (magnetic ultrasonic stimulation), and their performing process and physical mechanism, stimulation waveforms as well as mathematical expressions.

Figure 4: The impact of the strength of cortico-hippocampal excitatory connections on their firing rate and their facilitation effects to memory consolidation. It is shown that this excitatory connection has significant implications for the promotion of memory consolidation.

Figure 5: The impact of varying connection strengths on the firing rate of thalamic neurons. Under varying connection strengths among different neurons, there is almost no effect on the firing rate of thalamic neurons.

Figure 6: Under a fixed connection strength, changing the stimulus intensity has little effect on the discharge rate of the nucleus, further explaining the important role of excitatory connections in the cortical-hippocampal nucleus neurons in promoting memory consolidation.

Figure 7: Numerical simulations reproduce the experimental results, namely that under real-time closed-loop stimulation, synchronization increases and the number of ripple events decreases, while the number of other events increases; without precise temporal stimulation, the results are qualitatively consistent with the experimental findings. The significant reduction in the number of slow oscillation events may counteract the decreased synchronization between hippocampal ripples and cortical slow oscillations, leading to no significant changes after stimulation or potentially being detrimental to memory consolidation.

Figure 8: Heatmap of exponential changes under dual-parameter experimental stimulation. This further affirms the rationality of the experimental stimulation frequency (100Hz) chosen in the numerical simulations.

Figure 9: Results of the inhibitory stimulation protocol. The low-current inhibitory stimulation scheme is more effective than the existing experiments (with significant increases in synchronization values as well as the number and characteristics of events), further demonstrating the rationality and superiority of real-time closed-loop stimulation.

Figure 10: Dual-parameter inhibitory stimulation. Similarly, it also further confirms the rationality and superiority of our chosen stimulation frequency (500Hz).

Figure 11: Results of magneto-ultrasound stimulation, compared with the effects of experimental closed-loop intracranial stimulation. It indicates that the effects of magneto-ultrasound stimulation are comparable to those of experimental closed-loop intracranial stimulation. That is, the synchronization gain of thalamo-cortical spindle waves with hippocampal ripples and the increase in the number of cortical slow oscillation events show no significant difference, and the reduction in the number of ripple events is roughly consistent. The increase in spindle events under magneto-ultrasound stimulation is slightly inferior, but in comparison, the enhancement of cortical slow oscillation and hippocampal ripple synchronization under magneto-ultrasound stimulation is significantly higher than that under closed-loop intracranial electrical stimulation. This improvement may offset the insufficiency in the number of spindle events.

Figure S1: The time-frequency plots of the three types of waves and the percentage of their co-occurrence (So and spindle have approximately 85% co-occurrence, spindle and ripple have approximately 75% co-occurrence, So and ripple have approximately 50% co-occurrence).

Figure S2: Discharge rates of hippocampal and cortical nucleus neurons under different connection strengths. (Apart from the change in cortical excitatory connections to the hippocampus affecting the discharge rate of neurons, there are almost no changes in the others).

Figure S3: Changes in memory consolidation-related indicators with altered connection strengths other than the excitatory connections from the cortex to the hippocampal neurons. It does not promote memory consolidation.

Figure S4: Changes in memory consolidation indicators under different inhibitory stimulation intensities. None of the above stimulation intensities can simultaneously increase all indicators of memory consolidation, and may

even significantly impair memory consolidation.

Highlights

From experimental phenomena to computational models: Exploring the synchronization mechanisms of phase-locked stimulation in the hippocampal-thalamic-cortical circuit for memory consolidation

Denggui Fan, Jin Chen, Songan Hou, Zhengyong Song, Gerold Baier, Qingyun Wang

- **Based on the hippocampal-thalamic-cortical circuit dynamics network model, we provided the theoretical evidence for the experimental results, i.e., the promoting effect of real-time closed-loop electrical stimulation on memory consolidation**

In this study, we used a computational model to simulate the experimental stimulation process and quantify the memory consolidation indicators. We successfully reproduced the promoting effect of real-time closed-loop electrical stimulation on memory consolidation as designed in the experiment.

- **We proposed two type of improving stimulation therapies, i.e., the low current inhibitory stimulation and non-invasive magneto-ultrasonic stimulation.**

The results show that this inhibitory stimulation protocol can promote memory consolidation more efficiently. In addition, the predictive effects of non-invasive stimulation protocol is comparable to the commonly invasive intracranial stimulation, but has significant advantages in terms of side effects, cost, and difficulty of implementation. These findings provide new solutions for the treatment of memory disorders and may advance the development of clinical stimulation devices.

- **We verified the complex nonlinear properties of memory consolidation using the Mean Firing Rate (MFR) and the key role of excitatory connections between the cortex and the hippocampus in modulating dominantly memory consolidation, which providing new ideas for understanding the neural mechanism of memory process.**

From experimental phenomena to computational models: Exploring the synchronization mechanisms of phase-locked stimulation in the hippocampal-thalamic-cortical circuit for memory consolidation

Denggui Fan^a, Jin Chen^a, Songan Hou^b, Zhengyong Song^a, Gerold Baier^c,
Qingyun Wang^b

*^aSchool of Mathematics and Physics, University of Science and Technology
Beijing, Beijing, 100083, China*

^bDynamics and Control, Beihang University, Beijing, 100191, China

*^cCell and Developmental Biology, University College London, London, London WC1E
6BT, United Kingdom*

Abstract

Closed-loop phase-locking stimulation has been experimentally demonstrated to facilitate memory consolidation, which is believed to rely on the coordinated interactions among slow waves in multi-regional cortex, thalamocortical sleep spindles, and hippocampal ripples. However, the mechanisms through which this stimulation influences memory consolidation have not been thoroughly investigated. Therefore, starting from experimental phenomena, we computationally explored the synchronization mechanisms of memory consolidation in the hippocampal-thalamocortical (HTC) loop based on a firing rate model, and further reproduced the established effects of stimulation therapy on memory consolidation. The results indicate that excitatory connections between the cortex and hippocampus play a crucial role in the memory consolidation process. Additionally, our improved inhibitory closed-loop phase-locking stimulation protocol exhibits a more enhanced effect on memory consolidation compared to previous experimental stimulation schemes. Moreover, non-invasive stimulation shows lower side effects, costs, and implementation difficulties compared to invasive stimulation. Consequently, we further designed and explored the modulatory effects of a non-invasive magnetic-acoustic stimulation protocol. The results suggest that

this non-invasive magnetic-acoustic stimulation yields effects comparable to those of existing invasive experimental deep brain stimulation. Our findings may provide new evidence and perspectives for understanding the neural mechanisms of memory processes and offer potential theoretical foundations for innovative non-invasive therapeutic strategies.

Keywords: Memory consolidation;hippocampal-thalamocortical (HTC);circuit closed-loop electrical stimulation;magnetic ultrasonic stimulation;mass discharge rate

1. Introduction

Precise timing relationships among the three primary non-rapid eye movement (NREM) rhythms cortical slow oscillations (SOs), thalamic spindle waves, and hippocampal ripples—are deemed crucial for memory consolidation during sleep [1, 2, 3, 4, 5]. The interlocking of these distinct NREM rhythms serves as the coupled mechanism for memory consolidation [6, 7, 8, 9, 10, 11, 12].

Electrical stimulation has been extensively applied in the treatment of various neurological disorders, such as epilepsy and Parkinson’s disease, serving as a complementary approach to pharmacotherapy and playing a significant role in the management of these conditions [13, 14, 15, 16]. In relation to neurodegenerative diseases associated with cognitive impairment, electrical stimulation has also demonstrated the potential to improve cognitive functions. Meanwhile, external intervention can facilitate memory consolidation, with the majority of evidence supporting these theories derived from studies involving either non-invasive experiments on humans or neuronal recordings in rodents. For instance, closed-loop acoustic stimulation is employed to demonstrate that bolstering slow-wave oscillations and sleep spindles in the neocortex enhances memory [17, 18]; By enhancing the synchronization of hippocampal prefrontal neurons during sleep through closed-loop electrical stimulation, human memory consolidation is strengthened [19]; Transcranial electrical stimulation influences sleep-related memory consolidation by altering the excitability of nerve cells, thereby modifying the resting potential to achieve depolarization or hyperpolarization, which in turn fosters more slow-wave oscillatory activity and enhances memory consolidation [20, 21]. However, the effects of stimulus regulation in the aforementioned protocols have thus far been validated solely through physiological means, with a no-

table absence of direct computational theoretical evidence, the dynamics of memory consolidation remain unclear, and the outcomes of current experimental protocols fall short of enhancing various criteria pertinent to memory consolidation.

Modeling the nervous system provides a more diverse arsenal for the study of various neural functions, offering theoretical and simulation support for clinical trials[22, 23, 24, 25]. Currently, numerous neurodynamic models focused on the cortex, hippocampus, and thalamus have significantly contributed to the understanding of related neurological disorders and the mechanisms underlying brain function [26, 27, 28, 29, 30]. Prior model studies were confined to either the hippocampal-cortical or cortical-thalamic networks alone [31]. Taking into account the mediating role of thalamic spindle waves, this study employs the simplified hippocampal-thalamic-cortical neural mass model (HTC) introduced by Azimi et al. to investigate the network dynamics underlying memory consolidation [9]. This model is capable of spontaneously generating slow oscillations, slow/fast spindles, and hippocampal ripples. Without providing any code, we utilized this model to simulate the neuronal membrane potentials in the hippocampus, thalamus, and cortex. Through filtering, we identified the slow oscillations, slow/fast spindles, and hippocampal ripple events that occur during the memory consolidation process. Using the events detected post-filtering, we will explore the intrinsic mechanism of memory consolidation and study the effect of different electrical stimulation schemes on enhancing brain memory consolidation[32, 33, 34, 35].

Inspired by the above, this paper will explore the promoting effect of stimulus regulation on memory consolidation from the perspective of calculation. Referring to the experimental scheme of intracranial real-time closed-loop electrical stimulation promoting memory consolidation recently proposed in nature neuroscience [19], we will conduct numerical simulation of the experimental process through the model to make up for the shortage of computational evidence. Although the participants in the experiment were patients with medically intractable temporal lobe epilepsy, it was clearly explained that there was no correlation between the accuracy of recognition memory and the impact of stimuli on interactive epileptiform discharges (IED). It shows that epilepsy patients as the re-search object in this experiment do not affect the regulation of stimulus on memory consolidation. Therefore, we combined the HTC model to simulate the numerical calculation of the human stimulation experiment and verified the results of experiment [19]. In addition, we also designed a specific real-time closed-loop inhibitory stimulus,

and verified for the first time that adding a specific low current inhibitory stimulus can also improve the indicators related to memory consolidation, thus promoting memory consolidation. In contrast, the same stimulus without such precise time locking has no good effect on memory consolidation, which reflects the scientificity and rationality of real-time closed-loop to a certain extent. In particular, our proposed electrical stimulation scheme may better promote memory consolidation. More importantly, we have also developed a promising noninvasive stimulation scheme, namely, magnetic ultrasound stimulation, which has the same effect as experimental intracranial stimulation. All these may contribute to the development of clinical stimulation equipment for memory impairment and dementia in the future, and provide a new means to solve memory impairment. In addition, the model also predicted that altering the excitatory connection between the cortex and hippocampus has a greater impact on the discharge rate of the nucleus. Under the same stimulation, a larger change in discharge rate, compared to a smaller one, would positively enhance memory consolidation. It provides new ideas for promoting memory consolidation.

2. Materials and Methods

2.1. *Experimental Data*

This paper is referring to the experimental data from eighteen participants with pharmacologically intractable temporal lobe epilepsy. It was shown that epilepsy patients as the research object in this experiment do not affect the regulation of stimulus on recognition memory consolidation [15]. Participants were tested in two experimental nights: intervention night and undisturbed night. At the intervention night, real-time closed-loop (RTCL) stimulation was used in NREM early sleep. One intracranial electroencephalogram (iEEG) electrode in the medial temporary lobe is used as a synchronous probe to determine the time of closed-loop control, while the second neocortical iEEG electrode is used as a stimulation site (usually in the white matter of the orbital frontal cortex, 15 of the 19 stimulation nights). The slow wave activity of the probe was monitored and analyzed in real time to trigger a short (50ms) high frequency (100Hz) electrical stimulation event at the neocortical stimulation site about every 4 seconds. There are two operation modes of intervention, namely (I) "synchronous stimulation" (II) "mixed stage stimulation", which are respectively applied to two groups of different participants.

2.2. Structure of HTC

As shown in Figure 1, this HTC circuit structure consists of two hippocampal networks, representing the CA1-CA3 network, one thalamic network, and two cortical networks, respectively. The strength of short-range synaptic connections between neurons in a separate CA3-CA1 network and a separate cortical thalamic network is much greater than that of the CA3-CA1 network and cortical network neurons in remote synaptic connections, similar to the three small world networks[9].

2.3. Network Dynamics of HTC

The HTC network is modelled with the rate model[9]:

$$\begin{aligned} \frac{dV_q^k}{dt} = & -\frac{V_q^k}{\tau_q} - \sum_{n=1}^3 x_n N_{j_n}^{k_{n1}} P_{j_n i}^{k_n} J_{j_n i}^{k_n} (c^k) r(V_{j_n}^{k_{n1}}) \\ & + \sum_{m=1}^5 x_m N_{j_m}^{k_{m1}} P_{j_m q}^{k_m} J_{j_m q}^{k_m} r(V_{j_m}^{k_{m1}}) + k_l \frac{f(u_l)}{A_l} \end{aligned} \quad (1)$$

$$\frac{dc^k}{dt} = -\frac{c^k}{\tau_c} + \sum_{n=1}^3 y_n N_e^{k_n} P_{ee}^{k_{n1}} \Delta c^k r(V_e^{k_n}) \quad (2)$$

where, V_q^k is the membrane potentials, A_l is the specific membrane capacitance, c^k and Δc^k are respectively the adaptation variable of neuron k and its increment, $N_{j_n}^{k_{n1}}$ and $N_{j_m}^{k_{m1}}$ are the number of neurons, where $x_n, x_m, y_n, k_l \in \{-1, 0, 1\}$; $n = 1, 2, 3$; $m = 1, 2, 3, 4, 5$; $l \in \{t, r\}$; $q, j_n \in \{i, e, t, r\}$; $k, k_{n1} \in \{CA1, CA3, CX1, CX2, TH\}$; $k_n, k_m \in \{CA1, CA3, CX1, CX2, TH, CA3 - CA1, CX1 - CA1, CA1 - CX, CX2 - CA3, CX2 - CX1, CX1 - TH, TH - CX1, CX2 - TH\}$.

The probability and strength of the network from neurons m to neurons n are determined by P_{mn}^{k-h} and J_{mn}^{k-h} , where k and h can be CA1, CA3, CX (representing the cortex) or TH (representing the thalamus), n can take t (representing TC neurons), r (representing thalamic RE neurons), e (representing cortical or hippocampal excitatory neurons), and i (representing cortical or hippocampal inhibitory neurons), while m can only take one of the excitatory neurons t or e .

The firing rate (r) of Hippocampal and cortical neurons is a sigmoid function of the membrane potential (V_m^k) as follows:

$$r(V_m^k) = r_0 + \frac{r_1}{1 + \exp[-(V_m^k - V_m^{*k})/g_m^k]} \quad (3)$$

$$\{m\} \in \{e, i\}, \{k\} \in \{CA1, CA3, CX\}$$

where $r_1(r_0)$ is the maximum (minimum) discharge rate of neurons m in a completely depolarized state, V_m^{*k} is the threshold discharge potential of neurons m , g_m^k is the dependence of discharge rate on membrane potential.

J_{mn}^k indicates the strength of the connection from neuron m to neuron n . Dendritic spike frequency adaptation (DSFA) is considered applicable to all excitatory to excitatory connections, J_{ee}^k is a decreasing sigmoid function of an adaptation variable, c , representing the mean adaptation level of an excitatory neuron:

$$J_{ee}^k(c^n) = \frac{J0_{ee}^k}{1 + \exp[(c^n - c^*)/g_c]} \quad (4)$$

$$\{n\} \in \{CA3, CA1\}, \{k\} \in \{CA3, CA3 - CA1\}$$

where, $J0_{ee}^k$ is the maximal synaptic strength corresponding to adaptation level at equilibrium value (set to be zero). $c^* = 10$ is the threshold adaptation level and $g_c = 3$ shows the sharpness of the excitatory to excitatory connection dependence on the adaptation variable. The adaptation level increases by Δc_n .

The function $f(u_l)$ in Eq.(1) is a sigmoid function that can be expressed as:

$$f(u_l) = \frac{-f_l^{\max}}{1 + \exp\left[\frac{(u_l + f_{th}^l)}{q_l}\right]}, \{l\} \in \{t, r\} \quad (5)$$

where u_l is a bursting variable particularly defined for thalamic neurons to model T-type calcium currents:

$$\frac{du_l}{dt} = \frac{b_l - u_l}{\tau_l^u} \quad (6)$$

where τ_l^u is the time constant, $b_l = 0$ is $V_r^{TH} > 0mV$ or $V_t^{TH} > -0.1mV$, otherwise $b_l = -200mA$. Then the discharge rate of thalamic neurons is

defined as:

$$r(V_m^{TH}) = \frac{R_m^T}{1 + \exp\left[\frac{V_m^{TH} - V_m^T}{g_m^T}\right]} (\exp[L_m u_m]) + \frac{R_m^B}{1 + \exp\left[\frac{V_m^{TH} - V_m^B}{g_m^B}\right]} (1 - \exp[L_m u_m]) \quad (7)$$

where, R_m^T (R_m^B), V_m^T (V_m^B) and g_m^T (g_m^B) is maximum firing rate, threshold firing potential, and the sharpness of the firing rate.

The corresponding parameter values of HTC model network can be found in Supplementary Materials. The numerical calculation is conducted by the MATLAB software and using the fourth-order Runge Kutta method with a time step of $1ms$.

2.4. Transcranial magneto-acoustical stimulation

Utilized standard Cartesian coordinates, assuming longitudinal pressure waves along the z axis and a magnetostatic field along the x axis, with current density aligned with the y axis. The longitudinal wave follows the classical wave equation[32].

$$\frac{\partial^2 u}{\partial z^2} = \frac{1}{c_0^2} \frac{\partial^2 u}{\partial t^2} \quad (8)$$

The displacement u represents the distance of an ion from its equilibrium position, with c_0 denoting the ultrasonic velocity. For a progressive sine wave, the instantaneous velocity v of an ion can be described as:

$$v_z = W \sin(\omega t - \varphi) \quad (9)$$

where W is the ion velocity, $\omega = 2\pi f$ is the angular frequency, and f is the ultrasonic frequency. The relationship between fluid velocity and instantaneous pressure P can be expressed as

$$P = \rho c_0 \omega \quad (10)$$

where ρ is the tissue density. According to Montalibet's theory, the current density J_y can be expressed as

$$J_y = \sigma \frac{w B_x}{1 + \tan^2 \psi} \sin(\omega t - \psi) \quad (11)$$

where σ is the tissue conductivity, with a typical value of 0.5 siemens /m. B_x is the static magnetic field strength, and ψ is the phase angle.

$$\tan \psi = \omega \tau \quad (12)$$

where τ is the time constant, typically femtoseconds for an electrolyte, and can be neglected for medical ultrasonic frequencies (200 – 700kHz) . From this, we derive a simplified formula for neuronal discharge induced by ultrasound:

$$J_y \approx \sigma w B_x \sin \omega t \quad (13)$$

The relationship between ultrasonic power intensity and ultrasonic pressure satisfies the following equation

$$\Gamma = \frac{1}{2} \frac{P^2}{\rho c_0} \quad (14)$$

Combine the above equations to get the final formula

$$J_y \approx \sigma B_x \sqrt{\frac{2\Gamma}{\rho c_0}} \sin(2\pi f t) \quad (15)$$

Thus, in transcranial Magnetoacoustic stimulation, we can intermittently switch the magnetic field stimulation, so that the pulse ultrasound can better simulate the pulse current in DBS.

2.5. Firing Characteristics of HTC on the Memory Consolidation

2.5.1. Events Detection Methods

In the second stage of non rapid eye movement sleep, the appearance of spindle waves marks a specific pattern of brain activity, closely related to cognitive functions such as sensory signal transmission, synaptic plasticity, memory consolidation, and intellectual development. Ripple waves mainly appear in the hippocampus and are related to the process of memory consolidation, although they have also been observed in areas outside the hippocampus. Slow waves and oscillations are associated with deep sleep and are important manifestations of synchronized brain activity. The specific detection method is as follows:

Spindle Similar to existing methods [36], The 4th order zero phase delay Butterworth bandpass filter is applied to the local field potential (LFP)

of cortical network 2, and the frequency is adjusted to 9Hz-16Hz. In the experiment, it is adjusted to 12Hz-16Hz. Then we use Hilbert transform to extract the phase and calculate the instantaneous amplitude, which is smoothed through a 300 millisecond Gauss window (standard deviation=0.65). Spindle events are identified by amplitude exceeding the threshold by one standard deviation and duration between 0.5 and 3.5 seconds. Adjacent events with an interval of less than 0.5 seconds are merged.

Ripple Similar to previous research [37], firstly, the fourth-order zero phase delay Butterworth bandpass filter was applied to the membrane potential of CA1 pyramidal neurons. The target frequency range was 80hz-150hz, and the experimental focus was 80hz-100hz. The instantaneous amplitude is calculated by deriving the phase through Hilbert transform. Subsequently, a 50 millisecond Gaussian smoothing window is used to enhance the signal definition. Our criteria for identifying ripple events include amplitude exceeding the median plus two standard deviations and a minimum duration of 30 milliseconds.

Slow Oscillation Similar to [9], we first perform the bandpass filtering (12Hz-16 Hz, 3th order zero phase delay Butterworth) to the membrane potential of excitatory neuron of cortical network 2. Afterwards, the positive and negative peaks of the signal are calculated. When the distance between two consecutive positive and negative zeros in different directions is between 0.5s and 2s (corresponding to 0.5Hz to 2 Hz), the difference between the positive and negative peaks of the signal is greater than the threshold (1.4SD of the average negative peak), and the negative peak is greater than the threshold (1.4SD of the average negative peak), an slow oscillation (So) event can be identified.

Slow Wave Refer to [38], firstly, the membrane potential signal of excitatory neuron of the hippocampal network is band-pass filtered (0.125Hz-1.6Hz, two pass fir band pass filter, order = three cycles of the low frequency cut-off); Secondly, the positive and negative peaks of the signal are calculated. When the distance between the positive and negative zeros in two consecutive directions is between 0.8s and 2s, and the amplitude standard is met at the same time, the difference between the positive and negative peaks of the signal is greater than the threshold (1.4SD of the average negative peak), and the negative peak is greater than the threshold (1.4SD of the average negative peak), the slow wave event can be identified.

2.5.2. Temporal nesting of cortical slow oscillations, thalamic spindles, and hippocampal ripples

The neuronal membrane potentials of the hippocampus and thalamic cortex were processed using the aforementioned filtering methods to obtain ripple (100-250Hz), So (0.5-2Hz), and spindle waves (12-16Hz) (Figure 2a). Their time-frequency charts (see Figure S1, using a Molet wavelet transform with a cycle of 3 and scaling factor of 0.8) and ripple frequency spectra (Walch's method) (Figure 2b) can be derived from the eeglab toolbox. Existing experiments demonstrate that during the slow-wave sleep (SWS) process, most ripples and slow oscillations coincide with spindle waves [9, 39]. To investigate the coupling mechanisms among spindle waves, ripples and slow oscillations, we contrasted the characteristics of spindle waves both isolated (8Hz-12Hz, 12Hz-16Hz) and in conjunction with ripples (100Hz-250Hz), measuring the amplitude and duration of those occurring concurrently with the ripples (within ± 0.1 s of the ripple's peak) and those not. Our simulation findings align with experimental results presented in Figure 10 (f) of [10]. Slow and fast spindle waves, in conjunction with ripples, exhibit greater duration and amplitude than those occurring in isolation. Specifically, fast (or slow) spindle waves synchronized with ripples demonstrate a higher amplitude and longer duration than isolated ones. Differently, 72.59% of fast spindle waves are coupled with ripples, while 83.47% of slow spindle waves are coupled with ripples (Figure 2d,e).

Additionally, during the SWS process, slow oscillations, spindle waves, and ripples tend to co-occur, fostering memory consolidation. To further investigate the interactions among these factors in enhancing memory consolidation, we will calculate the percentage of pairwise co-occurrences, using the same detection method as before. Our numerical findings align with existing experimental results [9] (Figure 2c, Figure S1).

2.6. Indexes measuring memory consolidation

2.6.1. Phase Locked Value (PLV)

The signal should first be filtered and the phase is obtained by Hilbert transform. The closer the PLV is to 1, the closer the two signals are to synchronization, which is calculated by:

$$PLV = \frac{1}{N} \left| \sum_{n=1}^N \exp(j\theta(t, n)) \right| \quad (16)$$

where N represents the number of trials, i.e. trials $n[1 \dots N]$, $\theta(t, n)$ represents the instantaneous phase difference of the same trial for different leads, $\exp(j\theta(t, n))$ represents the using of Euler's formula to obtain complex phase, $\sum_{n=1}^N$ overlays the complex signals of all trials, $\frac{1}{N} |\cdot|$ obtain the amplitude of the superimposed complex signal and calculate the average.

2.6.2. Duration of slow wave sleep ripple

Ripples, typically occurring within the valleys of spindle waves, signify the active phase of these oscillations. Prior research indicates that optogenetic stimulation can extend the duration of spontaneous hippocampal ripples, thereby enhancing memory consolidation. Consequently, the total duration of ripples is a key metric for assessing the impact of stimulation protocols on memory consolidation during spatial learning tasks.

2.6.3. Amplitude, duration and number of spindles in slow wave sleep

Sleep spindles, characteristic of stage 2 NREM sleep, are linked to enhanced memory consolidation through their amplitude and duration[40, 41, 42, 43], which reflect multiregional brain interactions. Evidence supports the positive correlation between spindle characteristics and memory improvement. Here, we focus on the total count, cumulative duration, and average amplitude of spindles to explore their role in memory consolidation.

2.6.4. Number of slow wave sleep So

Transcranial electrical stimulation (tDCS) experiments[44] have shown that enhancing slow oscillation activity during sleep bolsters memory consolidation. Accordingly, we will assess the total slow oscillation (So) activity generated during sleep for its impact on memory.

2.6.5. Percentage of co-occurring oscillations

Memory consolidation at night is closely tied to the synchronized presence of spindle waves, slow oscillations (So)[45], and hippocampal ripples. Direct evidence indicates that their combined occurrence extends both their duration and amplitude, which is more effective than when they occur alone. Increasing the co-occurrence of these oscillations is key to improving memory consolidation.

2.7. Stimulation settings

Stimulation protocols will be introduced into the cortical subnetwork of HTC circuit to regulate cortical activity during sleep, and to assess its impact

on sleep electrophysiology and the consolidation of memory throughout the night.

2.7.1. *Experiment Protocol*

The experiment [19] used a real-time closed-loop method to monitor and analyze slow-wave activity in the hippocampus, with a five-minute pause block, and a short (50 ms) high-frequency (100 Hz) electrical stimulation event was triggered at neocortical stimulation sites approximately once every 4s with a 5-min stimulation block of 1 ms per pulse width (Figure 3). For stimulation open-loop control, the method was added directly to the cerebral cortex, unlike high-frequency stimuli with a fixed interval of 4s and 50ms (Figure 3). For model calculations, besides to setting the total duration to 1200s, we basically carry out the stimulation according to the experimental protocol.

2.7.2. *Inhibitory stimulus*

Hippocampal ripples, recognized for their pivotal role in memory consolidation and their profound impact on neocortical activity during sleep, are central to our investigation into real-time closed-loop stimulation [46, 47]. Our stimulation form was consistent with the experiment, with a distinct addition: brief stimulation bursts of 10 milliseconds are delivered at 10-millisecond intervals within 100-millisecond blocks, interspersed with 100-millisecond pause blocks to allow for no stimulation during these intervals (Figure 3). A preliminary 1-second ignition phase ensures system stability by dampening the effects of initial perturbations. The detection window is set at 200 milliseconds, reflecting the transient nature of ripple events, which do not exceed 200 milliseconds in duration. Upon ripple detection, a 6-second stimulation cycle on the cortex is initiated, proceeding without additional testing in a continuous sequence. Consistently, the closed-loop system modulates the intervals between stimuli based on the ripple events detected. Among them, the pause block was also detected, but the stimulus intensity was 0 (Figure 3).

It comprises a sequence of equidistant rectangular pulses, with each pulse lasting for $stitime$ and the interval between pulses being determined by the signal's frequency:

$$s[n] = \text{strength} \cdot 1_{\left[\left\lfloor \frac{n}{10h} \right\rfloor \cdot \frac{1}{\text{freq}}, \left\lfloor \frac{n}{10h} \right\rfloor \cdot \frac{1}{\text{freq}} + \frac{stitime}{h} \right)}(n) \quad (17)$$

where, freq is the frequency of the pulse (Unit:Hz) and strength is the amplitude of the pulse, h is the sampling interval (Unit:s) stitime is the duration of a single pulse (Unit:s), duration is the duration of the entire signal (Unit:s). $s[n]$ is the signal value at the n^{th} sampling point, n is the index of the sampling point, $n = 1:\text{floor}(1000/\text{freq}):N$, where $N = \text{duration}/h$ is the total number of sampling points. $1[a, b)$ is an indicator function, when $a \leq x < b$, $1[a, b)(x) = 1$, else $1[a, b)(x) = 0$. $\lfloor x \rfloor$ indicates the rounding down of x .

2.7.3. Transcranial magneto-acoustical stimulation (TMAS)

All the aforementioned stimulation methods are intracranial, therefore, we here introduce the non-intracranial magneto-acoustical stimulation (Figure 3) to search for the comparable effects of experimental intracranial closed-loop stimulation with the aim of providing the promising clinical stimulation therapy[32].

The principle of TMAS is that the action of a focused ultrasonic wave moves charged ions in the nerve tissue. Because a magnetostatic field is perpendicular to the movement direction of the charged ions, the Lorentz force on the ions can be induced in the tissue. The Lorentz force separates the positive and negative ions in opposite directions, thereby forming the electric current I_{ext} to stimulate neurons. The TMAS current can be finally expressed as follows (see the detailed derivation from the supplementary materials):

$$J_y \approx \sigma B_x \sqrt{\frac{2\Gamma}{\rho c_0}} \sin(2\pi f t + bias) \quad (18)$$

We added a bias on this basis, where in order to generate an action potential, the ultrasonic wave needs to be a sine wave with bias. Thus, during the magnetoacoustic stimulation, we can intermittently switch the magnetic field stimulation, so that the pulse ultrasound can simulate the pulse current in DBS, which can be modeled as:

$$x(t) = \begin{cases} 1 & (n-1)\frac{1}{RF} < t \leq [(n-1) + DC]\frac{1}{RF}, n = 1, 2, 3 \dots \\ 0 & \text{Others} \end{cases} \quad (19)$$

where RF is the repetition frequency and DC is the duty cycle. So the experimental stimulation process can be submitted by the TMAS stimulation,

i.e.:

$$S_{TMAS} = J_y \times x(t) \quad (20)$$

3. RESULTS

3.1. *Reproduction of the Experimental DBS*

3.1.1. *Dynamic explanation of memory consolidation enhancement*

Memory consolidation is intricately connected to the dynamics of the brain. To gain deeper insights into the kinetic mechanisms that drive changes in memory consolidation, we meticulously calculated the mean firing rate (MFR) of neurons nuclei within the HTC network. By adjusting the strength of the connections between the hippocampus and cortex, we unveiled the pivotal role of excitatory interactions from the cortex to the hippocampus in regulating neuronal firing rates and the dynamics of memory consolidation.

Under conditions that enhance excitatory connectivity from the cortex to the hippocampus, there were significant alterations in nuclear firing rates, particularly a marked increase in the MFR of excitatory neurons in the CA1 region(Figure 4a). This discovery highlights the system’s acute sensitivity to these connections. In contrast, modifications to the strength of other connections had a negligible impact on the firing rates of the network (see Figure S2). Naturally, since the changes pertain to the strength of connections between the hippocampus and neocortex, they do not substantially affect the firing rates of neurons in the thalamic nuclei (see Figure 5). We found that nuclear firing rates with significant changes had a positive effect on the promotion of memory consolidation (Figure 4b). Employing an experimental stimulation method with an intensity of 3200mV, the outcomes qualitatively align with experimental results (Reference [19], Figure 1f). That is, closed-loop stimulation promotes synchronization between the hippocampus and cortex, increasing spindle waves events and slow oscillations events while concurrently reducing hippocampal ripples.Stimuli that lack precise temporal control do not significantly affect memory consolidation. A general decline in the synchronization of thalamocortical spindles and hippocampal ripples, coupled with a significant decrease in the number of cortical slow oscillations, may lead to a decline in the function of memory consolidation. However, the synchronization of cortical slow oscillations with hippocampal ripples and an overall increase in the number of spindles may counteract the adverse effects of the aforementioned indicators’ decline, ultimately yielding

results consistent with experimental qualitative analysis (Figure 4c). However, parameters that have little effect on nuclear firing rates do not promote memory consolidation (see Figure S3).

To further demonstrate that altering the strength of cortical-hippocampal excitatory connections can change the entire system’s modality, we calculated the variation in nuclear neuron firing rates as a function of stimulation intensity. Under experimental settings with fixed connection strength, the analysis of nuclear firing rates in response to varying stimulus intensities showed no significant changes, further underscoring the importance of the strength of cortical-hippocampal excitatory connections in memory consolidation (see Figure 6).

3.1.2. Stimulation results in the case of the experimental

According to the experimental parameter settings (stimulation current range of 0.5mA to 1.5mA, resistance range of 1-4 k Ω), we set a voltage range of 2500mV to 3500mV in the model to match the stimulation current size in the experiment as much as possible. Each stimulus intensity and no stimulus state were calculated at the same initial value, and we counted the results of 12 different random initial values to ensure the reliability and scientificity of the results. Given the importance of the temporal coupling between cortical slow oscillations and cortical thalamic spindles, as well as hippocampal ripples, in memory consolidation, we specifically explored slow oscillations (0.5Hz-2Hz) in the cortex rather than slow waves (0.16Hz-1.25Hz) in the model. In addition, we replace the phase locking ratio of neurons with the phase locking value between waveforms. Our numerical simulation results can be qualitatively compared with the "Results" section in reference [19]. Real-time closed-loop stimulation can improve the synchronization between cortical thalamic spindles and hippocampal ripples within a certain stimulation intensity (Wilcox-test) (Figure 7b(i)); It also improved the synchronization between cortical slow oscillations and hippocampal ripples (Wilcox-test) (Figure 7b(ii)). The observed increase in the number of spindle waves is consistent with experimental data, and the number of spindle waves significantly increases at specific stimulus intensities ($p = 0.0266$, $p = 0.0132$, $p = 0.0515$, $p = 0.0627$, representing stimulation intensities of 2500 mV, 2700 mV, 2800 mV, 3300 mV, respectively, Wilcox-test)(Figure 7b(iii)) ; The slow oscillation of the cortex also generally increased (Figure 7b(iv)); And the number of hippocampal ripple events decreased significantly under specific stimulus intensities, especially under high-intensity stimuli ($p = 0.00728$, $p = 0.0117$,

$p = 0.00699$, $p = 0.103$, $p = 0.0272$, $p = 0.00295$, representing stimulation intensities of 2600 mV, 3000 mV, 3200 mV, 3300 mV, 3400 mV, 3500mV, wilcox-test, respectively) (Figure 7b(v)). The results and changes of the above closed-loop events are significantly consistent with the experimental results, thus verifying the effectiveness of the model in reflecting the complex dynamics of memory consolidation processes.

For stimuli that were not precisely timing-locked (Figure 7a), qualitative results were also obtained with the model. This form of stimulation enhanced the synchronization between hippocampal ripples and cortical slow oscillations (Figure 7a(ii)). Notably, this effect was pronounced at specific stimulus intensities(p values of 0.00466, 0.0281, 0.0148, and 0.00295 corresponding to 2700 mV, 2800 mV, 3200 mV, and 3500 mV, respectively Wilcox-test), as well as the number of spindle events (Figure 7a(iii)). However, there was a general decline in the synchronization between hippocampal ripples and thalamocortical spindles (Figure 7a(i)). Particularly concerning the cortical slow oscillations, a significant reduction was observed across all stimulus intensities, indicating a detrimental effect on memory consolidation (Figure 7a(iv)) (mean p value of 0.00276 Wilcox-test). The number of individual ripple events also decreased, consistent with the experimental results, suggesting that this form of stimulation leads to a general reduction in hippocampal ripples (Figure 7a(v)). These results reflect the nuanced impact of open-loop stimulation on memory consolidation. The observed decrease in synchronization between hippocampal ripples and thalamocortical spindles, along with a significant reduction in the number of cortical slow oscillations, directly contributes to the weakening of memory consolidation function. However, the increased synchronization between hippocampal ripples and cortical slow oscillations, coupled with a significant rise in spindle events, may counteract these effects, resulting in no significant overall change in the outcome of stimulation.

3.1.3. *Experimental two-parameter prediction*

For the experiment, the stimulus intensity was varied from 0.5mA to 1.5mA, while the frequency was consistently set at 100Hz, a parameter likely determined through meticulous tuning as referenced in study [19]. Our computational simulations qualitatively reproduced the experimental outcomes, indicating that an optimal stimulation intensity at the fixed 100Hz frequency was not discernible. To numerically validate the experimental frequency and explore potential superior frequencies, the stimulation frequency was sys-

tematically altered to 40Hz, 100Hz, 200Hz, 300Hz, 400Hz, and 500Hz, with constant voltage and consistent methodology. The total simulation time is 1200s. Given the challenge of using the diminishing count of ripple events as an indicator of memory consolidation, we focused on four alternative metrics. A heatmap in Figure 8, except for the number of So, which did not show significant improvement, all other indicators showed clear advantages, so we can consider that the 100Hz frequency is indeed more favorable. This finding from our numerical simulations corroborates the rationality of the frequency selection in the original experiments.

3.2. Improvement for the Experimental DBS

3.2.1. Inhibitive stimulation

During sleep, extensive interactions occur between the hippocampus and the neocortex, and active intracranial interventions can promote memory consolidation to a certain extent. In this study, we designed a real-time closed-loop inhibitory electrical stimulation scheme, incorporating seven indicators related to memory consolidation to assess the efficacy of the stimulation protocol. The stimulation was set to low voltage (50 mV to 250 mV) and high frequency (500 Hz) inhibitory stimulation, which is well below the safe maximum values for both long-term and short-term stimulation [48], with a total simulation duration of 600 seconds. To facilitate the observation of changes in indicator values, we made some proportional adjustments.

Our results indicate that regardless of the magnitude of inhibitory stimulation added, the PLV values of spindle waves and ripples are increased. The PLV values between So and spindle waves, as well as between So and ripples, are universally enhanced. However, other indicators, not limited to the number of events, including percentages, the amplitude of events (spindle), and the duration of events (spindle and ripple), generally decrease under intermediate stimulation intensities, with some showing significant declines (Figure 9b, Figure S4). To further select the optimal stimulation intensity, each stimulation intensity was compared with the results under no stimulation conditions. For closed-loop stimulation, two stimulation intensities (90 mV, 70 mV) were identified, where all indicators showed universal improvement, with most showing significant enhancement. At a stimulation intensity of 90 mV, the synchronization values among the three, the number of spindle events, the number of ripple events, the average amplitude of spindle events, the total duration of ripple events, and the percentage of all co-occurrences were all significantly increased ($p < 0.001$, mean: $p = 0.00013$, Wilcoxon-test),

with no significant difference in other indicators. At 70 mV, similar improvements were observed, with significant increases in PLV values, the number of So and ripple events, the average amplitude of spindle events, and the percentage of co-occurrence between So and ripples ($p < 0.001$, mean: $p = 0.00002$, Wilcoxon-test), again with no significant difference in other indicators (Figure 9d).

In open-loop stimulation, there is no need to detect hippocampal ripples; instead, the same stimulation is directly applied to the cerebral cortex (Figure 3). Similar to closed-loop stimulation, the PLV values of spindle waves and ripples are increased, and the PLV values between So and spindle waves, as well as between So and ripples, are generally improved. However, other values, including the number of events, percentages, event amplitude (spindle waves), and duration (spindle waves and ripples), are usually reduced under moderate stimulation intensities, with some even showing significant decreases (Figure 9a). Similarly, three optimal stimulation intensities were selected for comparison (130 mV, 110 mV, and 90 mV). Compared to the no-stimulation condition, there was a general improvement in indicator values. At stimulation intensities of 130 mV and 110 mV, the PLV values, the number of spindle events, the number of So and ripple events, the average amplitude and total duration of spindle events, and the percentage of all co-occurrences were significantly increased ($p < 0.001$, mean: $p = 0.0004$ for 130 mV, and $p = 0.0007$ for 110 mV, Wilcoxon-test). At a stimulation intensity of 90 mV, similar improvements were noted, with significant increases in PLV values, the number of So and ripple events, the average amplitude and total duration of spindle events, and the percentage of co-occurrence between So and ripples ($p < 0.001$, mean: $p = 0.0009$, Wilcoxon-test)(Figure 9c).

To evaluate the comparative efficacy of open-loop and closed-loop stimulation on memory consolidation, we calculated the percentage increase in various indicators compared to the no-stimulation condition at three open-loop and two closed-loop stimulation intensities (Figure 9e, Left). The analysis revealed that the optimal intensity for open-loop stimulation was 110 mV, while the most effective intensity for closed-loop stimulation was 90 mV. A direct comparison between the most effective open-loop (110 mV) and closed-loop (90 mV) stimulation intensities indicated that closed-loop stimulation achieved superior results (Figure 9e, Right). This suggests that closed-loop stimulation is more effective in enhancing memory consolidation even at lower stimulation intensities, highlighting its advantages and aligning with the experimental conditions.

Furthermore, a numerical comparison with experimental data showed that the maximum increase in the phase-locking value (PLV) between So and ripples in experiment [19] was 14.19%, and the maximum increase in the PLV between spindle waves and ripples was 19.54%. The maximum increase in the number of spindle events was 11.14%, and the maximum increase in the number of SO events was 6.04%. Clearly, our inhibitory stimulation protocol achieved a greater enhancement compared to the experimental results (Figure 9e).

3.2.2. Two-parameter prediction of inhibitory stimulation

To delve deeper into the impact of stimulus frequency on memory consolidation, we selected a range of stimulus frequencies (100Hz, 200Hz, 250Hz, 400Hz, and 500Hz), based on the outcomes of inhibitory stimuli, selected low stimulation intensities (below 150 mV) for both open-loop and closed-loop experiments. Aligning with experimental benchmarks, we analyzed changes in the number of events and the synchronization between the cortex and hippocampus. The total simulation time is 600s. Simulation results revealed that, regardless of the stimulation intensity or frequency, stimulation at 90mV to 150 mV consistently outperformed the no-stimulation condition (Figure 10a). Furthermore, the overall performance of closed-loop stimulation was superior to that of open-loop stimulation. Additional analyses of the impact of stimulation frequency at average stimulation intensities indicated that, except for the minimal number of So events at the high frequency of 500Hz, other indicators generally increased with increasing stimulation frequency (Figure 10b). These findings reaffirm the rationality of our chosen stimulation frequencies.

3.3. Comparable effect of non-invasive Transcranial Stimulation

In this study, we investigated the feasibility of enhancing memory consolidation using a composite magnetic and ultrasonic stimulation. Given that the induced current is a product of the magnetic field and ultrasonic waves, the primary resistance in our model is attributed to the cerebral cortex. Previous studies have shown that the resistance of the cerebral cortex is approximately between several thousand to tens of thousands of ohms, therefore, to better align with the resistance provided by the cortex, the resistance was set to a high value (15 k Ω) in our simulations. Through iterative testing, we identified a set of optimal parameters (see Table S2). With these parameters held constant, adjusting the bias range from 1 to 4 yielded favorable outcomes

for memory consolidation (Figure 11a), particularly in the number of ripple events, which corresponded with the results from experimental closed-loop intracranial stimulation (Figure 11a(ii)). To further assess the effectiveness of magneto-ultrasonic stimulation in enhancing memory consolidation, we compared it with the results from closed-loop intracranial experiments, with a simulation duration set to 20 minutes.

Numerical simulation results demonstrate that both stimulation methods are equally effective in promoting memory consolidation. To ensure a fair comparison, we performed a differential analysis of five indicators under various initial conditions in the absence of stimulation, revealing that the experimental outcomes are largely independent of initial values (Wilcox-test) (Figure 11b). Subsequently, we compared the outcomes of the two stimulation methods and conducted a significant difference analysis. In magneto-ultrasonic stimulation, only the bias was varied (1-4). For closed-loop intracranial stimulation, parameters remained consistent, with adjustments made to the voltage range (2500mV-3500mV). The synchronization gain between thalamocortical spindles and hippocampal ripples, along with the increase in the number of cortical slow oscillation events, did not exhibit significant differences ($p=0.7646484$ for spindle-ripple PLV, $p=0.0673828$ for the number of So events, Wilcox-test) (Figure 11c(iii,iv)). Furthermore, the reduction in the number of ripple events was found to be largely consistent between magneto-ultrasonic stimulation and closed-loop intracranial electrical stimulation ($p=0.2783203$, Wilcox-test) (Figure 11c(ii)). However, the increase in the number of spindle events was significantly lower with magneto-ultrasonic stimulation compared to closed-loop intracranial stimulation ($p=0.0097284$, Wilcox-test) (Figure 11c(i)). In contrast, the enhancement of synchronization values between cortical slow oscillations and hippocampal ripples was markedly higher with magneto-ultrasonic stimulation than with closed-loop intracranial electrical stimulation ($p=0.0048828$, Wilcox-test) (Figure 11c(v)). Although this improvement may offset the deficiency in the number of spindle events, the actual effects necessitate further experimental confirmation. We do not assert that the selected parameters are the best possible, but we propose that TMAS, under conditions of comparable efficacy, has the potential to serve as a potent non-invasive method for disrupting brain rhythms, with implications for both diagnostic and therapeutic applications. The substitution of magneto-ultrasonic stimulation for closed-loop intracranial stimulation could be advantageous for patient care and cost considerations.

4. Conclusion and Discussion

Existing research indicates that physiological experiments including closed-loop auditory, electrical, magnetic, and transcranial electrical stimulation can enhance memory [13, 19, 35, 49]. Yet, research into the dynamics of external stimuli in regulating memory consolidation within the HTC network during sleep is relatively scarce [34, 36]. This study employed the HTC network model to explore the generation and coupling mechanisms of slow-wave sleep rhythms [50, 51, 52, 53]. The existence of a two-way communication between the PFC (anterior cingulate cortex) and hippocampus has been reported previously [54]. Hence similar to a recent modeling study [55] in the full model consisting of CA3-CA1 networks and the thalamocortical networks, the cortical networks are recurrently connected to CA3-CA1 network so that all the anatomical connections from the thalamocortical network to the hippocampus are modeled by one projection from the cortex to the hippocampus. Our computational approach unveiled the intrinsic regulatory mechanisms of memory consolidation under external stimuli and introduced a novel inhibitory intracranial stimulation protocol to bolster memory consolidation. We identified seven markers linked to memory consolidation based on experimental findings, and quantified how various stimulus intensities and frequencies impact memory consolidation using a model of the HTC network, allowing for concurrent observation of multiple marker changes.

Earlier studies have demonstrated an association between increased spindle wave frequency during NREM in older subjects and memory impairment [43], as well as an inverse correlation between spindle wave frequency and cognitive ability in children [46, 47, 48]. Consequently, spindle wave frequency should be incorporated into subsequent research. Similarly, we will consider an increasing array of indicators for memory consolidation in the future to enhance the precision of our stimulation protocols. We have successfully replicated the effects of prior experimental techniques using this model. Hence, going forward, we will employ this model to replicate existing experiments, devise diverse and reliable electrical stimulation protocols. Furthermore, we will apply varying or identical stimuli to distinct brain regions simultaneously, continually adapting stimulation protocols to predict experimental outcomes. We can also observe the impact of external stimuli on the network manifold structure, among other effects.

Several features of our experimental design enhance its rationality. These include: (i) incorporating electrical stimulation to the cortex, based on the

detection of hippocampal ripples, to influence the hippocampal-neocortical pathway; (ii) synchronizing electrical stimulation with the hippocampal ripples to synchronize more ripples; (iii) given that nerve damage appears closely related to excessive fiber activity, we developed an intermittent stimulation strategy. Additionally, considering the comfort and safety of electrical stimulation, this strategy features low stimulation intensity, high-frequency inhibition, and brief stimulation duration; (iv) our setup allows for continuous changes in stimulation amplitude and frequency to explore more effective, comfortable, and safe stimulation protocols; However, we do not assert that the specific timing and stimulation parameters in this paper are definitively optimal. Future research should investigate whether simultaneous refinement of stimulation timing and other parameters can further enhance memory consolidation.

In summary, our research transcends traditional models, employing a comprehensive hippocampal-cortical-thalamic model to explore how external stimuli influence the dynamics of slow oscillations, spindle waves, and ripples—key to memory consolidation. On the basis of accurately reproducing existing experimental results using this model, we ensured the scientific and accurate nature of the model, induct the concept of using inhibitory intracranial stimulation during sleep to enhance memory, challenge the norm of excitatory stimulation. showing that carefully designed inhibitory stimuli can also bolster memory. And the effect is better. In addition, we also explored an extracranial stimulation method using transcranial magnetic ultrasound stimulation to promote memory consolidation, and conducted in-depth research on the effects of connections between different neurons on memory consolidation. Our results enrich the knowledge basis of memory consolidation and may provide new paths and ideas for solving memory disorders or experimental findings [56, 57].

References

- [1] Helfrich, R.F., Mander, B.A., Jagust, W.J., et al.: Old Brains Come Uncoupled in Sleep: Slow Wave-Spindle Synchrony, Brain Atrophy, and Forgetting. *Neuron*. **97**, 221-230.e4 (2018)
- [2] Latchoumane, C.F.V., Ngo, H.V.V., Born, J., et al.: Thalamic Spindles Promote Memory Formation during Sleep through Triple Phase-Locking of Cortical, Thalamic, and Hippocampal Rhythms. *Neuron*. **95**, 424-435.e6 (2017)

- [3] Maingret, N., Girardeau, G., Todorova, R., et al.: Hippocampo-cortical coupling mediates memory consolidation during sleep. *Nat Neurosci.* **19**, 959–964 (2016)
- [4] Niknazar, M., Krishnan, G.P., Bazhenov, M., et al.: Coupling of Thalamocortical Sleep Oscillations Are Important for Memory Consolidation in Humans. *PLOS ONE.* **10**, e0144720 (2015)
- [5] Maquet, P.: The Role of Sleep in Learning and Memory. *Science.* **294**, 1048–1052 (2001)
- [6] Hruska, M., Cain, R.E., Dalva, M.B.: Nanoscale rules governing the organization of glutamate receptors in spine synapses are subunit specific. *Nat Commun.* **13**, 920 (2022)
- [7] Sekeres, M.J., Winocur, G., Moscovitch, M.: The hippocampus and related neocortical structures in memory transformation. *Neuroscience Letters.* **680**, 39–53 (2018)
- [8] Vaz, A.P., Inati, S.K., Brunel, N., et al.: Coupled ripple oscillations between the medial temporal lobe and neocortex retrieve human memory. *Science.* **363**, 975–978 (2019)
- [9] Azimi, A., Alizadeh, Z., Ghorbani, M.: The essential role of hippocampo-cortical connections in temporal coordination of spindles and ripples. *NeuroImage.* **243**, 118485 (2021)
- [10] Alizadeh, Z., Azimi, A., Ghorbani, M.: Enhancement of Hippocampal-Thalamocortical Temporal Coordination during Slow-Frequency Long-Duration Anterior Thalamic Spindles. *J. Neurosci.* **42**, 7222–7243 (2022)
- [11] Klinzing, J.G., Mölle, M., Weber, F., et al.: Spindle activity phase-locked to sleep slow oscillations. *NeuroImage.* **134**, 607–616 (2016)
- [12] Binder, S., Mölle, M., Lippert, M., et al.: Monosynaptic Hippocampal-Prefrontal Projections Contribute to Spatial Memory Consolidation in Mice. *J. Neurosci.* **39**, 6978–6991 (2019)
- [13] Yu, Y., Wang, H., Liu, X., et al.: Closed-loop transcranial electrical stimulation for inhibiting epileptic activity propagation: a whole-brain model study. *Nonlinear Dyn.* **112**, 21369–21387 (2024).

- [14] Wang, X., Yu, Y., Han, F., et al.: Dynamical mechanism of parkinsonian beta oscillation in a heterogenous subthalamopallidal network. *Nonlinear Dyn.* **111**, 10505–10527 (2023).
- [15] Hou, S., Fan, D., Wang, Q.: Novel perturbation mechanism underlying the network fragility evolution. *EPL.* **144**, 32002 (2023).
- [16] Yang, H., Han, F., Wang, Q.: A large-scale neuronal network modelling study: Stimulus size modulates gamma oscillations in the primary visual cortex by long-range connections. *European Journal of Neuroscience.* **60**, 4224–4243 (2024).
- [17] Leminen, M.M., Virkkala, J., Saure, E., et al.: Enhanced Memory Consolidation Via Automatic Sound Stimulation During Non-REM Sleep. *Sleep.* **40**, zsx003 (2017).
- [18] Ong, J.L., Lo, J.C., Chee, N.I.Y.N., et al.: Effects of phase-locked acoustic stimulation during a nap on EEG spectra and declarative memory consolidation. *Sleep Medicine.* **20**, 88–97 (2016)
- [19] Geva-Sagiv, M., Mankin, E.A., Eliashiv, D., et al.: Augmenting hippocampal–prefrontal neuronal synchrony during sleep enhances memory consolidation in humans. *Nat Neurosci.* **26**, 1100–1110 (2023)
- [20] Nikolin, S., Martin, D., Loo, C.K., et al.: Effects of TDCS dosage on working memory in healthy participants. *Brain Stimulation.* **11**, 518–527 (2018)
- [21] Coffman, B.A., Clark, V.P., Parasuraman, R.: Battery powered thought: Enhancement of attention, learning, and memory in healthy adults using transcranial direct current stimulation. *NeuroImage.* **85**, 895–908 (2014).
- [22] Zakary, O., Rachik, M., Elmouki, I.: On the analysis of a multi-regions discrete SIR epidemic model: an optimal control approach[J]. *International Journal of Dynamics and Control.* **5**, 917-930 (2017).
- [23] Horikawa, Y.: Bifurcations and chaos in a minimal neural network: Forced coupled neurons[J]. *International Journal of Bifurcation and Chaos.* **31**, 2150147 (2021).

- [24] Mehmood, S., Singh, J P.: A memristor-based magnetized Hopfield neural network for hidden scroll chaotic attractors and control analysis with reduced input[J]. *International Journal of Dynamics and Control*. 1-12(2024).
- [25] Stocco, A., Rice, P., Thomson, R. et al.: An Integrated Computational Framework for the Neurobiology of Memory Based on the ACT-R Declarative Memory System. *Comput Brain Behav* **7** 129–149 (2024).
- [26] Zhao, J., Yu, Y., Han, F., et al.: Regulating epileptiform discharges by heterogeneous interneurons in thalamocortical model. *Chaos: An Interdisciplinary Journal of Nonlinear Science*. **33**, 083128 (2023).
- [27] Fan, D., Wang, Y., Wu, J., et al.: The preview control of a corticothalamic model with disturbance. *era*. **32**, 812–835 (2024).
- [28] Yin, L., Han, F., Yu, Y., et al.: A computational network dynamical modeling for abnormal oscillation and deep brain stimulation control of obsessive–compulsive disorder. *Cogn Neurodyn*. **17**, 1167–1184 (2023).
- [29] Gosak, M., Milojević, M., Duh, M., et al.: Networks behind the morphology and structural design of living systems. *Physics of Life Reviews*. **41**, 1-21 (2022).
- [30] Gosak, M., Markovič, R., Dolenšek, J., et al.: Network science of biological systems at different scales: A review. *Physics of life reviews*. **24**,118-135(2018).
- [31] Hashemi, N.S., Dehnavi, F., Moghimi, S., et al.: Slow spindles are associated with cortical high frequency activity. *NeuroImage*. **189**, 71–84 (2019)
- [32] Yuan, Y., Chen, Y., Li, X.: Theoretical Analysis of Transcranial Magneto-Acoustical Stimulation with Hodgkin-Huxley Neuron Model. *Front. Comput. Neurosci*. **10**(2016).
- [33] Klinzing, J.G., Niethard, N., Born, J.: Mechanisms of systems memory consolidation during sleep. *Nat Neurosci*. **22**, 1598–1610 (2019).
- [34] Helfrich, R.F., Mander, B.A., Jagust, W.J., et al.: Old Brains Come Uncoupled in Sleep: Slow Wave-Spindle Synchrony, Brain Atrophy, and Forgetting. *Neuron*. **97**, 221-230.e4 (2018).

- [35] Ladenbauer, J., Ladenbauer, J., Külzow, N., et al.: Promoting Sleep Oscillations and Their Functional Coupling by Transcranial Stimulation Enhances Memory Consolidation in Mild Cognitive Impairment. *J. Neurosci.* **37**, 7111–7124 (2017).
- [36] Staresina, B.P., Bergmann, T.O., Bonnefond, M., et al.: Hierarchical nesting of slow oscillations, spindles and ripples in the human hippocampus during sleep. *Nat Neurosci.* **18**, 1679–1686 (2015).
- [37] Levenstein, D., Buzsáki, G., Rinzl, J.: NREM sleep in the rodent neocortex and hippocampus reflects excitable dynamics. *Nat Commun.* **10**, 2478 (2019).
- [38] Staresina, B.P., Bergmann, T.O., Bonnefond, M., et al.: Hierarchical nesting of slow oscillations, spindles and ripples in the human hippocampus during sleep. *Nat Neurosci.* **18**, 1679–1686 (2015).
- [39] Adamantidis, A.R., Gutierrez Herrera, C., Gent, T.C.: Oscillating circuitries in the sleeping brain. *Nat Rev Neurosci.* **20**, 746–762 (2019).
- [40] Varela, C., Wilson, M.A.: mPFC spindle cycles organize sparse thalamic activation and recently active CA1 cells during non-REM sleep. *eLife.* **9**, e48881 (2020).
- [41] Diekelmann, S., Born, J.: The memory function of sleep. *Nat Rev Neurosci.* **11**, 114–126 (2010).
- [42] Fernández-Ruiz, A., Oliva, A., Fermino de Oliveira, E., et al.: Long-duration hippocampal sharp wave ripples improve memory. *Science.* 364, 1082–1086 (2019).
- [43] Fogel, S.M., Smith, C.T., Cote, K.A.: Dissociable learning-dependent changes in REM and non-REM sleep in declarative and procedural memory systems. *Behavioural Brain Research.* **180**, 48–61 (2007).
- [44] Ngo, H.-V.V., Martinetz, T., Born, J., et al.: Auditory Closed-Loop Stimulation of the Sleep Slow Oscillation Enhances Memory. *Neuron.* **78**, 545–553 (2013).

- [45] Nikolin, S., Loo, C.K., Bai, S., et al.: Focalised stimulation using high definition transcranial direct current stimulation (HD-tDCS) to investigate declarative verbal learning and memory functioning. *NeuroImage*. **117**, 11–19 (2015).
- [46] Logothetis, N.K., Eschenko, O., Murayama, Y., Augath, M., Steudel, T., Evrard, H.C., Besserve, M., Oeltermann, A.: Hippocampal–cortical interaction during periods of subcortical silence. *Nature*. **491**, 547–553 (2012).
- [47] Vaz, A.P., Inati, S.K., Brunel, N., Zaghloul, K.A.: Coupled ripple oscillations between the medial temporal lobe and neocortex retrieve human memory. *Science*. **363**, 975–978 (2019).
- [48] Gordon, B., Lesser, R.P., Rance, N.E., et al.: Parameters for direct cortical electrical stimulation in the human: histopathologic confirmation. *Electroencephalography and Clinical Neurophysiology*. **75**, 371–377 (1990).
- [49] Guskjolen, A., Cembrowski, M.S.: Engram neurons: Encoding, consolidation, retrieval, and forgetting of memory. *Mol Psychiatry*. **28**, 3207–3219 (2023).
- [50] Ngo, H.-V., Fell, J., Staresina, B.: Sleep spindles mediate hippocampal–neocortical coupling during long-duration ripples. *eLife*. **9**, e57011 (2020).
- [51] Phipps, C.J., Murman, D.L., Warren, D.E.: Stimulating Memory: Reviewing Interventions Using Repetitive Transcranial Magnetic Stimulation to Enhance or Restore Memory Abilities. *Brain Sciences*. **11**, 1283 (2021).
- [52] Traub, R.D., Whittington, M.A., Stanford, I.M., Jefferys, J.G.R.: A mechanism for generation of long-range synchronous fast oscillations in the cortex. *Nature*. **383**, 621–624 (1996).
- [53] Helfrich, R.F., Lendner, J.D., Mander, B.A., et al.: Bidirectional prefrontal–hippocampal dynamics organize information transfer during sleep in humans. *Nat Commun*. **10**, 3572 (2019).

- [54] Rajasethupathy, P., Sankaran, S., Marshel, et al.: Projections from neocortex mediate top-down control of memory retrieval. *Nature*. **526**, 653–659 (2015).
- [55] Sanda, P., Malerba, P., Jiang, X., et al.: Bidirectional interaction of hippocampal ripples and cortical slow waves leads to coordinated spiking activity during NREM sleep. *Cerebral Cortex*. **31**, 324-340(2021).
- [56] Li, Y., Briguglio, J. J., Romani, S., Magee, J. C.: Mechanisms of memory-supporting neuronal dynamics in hippocampal area CA3. *Cell*. **187**, 1-16(2024).
- [57] McHugh S.B., Lopes-Dos-Santos V., Castelli M., Gava G.P., Thompson S.E., Tam S.K.E., Hartwich K., Perry B., Toth R., Denison T., Sharott A., Dupret D.: Offline hippocampal reactivation during dentate spikes supports flexible memory. *Neuron*. **112**, 1-14(2024).

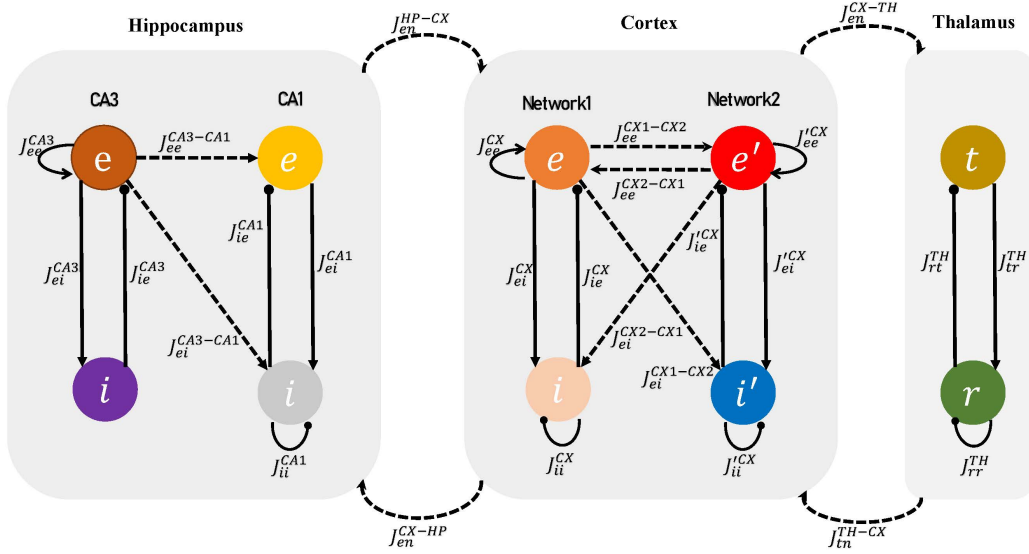


Figure 1: The structure of synaptic connections between neurons of the HTC network. This network model consists of three subnetworks: hippocampus, cortex, and thalamus. In the hippocampal subnetwork and the cortex subnetwork, the excitatory neurons (shown by “e”) and the inhibitory neurons (shown by “i”) in the CA1 and CA3 regions are connected using “J” synaptic strengths. The thalamocortical(TC) and the reticular(RE) neurons shown in the thalamus network are represented by “t” and “r”. Excitatory synaptic connections are indicated by arrows and inhibitory connections are shown as lines ending in a dot. Short-range connections are displayed with solid lines and long-range connections with dotted lines. “n” represents the receptor network.

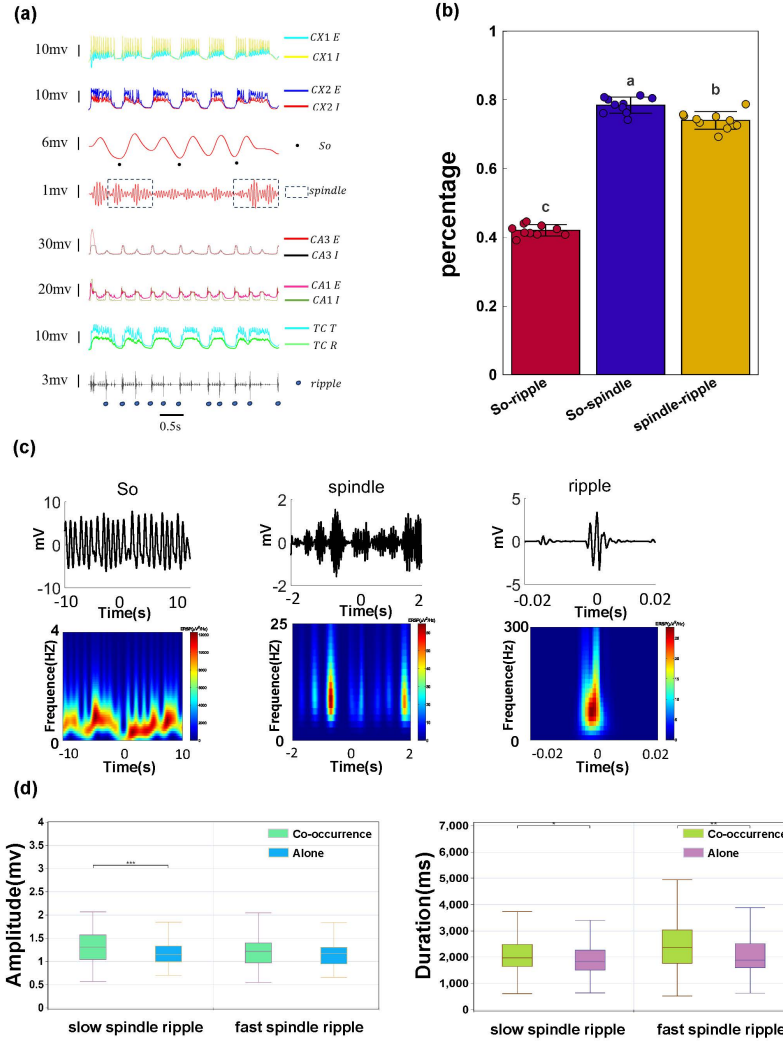


Figure 2: **Generation of SOs, spindles, and ripple in the full hippocampo-cortico-thalamic model and their firing characteristics.** (a) From top bottom respectively: Broadband traces of the membrane potential of the cortical networks 1 and 2, filtered traces of the membrane potential of the cortical network 2 excitatory neuron in the frequency range of So [0.5Hz–2Hz] and spindle [12Hz–16Hz] with detected SO troughs (filled circles) and spindles (dashed box), broadband traces of the membrane potential of CA3, CA1 and TC neurons, filtered [100Hz–250Hz] traces of the membrane potential of CA1 excitatory neurons with detected ripples (grey circles). (b) The percentage of the ripples co-occuring with spindles ($p=0.0000108$) and SOs ($p=0.0000108$), and spindles co-occuring with SOs ($p=0.00125$), respectively (Duncan’s Multiple Range Test; wilcox-test). The difference box diagram of the amplitude (c) From top to bottom, from left to right: Top, So, spindle events, one ripple event; Bottom, Corresponding spectrograms of the waveforms above. (d) and duration (e) of slow and fast spindles in conjunction with ripples and isolated spindles, respectively. The model duration was set to 10 minutes. Fast spindle: $p=0.01252$, $p=0.29371$, for duration and amplitude, respectively, Kruskal-Wallis test; mean duration=2.4323s and mean amplitude=1.1864mV, $n=143$ for spindles coupled with ripples; mean duration=2.0462s and mean amplitude=1.1435mV, $n=54$ for isolated spindles. Slow spindle: $p=0.09902$, $p=0.008306$, for duration and amplitude, respectively, Kruskal-Wallis test; mean duration=2.1620s and mean amplitude=1.3100mV, $n=197$ for spindles coupled to ripples; mean duration=1.9092s and mean amplitude=1.1514mV, $n=39$ for isolated spindles.

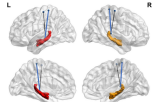
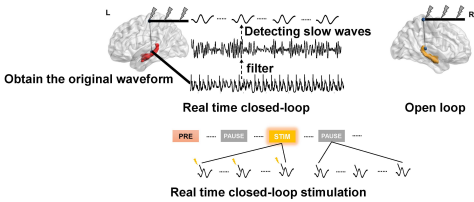
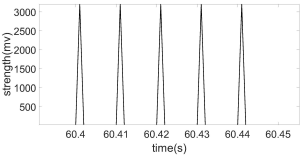
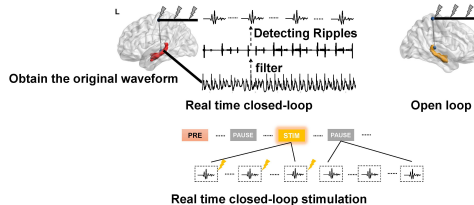
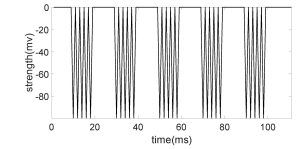
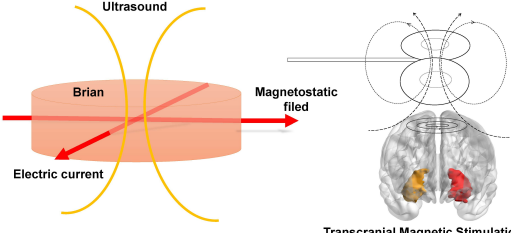
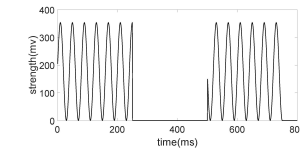
| Stimulation Protocol | Invasive (Yes/No) | Physical Principle | Stimulation Currents and Mathematical Expression |
|--|-------------------|--|--|
| Experimental Closed-loop Phase-locking Deep Brain Stimulation | Yes |  <p>— Sync-stimulation - cortex lobe — mixed-phase stimulation</p> | |
| Computational Closed-loop Phase-locking Excitable Stimulation | Yes |  <p>Obtain the original waveform</p> <p>Detecting slow waves</p> <p>filter</p> <p>Real time closed-loop</p> <p>Open loop</p> <p>PRE PAUSE STIM PAUSE</p> <p>Real time closed-loop stimulation</p> |  |
| Computational Closed-loop Phase-locking Inhibitive Stimulation | Yes |  <p>Obtain the original waveform</p> <p>Detecting Ripples</p> <p>filter</p> <p>Real time closed-loop</p> <p>Open loop</p> <p>PRE PAUSE STIM PAUSE</p> <p>Real time closed-loop stimulation</p> |  $s[n] = \text{strength} \cdot 1 \left(\left[\frac{n}{10h} \right] \cdot \frac{1}{\text{freq}} \cdot \left(\left[\frac{n}{10h} \right] \cdot \frac{1}{\text{freq}} + \frac{\text{sttime}}{h} \right) \right) (n)$ |
| Magnetic ultrasonic stimulation | No |  <p>Ultrasound</p> <p>Brain</p> <p>Magnetostatic field</p> <p>Electric current</p> <p>Transcranial Magnetic Stimulation</p> |  $x(t) \times (\sin(2\pi ft) + 1)$ $x(t) = \begin{cases} 1(n-1) \frac{1}{RF} < t \leq [(n-1) + DC] \frac{1}{RF}, n = 1, 2, 3, \dots \\ 0 & \text{others} \end{cases}$ |

Figure 3: Three type of invasive stimulus therapies and one type of non-invasive stimulation pattern (magnetic ultrasonic stimulation), and their performing process and physical mechanism, stimulation waveforms as well as mathematical expressions.

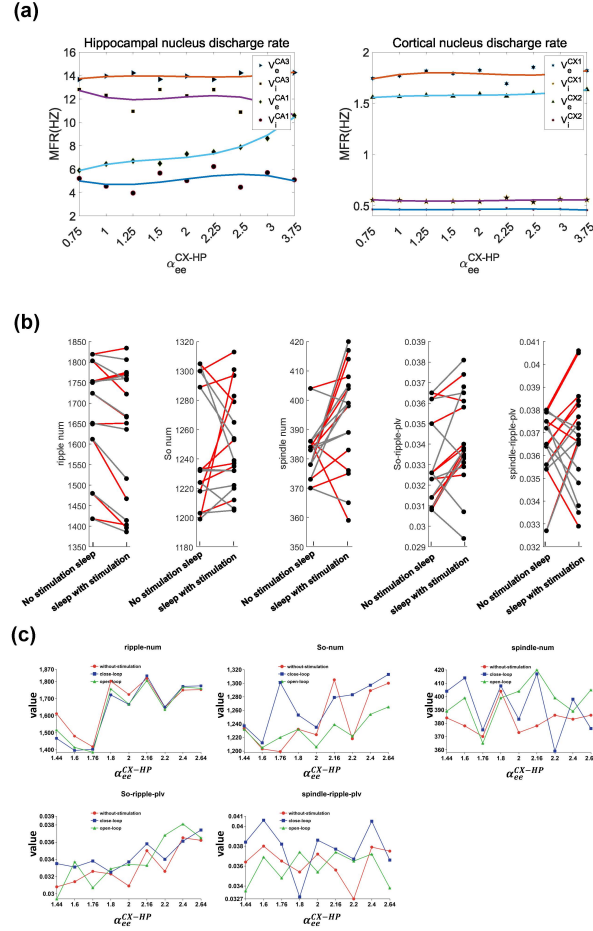


Figure 4: The impact of the strength of cortico-hippocampal excitatory connections on their firing rate and their facilitation effects to memory consolidation. It is shown that this excitatory connection has significant implications for the promotion of memory consolidation. **a** Left, Changes of cortical nucleus neuron firing rate with cortical hippocampal excitatory connection; Right, Changes in the firing rate of hippocampal nucleus neurons with cortical hippocampal excitatory connections (α_{ee}^{CX-HP} showing the factor multiplied to both J_{ee}^{CX-HP} and J'_{ee}^{CX-HP}). **b** The stimulation intensity was fixed (3200mV), and the corticohippocampal excitatory connection intensity parameters (α_{ee}^{CX-HP} showing the factor multiplied to both J_{ee}^{CX-HP} and J'_{ee}^{CX-HP}) were changed with reference to the experimental stimulation scheme, and the changes in five indicators of memory consolidation were observed (the number of ripple, the number of So, the number of spindle, the synchronization value of So and ripple, and the synchronization value of spindle and ripple). The black dots represent different connection strengths, the red lines represent closed loops, and the gray lines represent open loops. **c** Change of cortical-hippocampal excitatory connection strength parameters, specific numerical changes of the five index values, black dots represent different connection strength, red line represents no stimulus, blue line represents closed-loop stimulus, and green line represents open-loop stimulus

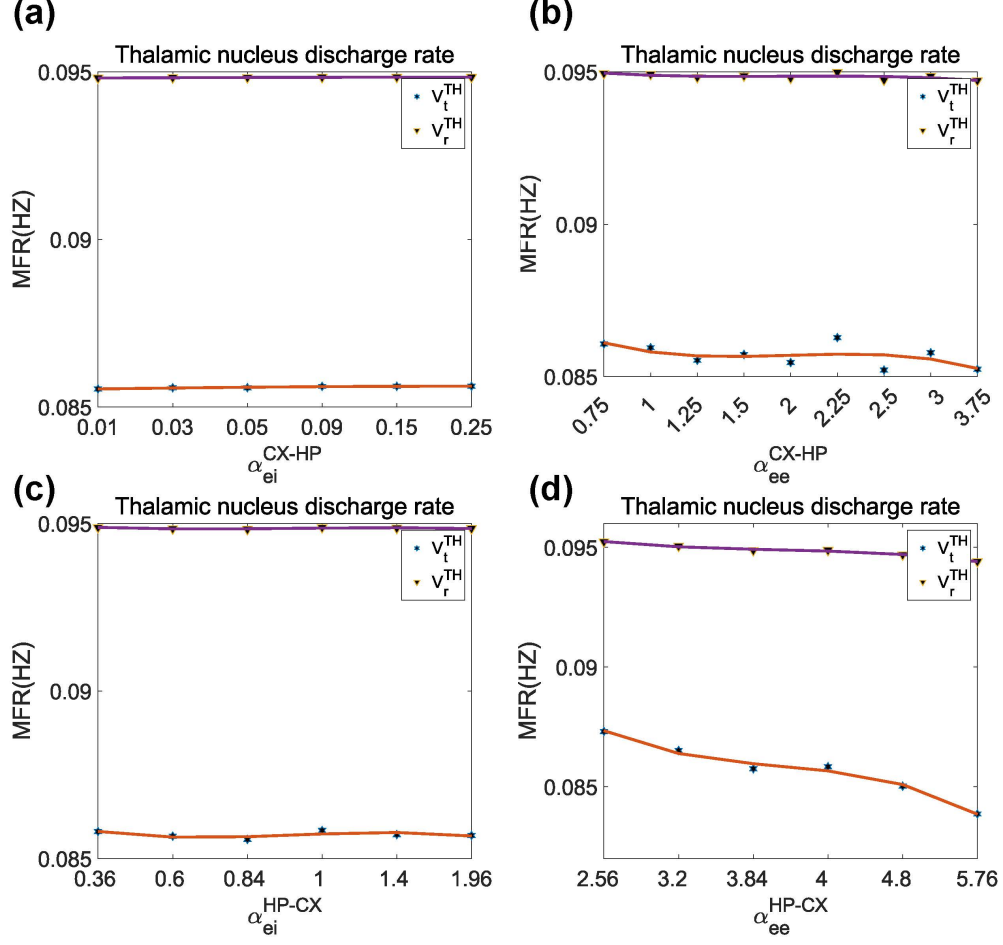


Figure 5: The impact of varying connection strengths on the firing rate of thalamic neurons. Under varying connection strengths among different neurons, there is almost no effect on the firing rate of thalamic neurons. **a** The firing frequency of thalamic nucleus neurons varies with the strength of cortical hippocampal excitatory inhibitory connections (α_{ei}^{CX-HP} showing the factor multiplied to both J_{ei}^{CX-HP} and J'_{ei}^{CX-HP}). **b** The firing frequency of thalamic nucleus neurons varies with the strength of cortical hippocampal excitatory connections (α_{ee}^{CX-HP} showing the factor multiplied to both J_{ee}^{CX-HP} and J'_{ee}^{CX-HP}). **c** The firing frequency of thalamic nucleus neurons varies with the strength of hippocampal cortical excitatory inhibitory connections (α_{ei}^{HP-CX} showing the factor multiplied to both J_{ei}^{HP-CX} and J'_{ei}^{HP-CX}). **d** The firing frequency of thalamic nucleus neurons varies with the strength of hippocampal cortical excitatory connections (α_{ee}^{HP-CX} showing the factor multiplied to both J_{ee}^{HP-CX} and J'_{ee}^{HP-CX}).

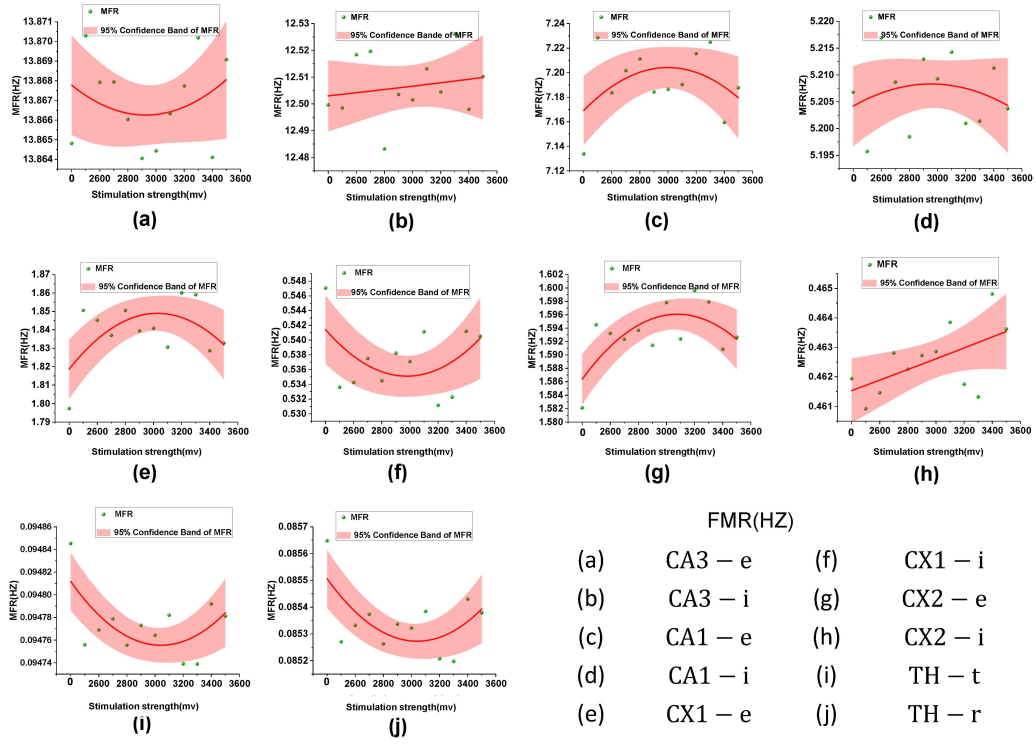


Figure 6: According to the experimental stimulus scheme [19], the effect of changing the stimulus intensity on the firing rate of neurons in HTC network was studied. Under a fixed connection strength, changing the stimulus intensity has little effect on the discharge rate of the nucleus, further explaining the important role of excitatory connections in the cortical-hippocampal neurons in promoting memory consolidation.

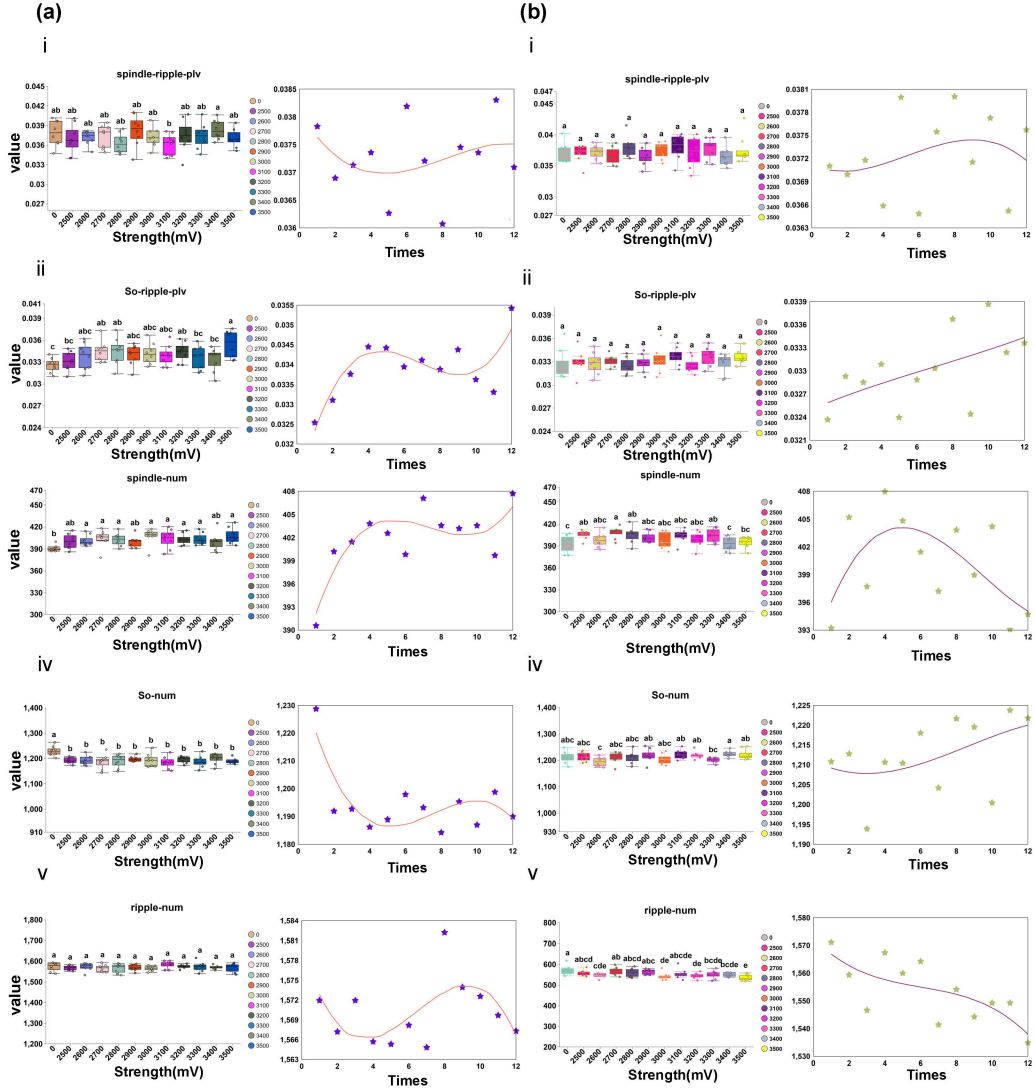


Figure 7: Numerical simulations reproduce the experimental results, namely that under real-time closed-loop stimulation, synchronization increases and the number of ripple events decreases, while the number of other events increases; without precise temporal stimulation, the results are qualitatively consistent with the experimental findings. The significant reduction in the number of slow oscillation events may counteract the decreased synchronization between hippocampal ripples and cortical slow oscillations, leading to no significant changes after stimulation or potentially being detrimental to memory consolidation. **a** The difference boxplot (Left) and the corresponding scatter fitting curve (Right) of five indices (i, spindle-ripple-plv; ii, So-ripple-plv; iii, spindle number; iv, So number; V, ripple number) were obtained by open-loop stimulation. **b** The difference boxplot (Left) and the corresponding scatter fitting curve (Right) of five indexes (i, spindle-ripple-plv; ii, So-ripple-plv; iii, spindle number; iv, So number; V, ripple number) by the closed-loop stimulation were studied.

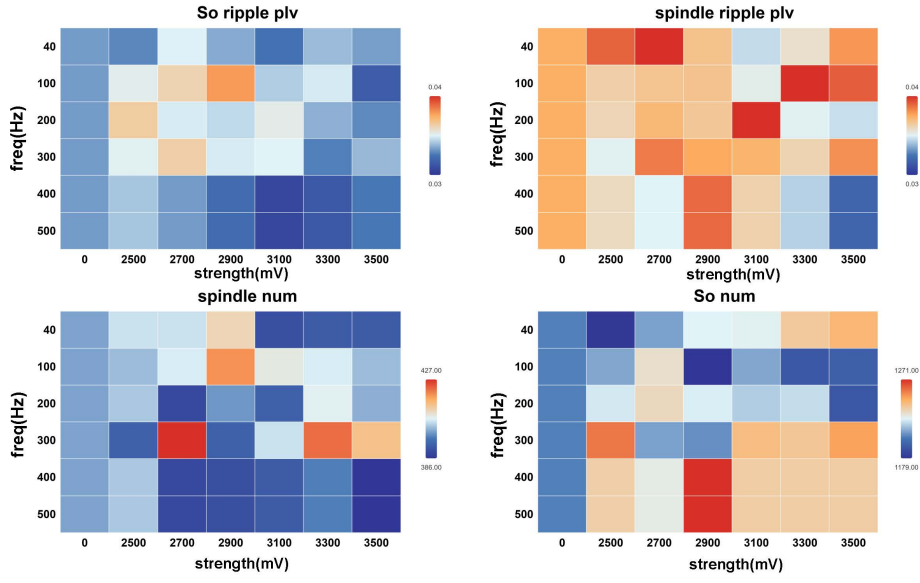


Figure 8: Heatmap of exponential changes under dual-parameter experimental stimulation. This further affirms the rationality of the experimental stimulation frequency (100Hz) chosen in the numerical simulations. From left to right, from top to bottom, the plv values of So and ripple, the plv values of spindle and ripple, the number of spindle and the number of So, and the abscordinate is the stimulus intensity. Each color depth represents the value, the bluer represents the larger value, and the reder represents the smaller value

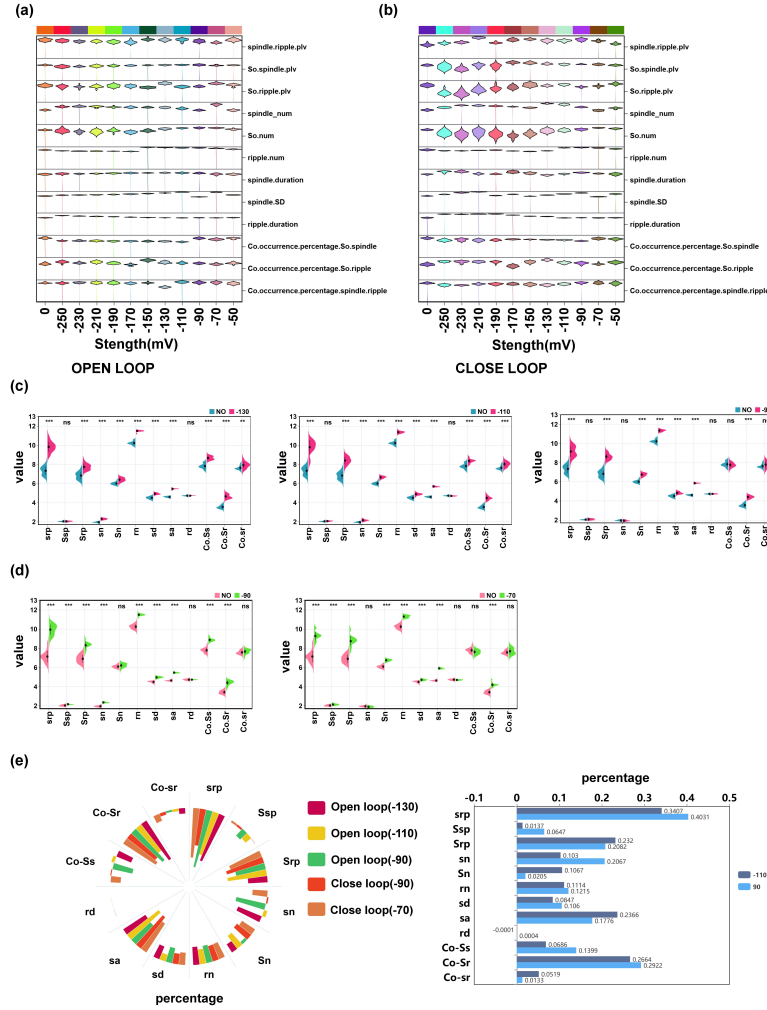
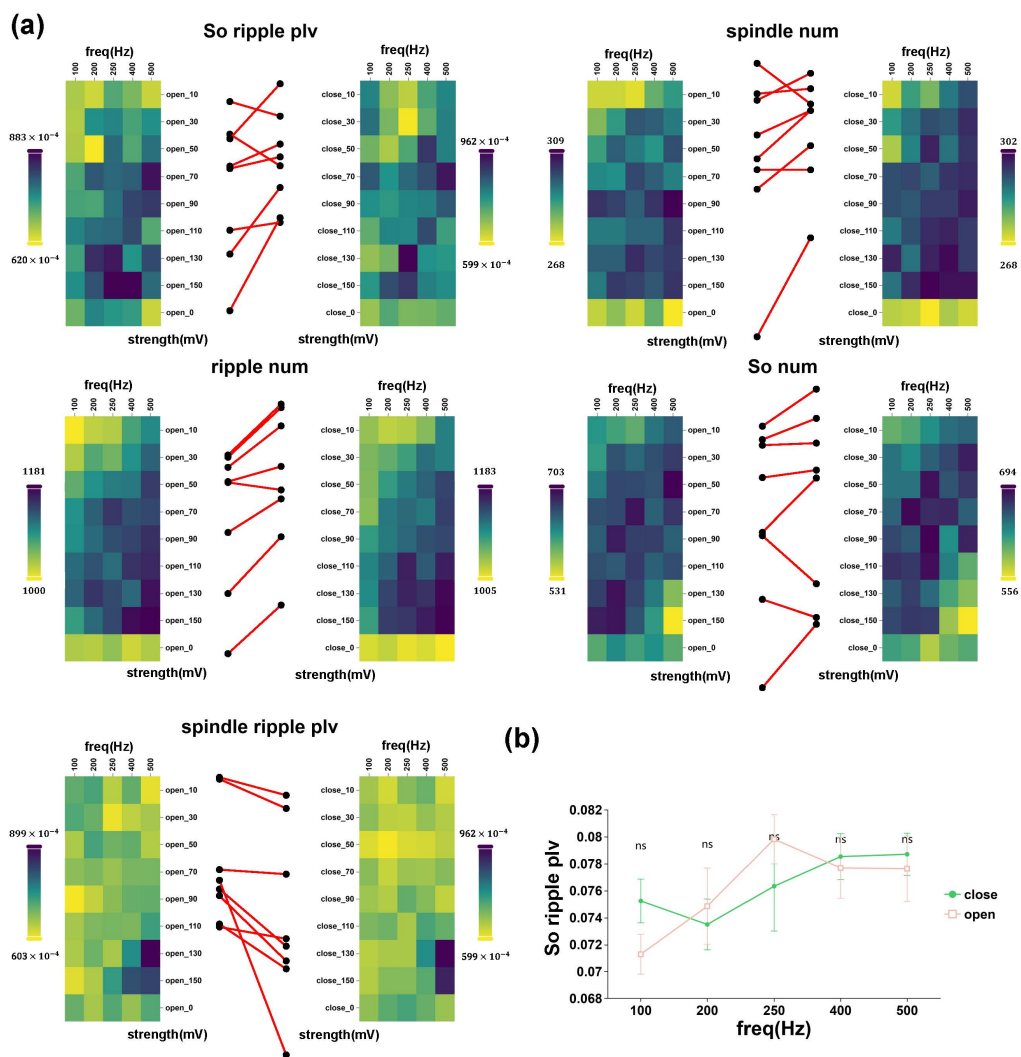


Figure 9: Results of the inhibitory stimulation protocol. The low-current inhibitory stimulation scheme is more effective than the existing experiments (with significant increases in synchronization values as well as the number and characteristics of events), further demonstrating the rationality and superiority of real-time closed-loop stimulation. **a** Violin diagram of inhibitory open-loop stimulus matrix, the horizontal coordinate is the stimulus intensity (negative sign represents the inhibitory stimulus), and the vertical coordinate represents each index value. **b** Like **d**, violin diagram of inhibitory closed loop matrix. **c** The intensity of open-loop inhibitory stimulation was 130 mV (left), 110 mV (middle), 90 mV (right) violin plots showing the index in the relatively unstimulated case. Difference analysis (***) indicates $p < 0.001$, ** indicates $p < 0.01$, * indicates $p < 0.05$, and ns indicates no significant difference). srp represents the plv value of spindle and ripple, Srp represents the plv value of So and spindle, Sn represents the number of spindle events, Sn represents the number of So events, rn represents the number of ripple events. sd represents the duration of spindle, sa represents the average amplitude of spindle, rd represents the duration of ripple, Co-Ss represents the percentage of So and spindle occurring together, Co-Sr represents the percentage of So co-occurring with ripple and Co-sr represents the percentage of spindle co-occurring with ripple. **d** The closed-loop inhibitory stimulus intensity was 90 mV (left), 70 mV (right), violin plot showing the index in the relatively unstimulated case. Difference analysis (***) indicates $p < 0.001$, ** indicates $p < 0.01$, * indicates $p < 0.05$, and ns indicates no significant difference. **e** left: The above polar graph shows the percentage (mean) increase of stimulus intensity relative to each index of non-stimulus; right: The percentage increase in each index relative to no stimulation was best for closed-loop stimulation inten-



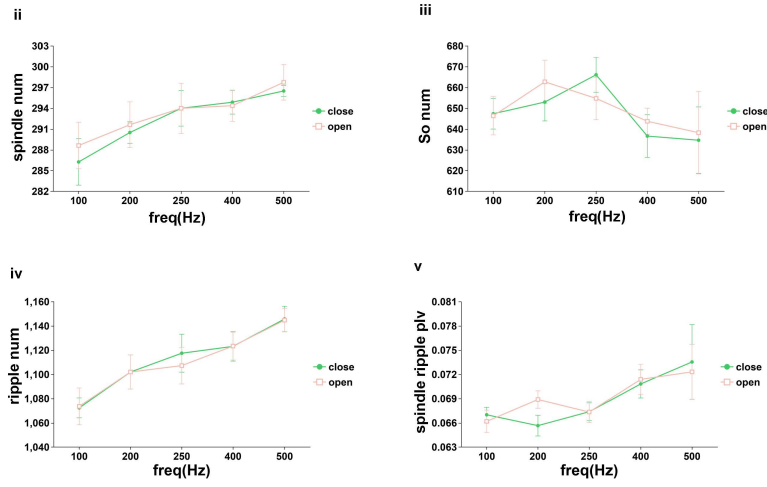


Figure 10: Dual-parameter inhibitory stimulation. Similarly, it also further confirms the rationality and superiority of our chosen stimulation frequency (500Hz). **a** Combined heat maps, the left side of each subgraph represents the open loop heat map results; On the right is the closed-loop thermal map result; Each point in the middle plot represents a different stimulus intensity, and the average stimulus frequency indicator is based on the percentage increase in no stimulus, with the left side being open loop and the right side being closed loop; i, ii, iii, iv, and v represent respectively the plv of So and ripple, the number of spindle events, the number of ripple events, the number of So events, and the plv of spindle and ripple. **b** Compare the open-loop (pink) and closed-loop (green) results

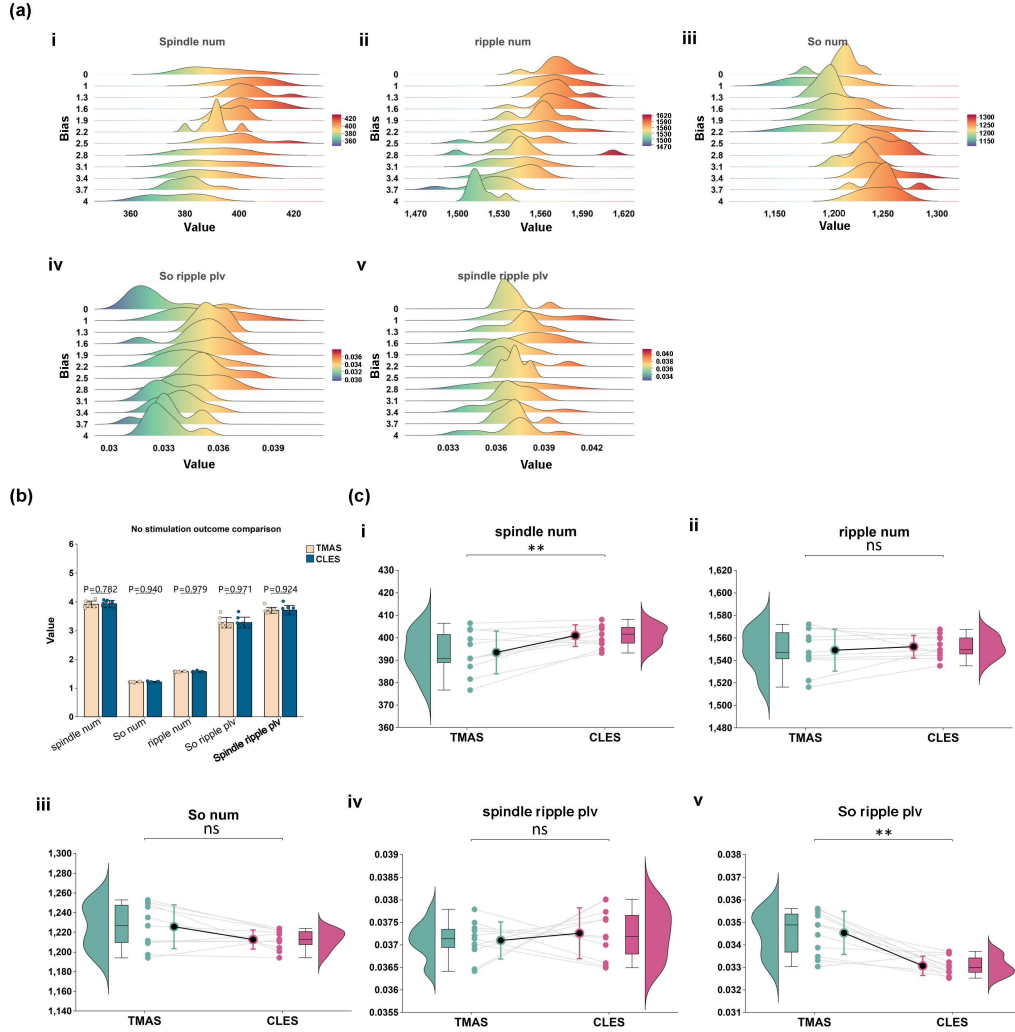


Figure 11: Results of magneto-ultrasound stimulation, compared with the effects of experimental closed-loop intracranial stimulation. It indicates that the effects of magneto-ultrasound stimulation are comparable to those of experimental closed-loop intracranial stimulation. That is, the synchronization gain of thalamo-cortical spindle waves with hippocampal ripples and the increase in the number of cortical slow oscillation events show no significant difference, and the reduction in the number of ripple events is roughly consistent. The increase in spindle events under magneto-ultrasound stimulation is slightly inferior, but in comparison, the enhancement of cortical slow oscillation and hippocampal ripple synchronization under magneto-ultrasound stimulation is significantly higher than that under closed-loop intracranial electrical stimulation. This improvement may offset the insufficiency in the number of spindle events. **a** Changes of magnetic ultrasound stimulation compared with no stimulation. **b** Comparison of index changes under different initial values. **c** Comparison of results between magnetic ultrasound stimulation and experimental closed-loop stimulation.